University of the West of England
BRISTOL

Waste and Wastewater Clean-up using Microbial Fuel Cells

Jiseon You

A thesis submitted in partial fulfilment of the requirements of the University of the West of England, Bristol for the degree of Doctor of Philosophy

Faculty of Environment and Technology, University of the West of England, Bristol

February 2016

Abstract

A sustainable energy portfolio should include a range of carbon-neutral and renewable energy technologies. Amongst the renewable energy technologies, MFCs can offer a solution for both sustainable energy and clean water demands. In order to take the MFC technology to a commercial level, more effort has to be spent to improve the performance and treatment efficiency. The goal for this thesis was to improve anode performance and waste utilisation. To achieve this goal, the approach taken was system scale-up through multiples of relatively small sized MFC units.

Two main aspects of the MFC anode, system design and parameters affecting anode biofilms were investigated in order to enhance the anode performance for waste/wastewater clean-up. Firstly, system design aspects such as, each MFC component, reactor designs as well as anodes were looked into. Through comparing nine commercially available ion exchange membranes, a cation exchange membrane (MI-C) was chosen for the rest of the work, since it showed the highest performance per unit cost of 20.72 mW/$100. Also, by replacing the previous plain carbon fibre veil electrode material with a carbon based microporous layer (MPL) modified anode and cathode, a 2.2 and 4.9 fold increase in power output was achieved respectively. Secondly, three different parameters affecting anode biofilms, temperature, external load and feedstock, were investigated to analyse and understand the dynamic characteristics of MFC anode biofilms, which could lead to methods of controlling anode biofilms in a desirable way. MFCs inoculated with thermophilic species and operated at 60 °C, showed the best performance at 60 °C, power output decreased above and below this temperature, which demonstrated their high sensitivity towards operating temperature. Accidental contamination which occurred during the work resulted in a power output increase, which revealed the potential for enhancing MFC performance by mixing

two or more anodophilic species. When comparing the effect of three different external loads, 100 Ω, 1 kΩ and 10 kΩ, on MFC performance during anode bacterial maturing period and beyond, MFCs loaded with 100 Ω and 1 kΩ showed P_{MAX} of 104.9 μW and 112.5 μW which are nearly twice higher than the value of MFCs with 10 kΩ (53.2 μW). However the underperformance of MFCs with the lightest load of 10 kΩ improved by 371.4 % when the external resistance values were changed to match the internal resistance. Hereby the importance of impedance matching that connects an MFC system with an external resistance value close to its internal resistance value was successfully demonstrated. Another experiment revealed the possibility of manipulating anodic biofilm metabolisms through exposure to different feedstock conditions. Two groups of anodic biofilm matured with two very different substrates, acetate and casein for 20-25 days, reached steady states and produced 80-87 μW and 20-29 μW consistently for 3 weeks, respectively. When the substrates were swapped, the casein-enriched group showed faster response to acetate and higher power output, compared to the acetate-enriched group. Also when the substrates were switched back to their original groups, the power output of both groups returned to the previous levels more quickly than when the substrates were swapped the first time, which supports the argument of possible manipulation of anodic biofilms. Community level physiological profiling also supported this finding.

For the final part of this thesis, these findings were used to implement the MFC technology for practical applications such as treating wastes and resource recovery as well as producing electrical energy. Two troublesome wastes, urine and uric salts showed great potential for being power sources of MFC electricity generation. Furthermore it was demonstrated that MFCs can contribute to recovery of resources such as nitrogen and phosphorus in the form of struvite. A 3-stage MFC/struvite extraction process system was developed and its feasibility tested in order to maximise urine utilisation in terms of electricity generation and struvite recovery. During the first stage, whilst generating

electrical energy, MFCs accelerated urea hydrolysis, which was beneficial for the struvite precipitation process in the following stage. After collecting struvite by adding magnesium into the initial effluent, the supernatant was used for the final stage for additional power and more efficient COD reduction. In total, 82 % of PO_4^{3-}–P and 20 % of COD of undiluted human urine were removed by the 3-stage system. Also 358 μW and 294 μW of power were produced from the 1st and 3rd stages of the system, respectively, during operation. Finally a commercial air freshener powered by a stack of 8 MFCs fed with neat human urine, was run continuously for over 4 weeks, which successfully demonstrated a great potential of the MFC technology for both electricity generation and waste treatment.

Acknowledgements

During the last 5 years of working on this PhD, I have sometimes dreamt about this moment when I am writing the Acknowledgements section of my thesis. And here it comes, at last. Like many other things in life, I know that I couldn't have made it this far without the help and guidance of others. There are so many people to thank for sharing my time of joy, excitement, challenges, frustration, and tiredness but above all, rewarding experience.

First of all, a million thanks should go to Professor Ioannis Ieropoulos for his guidance and support. He has always been able to keep on amazing me with his knowledge, ideas and insights. I also would like to express my gratitude to my other supervisors, Professor John Greenman and Professor Chris Melhuish for their encouragement and support. All of you have made my PhD life meaningful and unforgettable.

I also greatly appreciate all our dear members of Bristol BioEnergy Centre (B-BiC), George Papahalarabos, Iwona Gajda, Jonathan Winfield, Alexis Walter, Ben Tylor, Grzegorz Pasternak, Irene Jimenez, Pavlina Theodosiou, Hemma Philamore, Lily Chambers, Pablo Ledezma, Jean-Michel Maheu, Clare Backman for their companionship, productive discussions, emotional and physical help. Our fantastic technicians, Andrew Stinchcombe, Sam Forbes, Daniel Herranz should deserve my greatest thanks. I know I am lucky to have you and it was such a pleasure to work with all of you.

Big thanks to UWE technicians, Dave Corry, Dave Patton, Adele Ainger, Man-Kim Cheung, Debbie Lewis, Lee Graham, Saliha Saad, Dave Molesworth, Sam Coupland, Jason Welsby and especially to my technical super hero and dear friend, Ian Horsfield for his help and inspiration, many a late night discussing internally matched impedance! Jo, thank you for your spiritual guidance and reassurance during this time. I apologise if I bothered some of you too much sometimes, but you all have been so great and always kept a smile on your face.

I would like to express my sincere gratitude to my examiners of this thesis and viva, Dr Eileen Yu, Dr Yue Zhang, Professor Tim Hughes and Professor Darren Reynolds for their time and valuable comments. Special thanks to the collaborators Prof Larry Bull, Dr Richard Preen, Dr Carlo Santoro, Dr Pierangela Cristiani and Prof Baikun Li and for their help and valuable comments.

Lastly, I want to thank my best friend and beloved husband, Chris Bytheway, who gives me unfailing support and encouragement. Without you, I couldn't even dream of starting this journey. As I always said, whatever I have achieved for the last 5 years is yours too. I wish to share the joy of completing this thesis with you. And very finally, to my baby girl, Chloe, thank you for coming to me as my daughter, I love you so much.

Jiseon You

January 2016

"Experience life in all possible ways: good-bad, bitter-sweet, dark-light, summer-winter. Experience all the dualities. Don't be afraid of experience, because the more experience you have, the more mature you become."

— Osho

List of Abbreviations and Nomenclature

AC	Activated carbon
AEM	Anion exchange membrane
AS	Activated sludge
AUC	Area under curve
AWCD	Average well colour development
BES	Bioelectrochemical systems
BHI	Brain heart infusion
BOD	Biochemical oxygen demand
CAD	Computer-aided design
CC	Carbon cloth
CE	Coulombic efficiency
CEM	Cation exchange membrane
CFU	Colony forming unit
CI	Confidence interval
CL	Catalyst layer
CLED	Cystine lactose electrolyte deficient
CLPP	Community level physiological profiling
C-MFC	Circular MFC
COD	Chemical oxygen demand
CV	Carbon fibre veil
DET	Direct electron transfer
DGGE	Denaturing gradient gel electrophoresis
DIW	Deionised water
DNA	Deoxyribonucleic acid
DO	Dissolved oxygen
EDTA	Fe(III) ethylenediamineteraacetic acid
EPS	Extracellular polymeric substance
EPSRC	Engineering and Physical Sciences Research Council
GDL	Gas diffusion layer
H	Shannon-Wiener index
HRT	Hydraulic retention time
IEM	Ion exchange membrane
IPCC	Intergovernmental Panel on Climate Change
MEC	Microbial electrolysis cells
MET	Mediated electron transfer
MFC	Microbial fuel cell
MPL	Microporous layer
MPT	Maximum power transfer
MPTP	Maximum power transfer point
OCV	Open circuit voltage (unit: V)
OD	Optical density
OLR	Organic loading rate

ORP	Oxidation reduction potential
ORR	Organic removal rate
PAO	Polyphosphate accumulating organism
PBS	Phosphate buffered saline
PTFE	Polytetrafluoroethylene
R-MFC	Rectangular microbial fuel cell
RPM	Revolutions per minute
S.A.	Surface area
SEM	Scanning electron microscope
S-MFC	Spherical MFC
TGGE	Temperature gradient gel electrophoresis
TOC	Total organic carbon
TSA	Tryptic soy agar
TYE	Tryptone yeast extract
WWTP	Wastewater treatment plant
XRD	X-ray diffraction

Contents

List of Figures

List of Tables

1. Introduction

1.1. Overview

The Industrial Revolution was a major turning point in the history of humankind. It changed the way we live and the way we perceive utilities, commodities and values. Technical developments in this period resulted in mass production as well as mass consumption. As a result, the world has now more wealth and materials than before, but at the same time, it is facing some of its biggest challenges. World population growth, concentration of the population (urbanisation) and climate change have brought the threat of food, water and energy shortage. These now form part of the global grand challenges, known as the Energy-Water-Food Nexus. Therefore resolving or improving one challenge could well improve the others. In this respect, efforts for developing alternative energy sources, instead of combusting fossil fuels, have been intensified, and as a result, technologies relating to renewable energy sources such as solar, wind and biomass have progressed significantly. Nevertheless, none of these can be competitive with mainstream fossil fuel-based energy sources at this time, and this is why a new paradigm shift is required.

The rapidly growing microbial fuel cells (MFCs) technology is one example of a paradigm shift. MFCs are bioelectrochemical systems that convert energy contained in organic matter into electrical energy. They not only can provide electricity generation but also waste clean-up, via the microbial degradation of organic matter in the waste. From its inception over 100 years ago, the MFC technology development was very slow, and only recently accelerated, especially over the last two decades. The technology is now at an exciting point of showing great potential for clear cut practical and commercial applications. However, there is still a lot of effort required in order to take the technology from the laboratory to a commercial scale.

One of the key features that make MFCs unique is the fact that it is exploiting microbial metabolic activity. In order to optimise MFCs, it is important to establish good knowledge of

the anode half-cell, where bacterial activity takes place. Therefore the contention of this study is that:

MFC system performance and waste treatment efficiency can be significantly improved with a better understanding of the anode.

1.2. Thesis outline

The aim of this thesis was to **enhance anode performance and waste utilisation in terms of treatment efficiency and power generation,** which would lead to the development of power-packs for low power applications.

In order to achieve the aim, the following objectives were set;

(1) Compared to the previous materials used in the team, better performing components and designs of an MFC reactor will be selected. (Chapter 4)

(2) Parameters affecting anode biofilms performance will be evaluated and ways of controlling anode biofilms using these parameters will be sought. (Chapter 5)

(3) Utilisation of wastes that have not been tested much in MFC studies before, will be measured. (Chapter 6)

(4) A stack of MFCs will be built and run a commercial electrical appliance. (Chapter 6)

Chapter 2 will run through a brief introduction of current renewable energy technologies and where MFC technology fits in. The second part of the chapter will present principles and components of the MFC systems, highlighting some of the main technological breakthroughs achieved as well as identifying engineering hurdles. Lastly, MFC anode especially its biological aspect, will be covered in more detail since this was the main focus of this thesis.

Chapter 3: General materials and methods used in this work will be presented in detail. Some of the specific methods employed, in specific parts of the work, will be explained separately in the following chapters.

Chapter 4: Materials and designs of MFCs need to be selected carefully depending on the specific application of MFC operation (e.g. waste and wastewater clean-up in this work).

This chapter seeks improvement of the MFC performance and reduction of building cost through exploring better membrane materials, anode/cathode electrodes, and reactor designs. The materials showing good performance during the tests were employed for the subsequent experiments.

Chapter 5: Understanding the microbial community involved in electricity generation is imperative for MFC operation. This chapter will discuss the anodophilic microbial community's dynamic characteristics, under different running conditions such as temperature, external load and feedstock.

Chapter 6 explores the MFC ability of utilising urine and uric salts for power generation, which are considered as troublesome wastes to treat in conventional waste treatment processes. Furthermore recovering useful resource from urine was attempted and it was successfully shown that the MFC technology and conventional struvite recovery processes can complement each other. At the end of this work, a potential practical application of MFC stacks based on the findings of this thesis work will be demonstrated.

Chapter 7 provides conclusions of up to date current work and outlines possible directions for future work.

Figure 1.1 illustrates this thesis work.

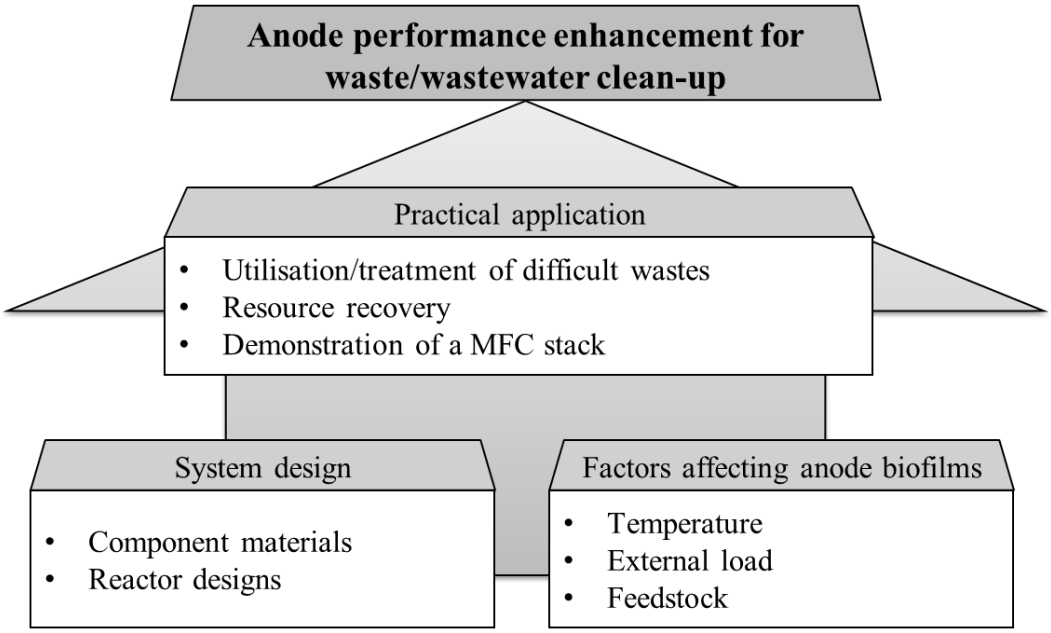

Figure 1.1 Overview of the work carried out in this study

2. Background – Microbial Fuel Cells and Anodes

2.1. Background to the Research

2.1.1. Global & UK Energy Issue: Energy Security & Climate Change

Currently the world is consuming 13,371 Mtoe (million tonnes of oil equivalent; 1 toe = 11,630 kWh) of energy and 81.7 % of this energy comes from fossil fuels (Figure 2.1, International Energy Agency, 2014). According to the IEA, the world's primary energy demand is expected to grow by 36 % between 2008 and 2035, or 1.2 % per year on average (International Energy Agency, 2010). Although there is controversy about how long fossil fuels will last, it is clear that current forms of fossil fuels are finite and limited, with a decreasing rate of available or accessible material. This rapid decline of limited resources causes the market price to increase. In fact, the price of crude oil has trebled over the last ten years (International Energy Agency, 2014).

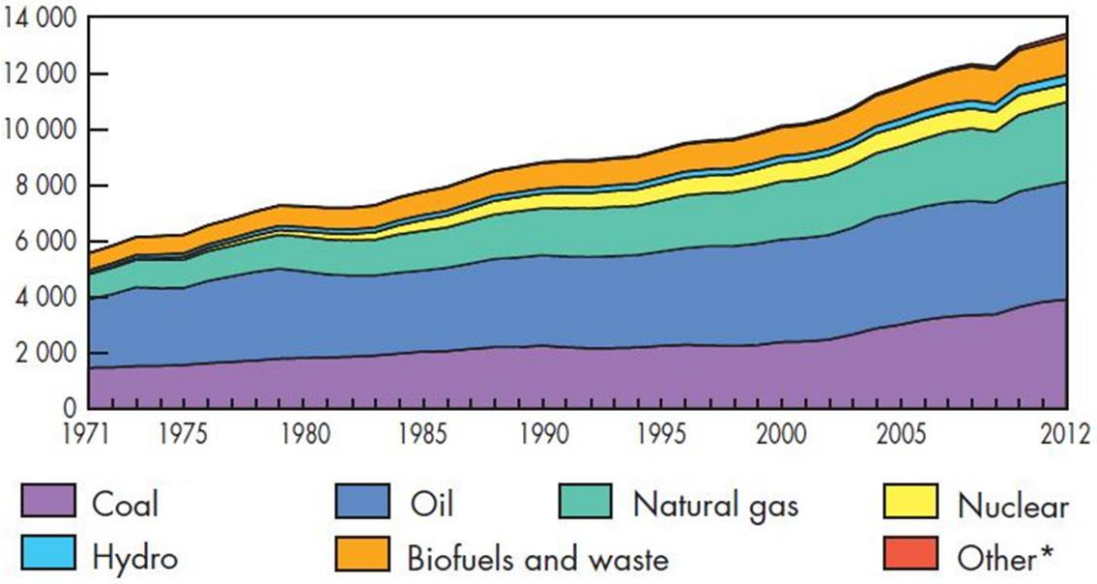

Figure 2.1 World total primary energy supply from 1971 to 2010 by fuel (Mtoe)
*includes geothermal, solar, wind, heat, etc.
(Source: © 2014 Key World Energy Statistics published by International Energy Agency.
Licence: https://www.iea.org/t&c/termsandconditions/)

Another problem of using fossil fuels is that they are high carbon emissions-intensive fuel sources. Using fossil fuels is the primary source of the global carbon emissions (IPCC, 2013). The concentration of atmospheric carbon dioxide has increased by 40 % since pre-industrial times and the global average temperature increased 0.85 degrees during the same period (Figure 2.2, IPCC, 2013).

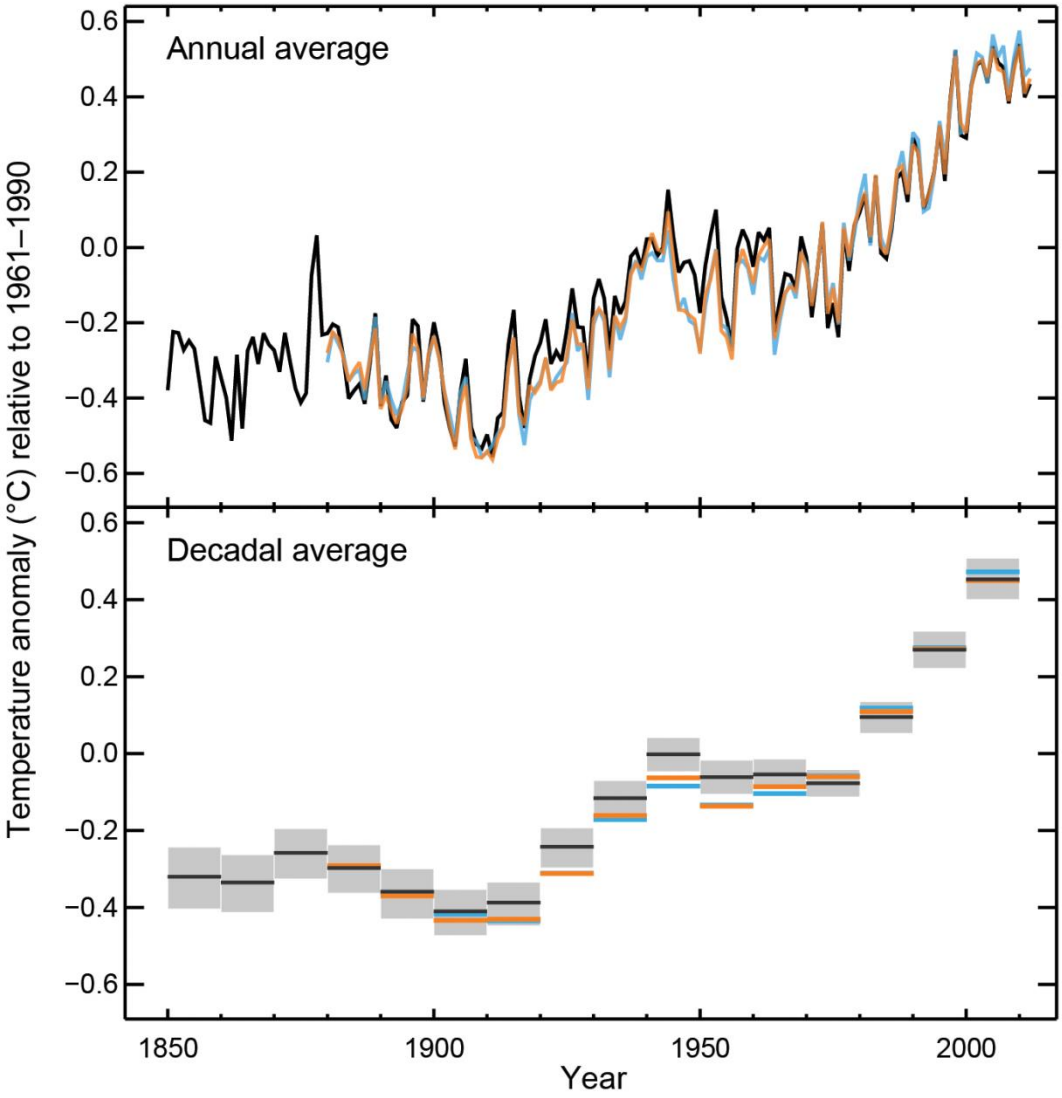

Figure 2.2 Observed globally averaged combined land and ocean surface temperature anomaly 1850-2012
(Source: Summary for Policymakers published by Intergovernmental Panel on Climate Change, 2013, Figure SPM.1(a), p.6)

In order to achieve energy security and tackle climate change, sustainable energy sources are required. Governments worldwide are committed to developing new national energy frameworks, in which renewable energy sources will have to play a central role, moving them onto a more secure, reliable and sustainable energy path.

In May 2011, the UK government committed to reducing carbon emissions by 50 % (from 1990 levels) during the fourth carbon budget period (2023-2027) and generating 15 % of the final energy consumption (calculated on a net calorific basis) from renewable sources by 2020. Although it is constantly increasing, only 5.2 % of the final energy consumption is from renewable sources in the UK at present (Department of Energy & Climate Change, 2014b).

2.1.2. Renewable Energy

Renewable energy is the energy created by sources, which are naturally replenished such as sunlight, rain, wind and tides. Although there is much debate about how to define and distinguish renewable energy from non-renewable, other energy types such as biomass, biofuel and anaerobic digestion are also widely considered as renewable energy. Some of the major renewable energy sources are as follows:

Solar Energy

Theoretically energy from the sun is the most abundant renewable electricity source on the earth and could supply more than enough of the energy the world needs (Lewis & Nocera, 2006; Aman *et al.*, 2015). Although the sun's movements are easily predictable, the possible amount of solar energy gaining highly depends on global location and climatic condition. One of the advantages of this technology is on-site electricity generation. It is flexible in terms of powering scale. For example, photovoltaic cells can be used for powering small

electrical devices such as watches and calculators as well as large grid-connected solar farms. It is also a relatively well-understood technology and low running costs make the technology more attractive. However the solar cell material is high-priced and its environmental impact should not be overlooked.

Wind Power

Wind energy can be converted into electricity (via wind turbines) and mechanical power (via wind mills). Again this is highly dependent on location. The UK has a big merit due to climatic condition. Consequently wind power (onshore and offshore) has been growing fast for the last decade in the UK (Fig. 2.3, Department of Energy & Climate Change, 2014).

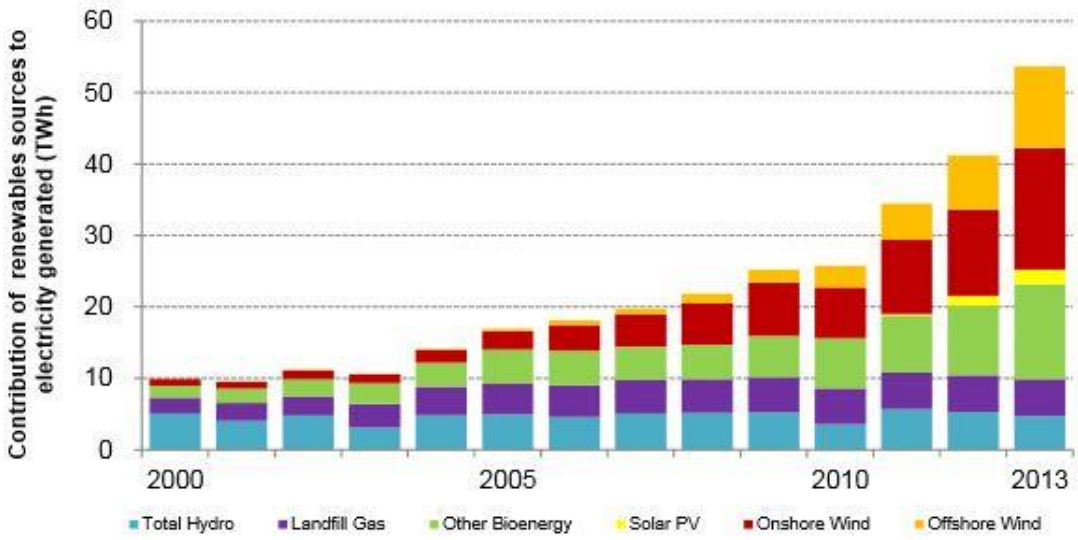

Figure 2.3 Electricity generation of the UK by main renewable source since 2000

* Note: Hydro bar includes shoreline wave/tidal (0.006 TWh in 2013)

(source: Energy Trends: June 2014, special feature articles - Renewable energy in 2013 published by Department of Energy & Climate Change, contains public sector information licensed under the Open Government Licence v3.0.)

Wind power is a readily available resource and does not emit air pollution. Onshore wind farms are relatively cheap to build and remove. Although offshore wind farms produce far more energy than onshore types, it is one of the most expensive ways of generating

electricity per unit due to the logistics of construction, connection and maintenance. Another disadvantage to consider is its impact on wildlife and local ecosystem (Baidya Roy, Pacala & Walko, 2004).

Hydropower

Hydropower is electricity converted from the kinetic energy of flowing water through a turbine. It is one of the oldest forms of electricity generation in the world. Hydropower is the largest renewable energy source and accounts for around 16.5 % of the world's electricity generation (International Renewable Energy Agency, 2012). Compared to other electricity generation facilities of a similar scale, hydropower plants are relatively cheap and easy to maintain. Also, they can be turned on and off as required. The downside of hydropower is its social and environmental cost. Building a power plant usually causes flooding of the nearby area and can bring damage to local ecosystems.

Tidal Power

Tidal power is a kind of hydropower that is converted from the kinetic energy of tides into electricity. It is not widely used as yet, but has attracted much attention recently. Tides can be more easily predicted than solar or wind energy, which enables more stable energy supply as firm power (Sleiti, 2015). However high cost for construction needs to be improved to make the technology cost-compatible on the global energy market.

Biomass

Biomass refers to organic material originated from living organisms. Broadly speaking, this can include organic matter of all kinds; plants, animals or waste from organic sources. It is one of the most plentiful and well-utilised sources of renewable energy on the planet. Biomass is considered to be a renewable energy source, because the organic carbon contained within it, is oxidised and released back into the atmosphere, but is only equivalent

to that which was captured by photosynthesis in the first place, and that which the biomass is bound to release as part of its natural cycle of food chains and respiration. It is therefore part of the planet's immediate carbon cycle, rather than being part of the geologic fossil fuel cycles. However, a cautious and considerate approach is needed for achieving truly sustainable biomass, although the types of biomass and range of technology for its use are very wide.

One of the biggest concerns surrounding biomass controversy is deforestation resulted from biomass production (plants in particular). This has been an on-going issue especially in the Developing World. Soil erosion, loss of biodiversity, increasing consumption of water and fertiliser can also be brought about by biomass production. Diverting the land use from food crops to biofuels may lead to an increase in food prices and hunger (International Energy Agency, 2010). The life-cycle greenhouse-gas emissions of biomass are again unclear. In 2010, the Manomet study reported that in the case of generating electricity in utility-scale plants, net carbon emissions are higher from biomass than fossil fuels, even taking forest regrowth into consideration (Manomet Center for Conservation Sciences, 2010). The study claimed that the net carbon emissions after 40 years, are higher from biomass than coal for generating electricity since more CO_2 is released than would be released if the equivalent coal, oil or natural gas was burnt. A recent study (Röder, Whittaker & Thornley, 2015) also pointed that greenhouse-gas emissions from bioenergy of forest residues can be worse than coal when considering the whole supply chain stages.

2.1.3. Energy from Waste

Despite of the multilateral efforts for improving the World's energy problems, it is quite clear that there is no 'panacea' or 'one perfect solution'. As discussed earlier, all the available renewable energy sources have their own limitations. Nevertheless these efforts should not be stopped and more technological innovations through research and innovation need to be achieved.

Although the term is often subjective, it is generally accepted that waste implies unwanted or unusable material that needs to be disposed of. However with the advancement of technology, waste can sometimes become a source of energy. Energy from waste is a very attractive option. The useable form of energy from waste can include electricity and heat. This approach is about reducing or recovering some of the energy that is spent in running the system; for example the energy cost of waste treatment and mass transfer. The most common way of implementation is incineration of waste. For the last few decades, the efficiency and unwanted emission of gases have been considerably improved for these treatments. But this approach is only suitable if the waste material is sufficiently dry; energy cannot be gained without additional energy input unless the water content of waste is below about 30 % (McCarty, Bae & Kim, 2011). Thus different approaches are required for recovering energy from 'wet waste' such as wastewater.

Over 10 billion litres of wastewater are produced on a daily basis, at domestic and industrial levels, in England and Wales. It takes approximately 6.34 GWh of energy per day to treat this volume of sewage, which accounts for almost 1 % of the daily electricity consumption in the country (Parliamentary Office of Science and Technology, 2007). Wastewater contains energy, in the form of biodegradable organic matter. According to Heidrich et al. (2011), the internal chemical energy contained in UK domestic wastewater is 7.6 kJ/L.

In this respect, microbial fuel cells (MFCs) that generate electricity by the break-down of organic matter (e.g. wastewater) have a great potential for the future energy and environmental challenges. MFCs are often compared with anaerobic digestion, which also uses microbial activity for breaking down organic matter in the absence of oxygen. Unlike anaerobic digestion, which is relatively well understood and already widely used in municipal wastewater treatment plants, MFCs have received far less attention and funding, hence the technology is still at laboratory level in its development. For example, a conventional anaerobic digestion reactor allows 1 kg of COD (chemical oxygen demand) to be converted to an energy amount of roughly 1 kWh. In the case of MFCs, only few studies have reported power generation exceeding this level, although 1 kg of COD can theoretically be converted to 4 kWh (Ge *et al.*, 2014). Yet MFCs have their own merits compared to anaerobic digestion. Firstly, MFCs generate electricity directly from organic matter, whereas anaerobic digestion produces biogas consisting of methane, carbon dioxide and other gases, which means that additional processes such as gas separation, purification and combustion are required in order to get usable forms of energy. Also this biogas is difficult to store, in addition to the fact that it contributes significantly to greenhouse gas emissions, when there are leakages. Secondly, MFCs can be operated at ambient temperature or even below 20 °C, and at low substrate concentration levels (Cheng, Xing & Logan, 2011; Catal *et al.*, 2011; Gil *et al.*, 2003; Pant *et al.*, 2010). Anaerobic digestion, on the other hand, is quite sensitive to both parameters as it requires high temperature and high substrate concentration (Verstraete *et al.*, 2005). Considering all these aspects, MFC and anaerobic digestion technologies do not seem to be competitive, rather both can be complementary to each other.

2.2. Microbial Fuel Cells

Technically microbial fuel cells are one of several types of fuel cell. Fuel cells are defined as electrochemical devices that continuously convert fuels directly to electrical energy, as long as reactants are supplied to their electrodes (Larminie & Dicks, 2003). In this way, fuel cells are distinguished from batteries, which stop producing electricity once the stored chemical reactants run out. For this reason, in earlier days, the same components used in conventional fuel cells were often employed in MFC studies.

Most fuel cells are powered by hydrogen, which can be fed to the fuel cell system directly or can be generated within the fuel cell system by reforming hydrogen-rich fuels such as gasoline, methane, propane, diesel, methanol and ethanol. This is one of the major drawbacks in the hydrogen technology. In order to get hydrogen, a reforming process is necessary because hydrogen in its raw form can be impure and difficult to store. For example, today's global hydrogen production is 48 % from natural gas, 30 % from oil, and 18 % from coal; water electrolysis accounts for only 4 % (World Nuclear Association, 2014). This reforming process is energy intensive and results in a considerable quantity of carbon dioxide emissions (each tonne of hydrogen produced gives rise to 11 tonnes of CO_2) (World Nuclear Association, 2014). Moreover pure hydrogen gas must be pressurised or liquefied to be used. Therefore hydrogen storage is again another energy consuming process.

On the other hand, MFCs can utilise a wide range of fuels as long as they contain organic matter, and this flexibility of fuel is one advantage that makes MFCs stand out. In theory, organic waste can be abundant, since organic detritus includes all human, animal and plant wastes, estuarine sediments, algal blooms, compost, sludge, leaf-litter, macro-algae, and floodwater.

The history of MFC began with the discovery of the link between electricity and metabolic processes of living organisms. In 1791, Luigi Galvani applied current to dead frog

legs and observed the legs twitching. From this work, he realised that biological reactions and electric current are closely related. This is one of the first attempts into the study of bioelectricity or animal electricity as it was named at the time (Piccolino, 1998). In 1911, Potter published the earliest MFC report on the ability of microorganisms to transform organic substrates (chemical energy) into electricity (Potter, 1911). He demonstrated the production of electrical energy from living cultures of either *Escherichia coli* or *Saccharomyces*. This was the first MFC proving that biological process produces bioelectricity (Bullen *et al.*, 2006; Shukla *et al.*, 2004). However this first discovery was nearly forgotten until 1931 when Cohen showed that a batch-biological fuel cell could produce more than 35 V (Cohen, 1931). In the 1960s, the USA NASA space programme showed interest in biological fuel cell technology since it could convert organic waste in space ships into electrical power (Putnam, 1971). Thanks to this, this technology drew some attention for a time, but it was soon replaced by other energy sources such as photovoltaic panels (Bullen *et al.*, 2006; Davis & Higson, 2007).

In 1976, Rao identified a clear principle of the biological fuel cell (Rao *et al.*, 1976). In the 1980s, H. Peter Bennetto succeeded in extracting electric power from MFCs by employing pure cultures to catalyse the oxidation of organics and utilising artificial electron mediators to facilitate electron transfer in the anode (Bennetto *et al.*, 1983; Roller *et al.*, 1984; Bennetto *et al.*, 1985). Habermann and Pommer (1991) demonstrated that additional exogenous mediators are not necessary for MFCs to generate electricity, since microorganisms could naturally produce such electron shuttle substances; this was also the first report of long-term wastewater utilisation using MFCs. Since then, rapid advances have been made in MFC research.

However MFC technology is still in its infancy due to the relatively short and interrupted development period. Unlike some conventional inorganic fuel cells that have already reached

an advanced state in their development, only very few MFC systems with reactor volumes bigger than 1L have been tested (The New York Times, 2007; Oxfam, 2015).

MFCs nevertheless possess a great potential to bring about innovation and become true alternatives to fossil fuel energy generation. In the early 2000s, two robots, Chew-Chew and EcoBot I, both powered by MFCs were developed (Wilkinson, 2000; Ieropoulos, Greenman & Melhuish, 2003). Biochemical oxygen demand (BOD) measuring sensors using MFCs are commercially available (HABS2000, KORBI) and benthic MFCs as on-site power sources for sensors and acoustic communication devices have also been reported (Reimers *et al.*, 2006). Recently a stack of 24 MFCs successfully charged a commercially available mobile phone directly (Ieropoulos *et al.*, 2013).

2.2.1. Principle of MFC Electricity Generation

MFCs are devices that convert chemical energy of feedstock into electricity through the metabolic activity of microorganisms. MFCs usually consist of two compartments; an anode and a cathode separated by an ion-permeable material. In the anode, microorganisms oxidise organic matter (fuel) and release CO_2, electrons and protons. Electrons produced in the anode flow to the cathode via an external circuit as the result of electrophilic attraction from the cathode electrode, whilst protons migrate from the anode to the cathode through the separator between the two compartments. The electrons and protons subsequently combine with oxygen (final electron acceptor) and this reduction reaction completes the circuit (Figure 2.4) (Li *et al.*, 2008; Chae *et al.*, 2008). The quantity of electrons flowing through the external circuit is the electricity being produced i.e. current.

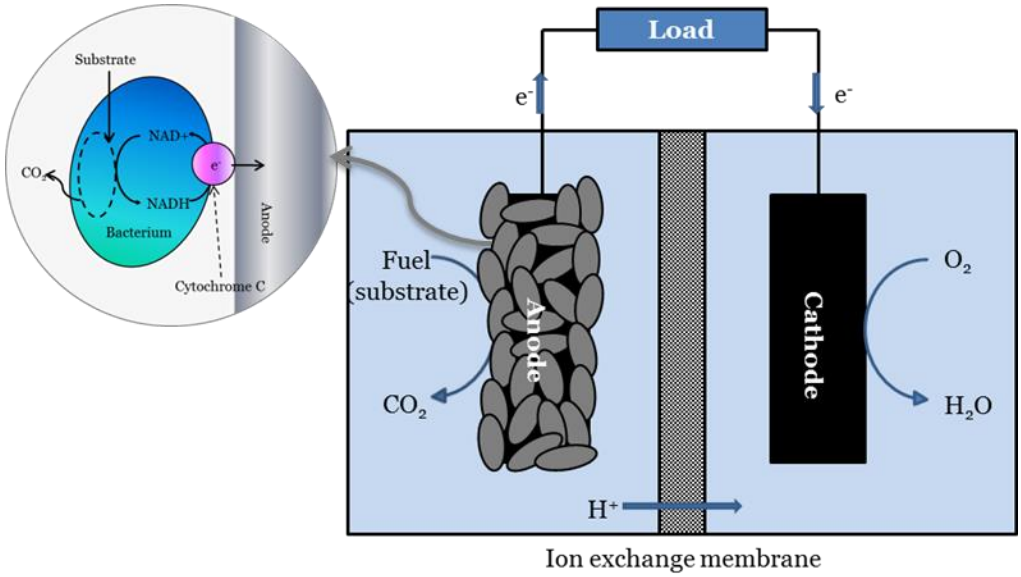

Figure 2.4 Schematic diagram of a microbial fuel cell

Other chemicals such as nitrate or sulphate can also serve as electron acceptors. Table 2.1 shows some exemplar electron donors and acceptors and their reactions on either anodes or cathodes.

Table 2.1 Electron donors and acceptors of MFCs

Electrode	Electron donor/acceptor	Reaction
Anode	Acetate	$C_2H_3O_2^- + 4H_2O \rightarrow 2HCO_3^{--} + 9H^+ + 8e^-$
	Glucose	$C_6H_{12}O_6 + H_2O \rightarrow 6CO_2 + 24H^+ + 24e^-$
	Butyrate	$C_4H_8O_2 + 2H_2O \rightarrow 2C_2H_4O_2 + 4H^+ + 4e^-$
	Glycerol	$C_3H_8O_3 + 6H_2O \rightarrow 3HCO_3^- + 17H^+ + 14e^-$
	Malate	$C_4H_5O_5^- + 7H_2O \rightarrow 4H_2CO_3 + 11H^+ + 12e^-$
	Citrate	$C_6H_5O_7^{3-} + 11H_2O \rightarrow 6H_2CO_3 + 15H^+ + 18e^-$
	Sulphide	$HS^- \rightarrow S^0 + H^+ + 2e^-$
Cathode	Oxygen	$O_2 + 4e^- + 4H^+ \rightarrow 2H_2O$
	Nitrate	$2NO_3^- + 12H^+ + 10e^- \rightarrow N_2 + 6H_2O$
	Nitrite	$NO_2^- + 2e^- + 2\,H^+ \rightarrow N_2 + H_2O$
	Permanganate	$MnO_4^- + 4\,H^+ + 3\,e^- \rightarrow MnO_2 + 2\,H_2O$
	Manganese dioxide	$MnO_2 + H^+ + e^- \rightarrow MnOOH(s)$
	Iron (III)	$Fe^{3+} + e^- \rightarrow Fe^{2+}$
	Copper (II)	$4\,Cu^{2+} + 8\,e^- \rightarrow 4\,Cu(s)$
	Potassium persulfate	$S_2O_8^{2-} + 2e^- \rightarrow 2SO_4^{2-}$
	Ferricyanide	$Fe(CN)_6^{3-} + e^- \rightarrow Fe(CN)_6^{4-}$

2.2.2. Components and Materials

Anode

Various materials have been investigated for MFC anodes in order to improve performance in terms of power output, durability and easier operation. Good anode materials are required to have large surface area for bacterial attachment and high electrical conductivity for the charge transfer, as well as good current collection capability. Since the anodes become biotic, they should be non-toxic to microorganisms, as well as inert to biochemical reactions. In order to prevent or minimise fouling, the structure of anodes needs

to be carefully chosen. Also they should be robust for long-term operation and economical, in terms of cost of production.

Carbon based materials such as carbon cloth (Li *et al.*, 2010; Santoro *et al.*, 2011), carbon fibre veil (Ieropoulos, Greenman & Melhuish, 2010; Winfield *et al.*, 2011), graphite felt (Biffinger *et al.*, 2007b; Aelterman *et al.*, 2008) and graphite granules (Aelterman *et al.*, 2006a; Jiang & Li, 2009; Deeke *et al.*, 2015) are the most commonly used materials in MFCs due to their chemical inertness, bio-fouling resistance, high conductivity, high surface area and relatively low cost. One of the limitations of these carbon based materials is clogging pores or spaces due to biofilm growth in systems running under poor fluid dynamics, which leads to anode electrocatalytic efficiency deterioration. Furthermore high background currents of carbon materials were pointed out, which makes in depth study of anodophilic biofilms difficult (Babauta *et al.*, 2012).

Metals such as gold (Crittenden, Sund & Sumner, 2006; Richter *et al.*, 2008), titanium (ter Heijne *et al.*, 2008) and stainless steel (Pocaznoi *et al.*, 2012) have been also employed for MFC anodes due to their excellent conductivity. Although some of these metal electrodes showed performance enhancement after surface modification, in order to improve the relatively small surface area and to introduce adhesive surfaces for bacterial attachment, when considering scale-up for waste/wastewater treatment, most of them seemed unsuitable as MFC anode due to the high cost, poor bacterial attachment or high risk of corrosion. Therefore physical or chemical surface modification seems indispensable for metal anodes.

Some researchers have tried metal-carbon composite anodes (Park & Zeikus, 2002, 2003; Lowy *et al.*, 2006; Lowy & Tender, 2008; Zhang *et al.*, 2007; Chen *et al.*, 2013). For these type of anodes, metals such as Mn4+, Mn2+, Ni2+, Sb(V) and aluminium-alloy mesh were applied with carbon based materials such as graphite rod, graphite paste and carbon cloth. These attempts showed anode performance improvement. However further studies about cost

evaluations, long-term stability, and understanding the mechanism of bacterial interaction with anode surface are required.

Diverse modifications have been made in order to improve the anode performance. This includes ammonia treatment of anode surface (Cheng & Logan, 2007; Velasquez-Orta, Curtis & Logan, 2009), acid treatment (Scott *et al.*, 2007; Feng *et al.*, 2010) and adding nanostructured materials (Sun *et al.*, 2010; Fan *et al.*, 2011; Xiao *et al.*, 2012). Especially nanostructured materials such as carbon nanotubes (CNTs), graphene (G) seem promising in terms of increasing power output. Coating anode materials with conductive polymers like polyaniline (PANI) or polypyrrole (PPY) also have received much attention due to high conductivity, good redox properties, environmental stability and relatively straightforward synthesis.

In order to enhance the anode performance, anode modification is thought to be an effective strategy. For waste/wastewater clean-up, however, long-term stability is an essential requirement thus more attention needs to be given in this aspect. An increasing risk for fouling due to biofilm growth in the anode structure also needs to be considered.

Cathode

In earlier years, MFC research mainly focused on the anode, because it was a unique feature that makes MFCs different to other conventional fuel cells. When considering the overall process, however, the cathode reaction is one of the major limiting factors of the MFC technology and in-depth research on the cathode side needs to be carried out, since different approaches to the MFC cathodes is required compared to other types of fuel cells, running at high temperatures and relatively rapid reaction rates. Recent work has started to focus more on the cathode but still most studies use expensive catalysts or unsustainable electrolytes (Lu & Li, 2012). Platinum is the most commonly used catalyst for oxygen reduction in the cathode due to its satisfactory catalytic ability (Liu & Logan, 2004; Oh, Min

& Logan, 2004; Pham *et al.*, 2004). Adding platinum, however, brings high costs for the system build-up. Ferricyanide ($Fe(CN)_6^{3-}$) is a very reliable laboratory standard, with a good performance, however it is limited because of its environmental toxicity to other living systems and frequent need for replenishment after consumption.

Recently, some researchers turned their attention to bio-cathodes and suggested several possible advantages of using such systems instead of abiotic half-cells (Aldrovandi *et al.*, 2009; Mao *et al.*, 2010). This may reduce the cost for system set-up and operation by eliminating the use of expensive catalysts. In addition, MFCs with bio-cathodes become more sustainable as there is no need for catalyst replenishment/replacement. Aelterman et al. (2006b) demonstrated the microbial reduction of Fe(III) and Mn(IV), which can take the role of terminal electron acceptors in the cathode, as an alternative method of extracting those metals from minerals. Rabaey and Keller (2008) showed current increases by growing a biofilm onto a cathode in comparison to a non-catalysed control and Gajda et al. (2013) achieved improvement of power generation using photosynthetic cathodes consisting of phototrophic organisms.

Another approach to resolve the catalyst problem is to increase the size of the cathode in proportion to the anode (Freguia *et al.*, 2007; Nevin *et al.*, 2008). Zuo et al. (2007) showed power output improvement with higher surface area of the cathode, but this change resulted in a constant volumetric power density since the volume of the cathodic chamber was required to be increased in order to accommodate for the larger cathodes. Removing the cathodic chamber can be a good option to avoid this kind of problem. Hence single chamber MFCs with open to air cathodes (i.e. R-MFC (B) and C-MFC described in section 3.2.1) have been widely used (Wei, Liang & Huang, 2011; El-Chakhtoura *et al.*, 2014; Gnana Kumar *et al.*, 2014; Papaharalabos *et al.*, 2014a; Chen *et al.*, 2015). Compared to aqueous cathodes, which are submerged in the cathodic chambers, open to air cathodes seem to be a

more attractive option for practical applications with better performance and no need for active aeration.

Cathode surface modification for higher surface area (Wang *et al.*, 2011) or catalytic efficiency (Duteanu *et al.*, 2010; Wang *et al.*, 2014) has been studied actively in the recent years. Non-Pt cathodes have been investigated to reduce the cathode material cost but still to enhance the ORR kinetics. Low-cost nonprecious metals and metal oxides such as cobalt, manganese dioxide, cobalt-tetramethylphenylporphyrin, pyrolyzed-Fe(II) phthalocyanine, lead dioxide, metal porphyrins and phthalocyanines have shown good performance comparable to Pt cathodes (Zhao *et al.*, 2005, 2006; Morris *et al.*, 2007; HaoYu *et al.*, 2007; Yu *et al.*, 2008; Lefebvre *et al.*, 2009; Zhang *et al.*, 2009). Nevertheless, the chance of metal discharge from the cathode and sensitivity of metal-based catalysts towards elevated pH values on the cathode should not be overlooked for practical applications of the MFC technology. Santoro et al. (2012) demonstrated platinum free cathodes modified with the addition of a micro porous layer (MPL), which outperformed platinum-based cathodes in a long term study. The same type of electrode was applied as the anode for a part of this work (section 4.2) which was a collaboration between three research groups; Bristol BioEnergy Centre (UK), Center for Clean Energy Engineering (USA) and RSE-Ricerca sul Sistema Energetico S.p.A. (Italy).

Ion exchange membrane (IEM)

The IEM is primarily used to physically separate the anode from the cathode whilst allowing protons to travel through to the cathode. The use of IEMs, however, has its drawbacks. The membrane contributes significantly to the internal resistance of a MFC and delays proton transfer from the anode chamber to the cathode chamber (Gil *et al.*, 2003; Rozendal, Hamelers & Buisman, 2006). In addition, it increases the overall cost of a MFC system. Previous work has shown that single-chamber MFCs without IEMs produce a higher

power density than MFCs with Nafion® membranes, which are the most commonly used IEM in MFCs (Liu & Logan, 2004; Liu, Cheng & Logan, 2005; Yang, Jia & Liu, 2009). However it has also been reported that the lack of IEM would increase oxygen and substrate diffusion, which would result in a reduction of microbial catalytic activity and consequently in a reduction in Coulombic efficiency (Zhang *et al.*, 2010). In this sense, a form of separator in the MFC is necessary (Lefebvre *et al.*, 2011; Li *et al.*, 2011).

Although attempts of using alternative materials to the IEM, (Biffinger *et al.*, 2007b; Venkata Mohan, Veer Raghavulu & Sarma, 2008; Sun *et al.*, 2009; Zhuang *et al.*, 2010a), IEMs are still widely used in MFC research due to their good performance. The most commonly used IEMs in MFCs are cation exchange membranes (CEMs) especially Nafion®. However it has been shown that relatively higher concentration of cation species, other than protons such as, Na^+, K^+, Ca^{2+}, Mg^{2+} and NH_4^+ transfer positive charge through the membrane (Rozendal, Hamelers & Buisman, 2006). Retarded proton transfer leads to pH splitting between the two chambers, and this gives a negative effect on microbial activity in the anode chamber and also reduces the cathode potential (Kim, Chang & Gadd, 2007; Torres, Kato Marcus & Rittmann, 2008; Harnisch, Schröder & Scholz, 2008). Anion exchange membranes (AEMs) have also been tested in MFCs and several studies have reported better performance compared to CEMs (Kim *et al.*, 2007; Mo *et al.*, 2009) because of the pH splitting problem of CEMs.

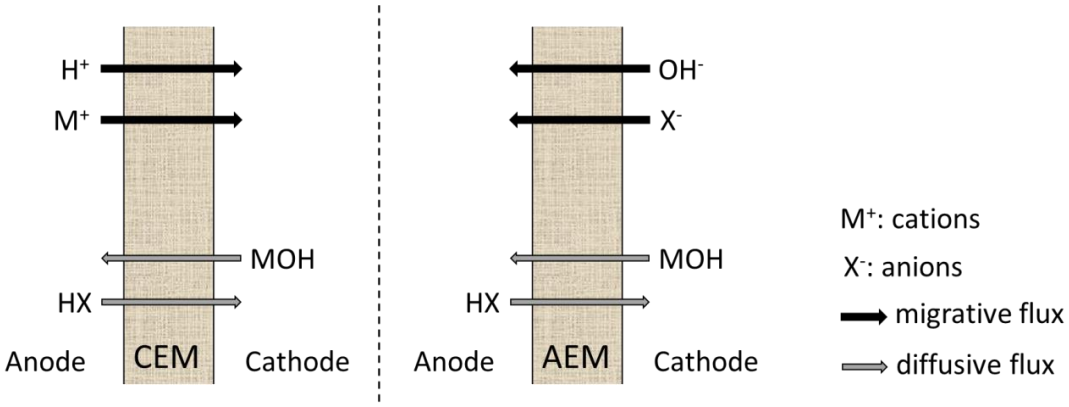

Figure 2.5 Schematic of ion and mass transfer across CEMs (left) and AEMs (right)
*Adapted from Harnisch *et al.*, 2009. Used with permission of Elsevier.

An ion exchange membrane either CEM or AEM is one of the largest costs for building an MFC. Recently relatively low cost material such as earthenware or terracotta has been tried as a separator (Jana, Behera & Ghangrekar, 2010; Winfield *et al.*, 2013). This is noteworthy since it would be convenient in developing countries where the material is readily available as well as reducing the building cost. Optimizing the IEM or seeking alternative separators depending on the final applications is one of the issues that need to be addressed for the benefit of the MFC technology.

2.2.3. Reactor Design

The MFC reactor should be designed accordingly depending on the end application. The H-type MFCs are probably the oldest design and still used widely. In an H-type MFC, the anode and the cathode are located in two separated chambers divided by a separator, and there is usually a longer distance involved between the anode/cathode electrodes and the membrane itself. H-type MFCs are useful for gas analysis due to the air-tight glass structure, but they usually suffer from high internal resistance due to the relatively bulky reactor volume which is prone to mass transfer losses.

Double-chamber cubic shaped MFCs have also been used, since the 1980's, following the design from Bennetto's (Bennetto, 1990). The design allows two electrodes located close to each other thus reducing the internal resistance (R_{INT}). A single-chamber cubic MFC is a modified design of the double-chamber cubic MFC, whereby the cathode is no longer submerged in liquid (catholyte) such as ferricyanide or aerated water, but is directly exposed to the air. Besides design simplicity, operational cost reduction and performance improvement are expected from single-chamber cubic MFCs.

In addition to the cubic (analytical) type, cylindrical or tubular shaped MFCs have also been tested. In these designs, the open-to-air cathode is wrapped around a central anode chamber (Kim *et al.*, 2009) or inversely the anode is wrapped around a central cathode part, where the cathode is exposed to air (Gajda *et al.*, 2015). The anode or cathode is not necessarily directly wrapped around the other. In this case, the cathode is placed in a cathode part like a single-chamber cubic MFC but the cylindrical shape of an anodic chamber helps the even distribution of feedstock by minimising dead space (You *et al.*, 2014).

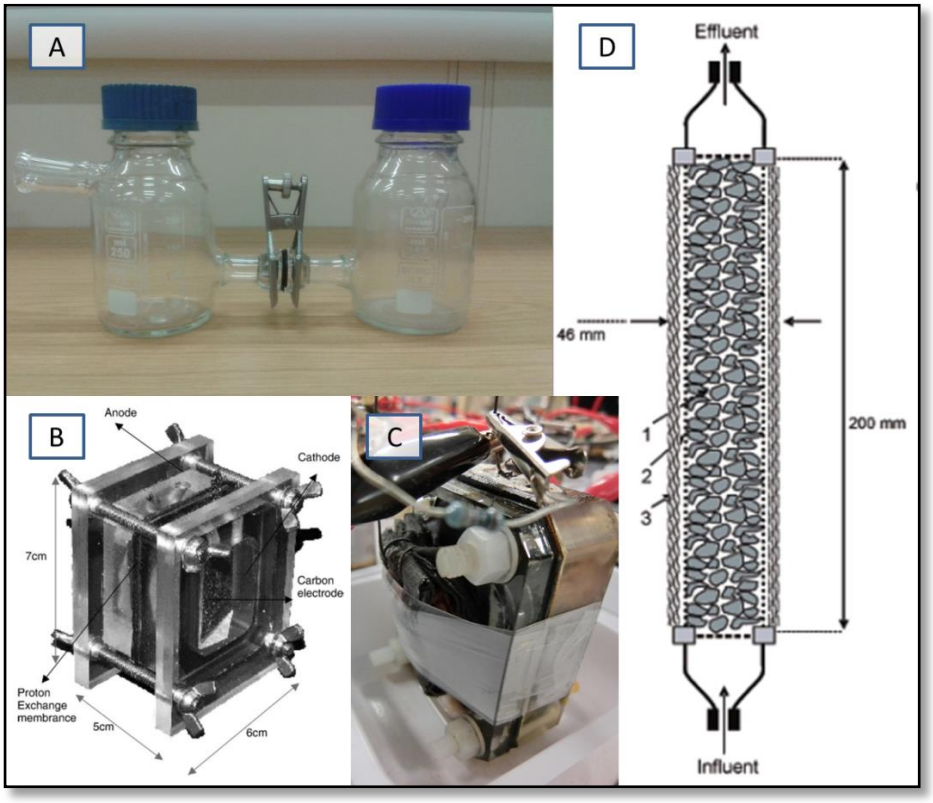

Figure 2.6 MFC reactor designs; H-type (A), double-chamber cubic shaped MFC (B)*, single-chamber cubic MFC (C), tubular shaped MFC (D)**

Adapted from * Ieropoulos *et al.*, 2005, ** Rabaey *et al.*, 2005.
Used with permission of * Elsevier, ** American Chemical Society.

2.2.4. Key Parameters Analysing the MFC Performance

In general, there are two main aspects when considering the performance of an MFC; the amount of power it can produce and how efficiently it is able to treat/utilise a given feedstock. Although measuring power output of an MFC is straightforward, reporting data to the research community is not simple and often causes confusion to readers. Due to the variation of MFC compartment materials, reactor designs and operation conditions adopted by researchers, there is a need for universally acceptable standard parameters. For example, power density is commonly used as a means of projecting the power output capability of an MFC, at larger scale. However it can be normalised by many different factors such as total size of anode or membrane or cathode, projected size of anode or cathode (Ieropoulos *et al.*,

2005; Oh & Logan, 2006; Logan *et al.*, 2006; Ieropoulos, Greenman & Melhuish, 2013). Sometimes power density is also expressed in terms of anodic, cathodic and liquid volume (Liu, Cheng & Logan, 2005; Aelterman *et al.*, 2006b; Biffinger *et al.*, 2007a; Ishii *et al.*, 2008; Capodaglio *et al.*, 2013; You *et al.*, 2015). Although many MFC researchers agree with the need for the same standard in this aspect, choosing a universally agreed uniform parameter has not been established yet. Reporting data in various parameters without presenting full information of reactor and component dimension makes it difficult to evaluate power performance of different systems and may lead to overestimation. Therefore absolute power values in addition to power density values, normalised by the total anodic volume or anode surface area (as in original size of an anode sheet before being folded or cut in square metres), are reported throughout this thesis.

Table 2.2 summarises the commonly used parameters for evaluating the MFC performance.

Table 2.2 Key parameters evaluating the MFC performance

Parameter	Unit	Calculation/measurement
Electrode potential	V	Measured between an electrode and a reference electrode
Open circuit voltage	V	OCV($V_{O/C}$), voltage at infinite resistance
Voltage	V	Measured between two ends under the applied external resistance (R_{EXT})
Current	A	$I = V/R$ R is the loaded external resistance value in ohms (Ω).
Power	W	$P = IV$ The maximum power (P_{MAX}) is calculated from the polarisation curve.
Current density	A/m^2, A/m^3	$j = I/A$, $j = I/V$ A is total/projected anode/cathode surface area in square metres (m^2) and V is the total reactor/anodic chamber/ cathodic chamber volume in cubic metre (m^3).

Power density	W/m^2, W/m^3	$P_D = P/A$, $P_D = P/V$ A and V are the same as above.
Coulombic efficiency	%	(for batch feed system) $$CE_{batch} = \frac{M \int_0^t I_{dt}}{FnV_{anodic}\Delta COD}$$ M is the molecular weight of oxygen (32), F is Faraday's constant, n is the number of electrons exchanged per mole of oxygen, V_{anodic} is the volume of liquid in the anodic chamber, and ΔCOD is the change in COD over time t. (for continuous feed system) $$CE_{cont} = \frac{MI}{FbQ\Delta COD}$$ This is on the basis of current generated under steady condition. Q is the volumetric influent flow rate and ΔCOD is the difference in the influent and effluent COD.
Internal resistance	Ω	(from polarisation curve) $P_{MAX} = V_{O/C}^2 R_{EXT}/(R_{INT} + R_{EXT})^2$ Or $R_{INT} = (V_{O/C}/I_L) - R_{EXT}$ I_L is the current under a load and R_{EXT} is the value of the applied resistance
Treatment efficiency	%	$\eta = \Delta C/C \times 100\%$ ΔC is removed substrate and C is the total substrate fed, this can be measured in BOD, COD (chemical oxygen demand) or TOC (total organic carbon).
Organic loading rate	$kg/m^3/day$	$OLR = COD \times V_{reactor}/V_{anodic}$ $V_{reactor}$ is the reactor volume.
Organic removal rate	$kg/m^3/day$	$ORR = \Delta COD \times V_{reactor}/V_{anodic}$
Hydraulic retention time	hour	$HRT = V_{anodic}/V_{reactor}$

2.2.5. Practical Applications and Scale-up

Potential applications of the MFC technology primarily include electricity generation, wastewater treatment, hydrogen production and bio-sensing (Greenman *et al.*, 2009; Ieropoulos, Greenman & Melhuish, 2012; Kim *et al.*, 2010; Liu *et al.*, 2010a; Kim *et al.*, 2003). Further developments may involve pollution treatment and resource recovery (Huang *et al.*, 2011; You *et al.*, 2015). Although further work is required in order to fully commercialise the technology, there have at least been some successful examples of practical applications.

For generating reasonable levels of electricity to power electrical applications, storing the electricity in rechargeable devices seems essential since it would be unrealistic to expect a high power density from a single MFC regardless of its volume (Ieropoulos, Greenman & Melhuish, 2003). The biologically inspired robot, EcoBot series have demonstrated this approach (Ieropoulos *et al.*, 2010; Papaharalabos *et al.*, 2014b). Benthic MFCs as a power source for remote sensing have shown their potential through running an experiment *in situ* (Tender *et al.*, 2002).

When aiming for wastewater treatment, scale-up is vital to treat a large volume of wastewater. For scale-up, two distinct approaches have been suggested. The first is to increase the size of an individual MFC as can be seen in the attempt made at Foster's brewery in Queensland, by the University of Queensland Australia. The second is to build a multitude of small MFCs and connect them electrically. In the case of the second approach, the output of an MFC system is amplified by the number of MFC units employed, similar to how batteries can be connected together. Increasing the size of MFC reactors leads to increases in R_{INT} (Clauwaert *et al.*, 2008; Ieropoulos, I., Greenman, J., Melhuish, 2008). Furthermore there would be a large volume of fluid in the anodic chamber that is not in contact with the anode electrode unless the anode is large enough to fill the whole chamber. Another aspect to consider for wastewater treatment application is the continuity of the

operation. For treating large volumes, continuous flow is more favourable. The approach that was taken in this thesis, therefore, is running multiple small-sized MFCs under continuous flow and this will be demonstrated in section 6.4.

2.3. Biological Aspect of MFC Anodes

Unlike chemical fuel cells, MFC anodes are 'bio-electrodes' consisting of living microorganisms on conductive solid material. The biological nature of MFCs makes the technology novel and there can be no doubt about the importance of understanding the MFC anode in order to put the technology to practical use. In this section, therefore the biological aspects of the MFC anodes will be discussed.

2.3.1. Anodophilic Microorganisms

Many microorganisms are capable of transferring the electrons derived from the metabolism of organic matter to the anode (Ieropoulos *et al.*, 2005; Niessen *et al.*, 2004; Zhang *et al.*, 2006). The electrochemical potential difference between the anode (NAD^+/NADH; E_0 = -0.32 V) and the electron acceptor at the cathode (e.g. $Fe(CN)_6^{3-}$ /$Fe(CN)_6^{4-}$; E_0 = +0.43 V or O_2/H_2O; E_0 = +0.82 V), enables the electrons to flow to the cathode (Logan & Regan, 2006).

The electron transfer mechanism in MFCs has been the subject of many studies that have been carried out in order to understand it better. It is generally accepted that two types of mechanisms exist; mediated electron transfer (MET) and direct electron transfer (DET).

In the earlier years of the MFC research, synthetic exogenous mediators such as thionine, quinone, Fe(III) ethylenediamineteraacetic acid (EDTA), methylene blue and neutral red were considered to be common practice for producing reasonable amounts of power from

MFCs (Kondo & Ikeda, 1999; Kim *et al.*, 2000; Lee *et al.*, 2002). Although these artificial mediators enhance power generation, their inherent toxicity, short half-life and instability limit their use in MFCs. Later it was found that some bacterial species are capable of self-mediating extracellular electron transfer directly to the anode (Habermann & Pommer, 1991; Kim *et al.*, 1999; Chaudhuri & Lovley, 2003). Without the addition of an artificial mediator, the electron transfer can be achieved through the use of natural mediators produced by the bacterium. For example, *Pseudomonas aeruginosa* produces phenazines that behave as mediators transferring electrons from within the bacterial cell to the anode. Following electrocatalytic oxidation of fuel at the electrodes, these molecules are recycled and used again (Rabaey *et al.*, 2004, 2005). The biosynthesis pathway of phenazines has been widely studied as well as the mechanism of electron transfer to phenazines (Mavrodi *et al.*, 2001; Price-Whelan, Dietrich & Newman, 2006; Watanabe *et al.*, 2009; Abbas & Sibirny, 2011). Since phenazines have a very similar basal molecular structure like other mediators such as neural red, anthraquinone-2,6-disulfonate (AQDS) and flavins, it is thought that electron transport to these mediators have the same mechanism which involves enzymatic reduction in the periplasmic space. These metabolites can also be utilised by other bacteria that would not otherwise be capable of electricity production (Pham *et al.*, 2008).

The second mechanism takes places via a physical contact of the bacterium cell with the fuel cell anode. Since microbial cells are generally thought to be non-conductive by nature, because cell membranes mostly consist of non-conductive materials such as polysaccharides, lipids and peptidoglycans, this type of mechanism has long been considered impossible. However DET can proceed via membrane bound electron transport proteins (c-type cytochromes). c-type cytochromes are redox proteins containing one or more heme groups, which mediate the respirational electron transport in many organisms. For the microbial DET, usually multi-heme c-type cytochromes located in the bacterial membranes are used (Shi *et al.*, 2007). Although the exact configurations of this electron transport chain for various

electrophilic bacteria remain unknown, for this type of mechanism, it was assumed that only bacteria in the first monolayer on the anode surface were electrochemically active, but DET is not limited to short-range interactions as it is also possible by using conductive pili (nanowires) or conductive biofilm matrices containing cytochromes (Lovley, 2006; Rabaey *et al.*, 2007; Schröder, 2007; Zhou *et al.*, 2013). Some species such as *Geobacter sulfurreducens* (Bond & Lovley, 2003), *Rhodoferex ferrireducens* (Chaudhuri & Lovley, 2003) and *Shewanella oneidensis* (Gorby *et al.*, 2006) have demonstrated DET.

There has been much discussion about power output of pure cultures compared with mixed bacterial cultures in the anode chamber. For example, Ishii et al. (2008) reported mixed culture derived from sewage sludge produced 22 % more power than a pure culture of *Geobacter sulfurreducens* in a single-chamber MFC with an air cathode. Whereas another study argued that *Geobacter sulfurreducens* produced more power than an enriched consortium in a dual-chamber MFC with ferricyanide catholyte (Nevin *et al.*, 2008). Direct comparison of power generation between mixed and pure cultures has been difficult since different systems have different limitations. It was also found that many bacteria enriched from an MFC could not be grown as pure cultures, and this is likely due to various interactions and interdependencies occurring in the original mixed cultures (Kim *et al.*, 2004; Parameswaran *et al.*, 2009).

Regardless of power output, pure culture studies could be a very useful tool to get a better understanding of the electricity production mechanisms and to seek strategies for optimising the process. However when dealing with waste or wastewater, a pure culture is not suitable as it will be limited in the range of utilisable substrates that it could consume, thus will have a lower metabolic diversity in comparison with having a mixed culture. For example, *Geobacter sulfurreducens* cannot use many carbon sources apart from simple short-chain organic acids such as acetate (Chaudhuri & Lovley, 2003). Moreover the nature of waste/wastewater can be a harsh environment for some pure cultures. For the current

thesis, although some work with pure cultures has been carried out, for reasons mentioned above, the main part of the work was carried out using mixed bacterial communities.

2.3.2. Anodic Biofilms

A biofilm is a group of either pure or mixed surface-associated microorganisms that is embedded within a self-produced matrix structure of extracellular polymeric substance (EPS) (Donlan, 2002). Biofilm EPS is generally composed of DNA, proteins and polysaccharides (Allesen-Holm *et al.*, 2006). Biofilms are permeable, thus allowing diffusion of substrates and metabolic products. The EPS matrix of anodic biofilms also acts as a conductive pathway that facilitates electron transfer from outer cells to the electrode surface (Torres, Kato Marcus & Rittmann, 2008). The microbial communities within a biofilm are a complex of many different individual species and they coexist through competition, communication and cooperation (Matz, 2011). Anodic biofilms consisting of mixed cultures contain anodophiles but may also hold non-anodophiles. Non-anodophiles in anodic biofilms could help anodophiles by breaking down complex substrates or secreting mediators that help anodophiles perform better.

The MFC anode chamber supports the growth of biofilm and planktonic microorganisms. While planktonic microorganisms can only perform MET, biofilm-forming microorganisms can do both MET and DET. Although planktonic cells have shown their contribution to electricity generation in fed-batch systems (Rabaey *et al.*, 2004; Bond & Lovley, 2005), anodic biofilms are key for increasing the MFC power producing performance in wastewater treatment applications that require continuous flow operation.

Anode biofilms are dynamic systems that can change their metabolic, physiological as well as ecological states depending on the given conditions. In the case of using mixed cultures for waste/wastewater treatment, selecting electroactive microbial communities from

the original inoculum, enhancing and maintaining its performance throughout the operation, are important. In the following section, some of these parameters affecting biofilm performance will be discussed.

2.3.3. Parameters Affecting Biofilm Performance

Anolyte (Feedstock)

Anolyte refers to the liquid solution inside the anodic chamber. It is a feedstock (substrate) for anodophilic microorganisms, providing carbon-energy, electrons and nutrients including minerals, salts and amino-acids. Substrate (fuel type, concentration and feeding rate) as an electron donor is one of the most important factors affecting the structure, composition and affinity of the microbial community, which can subsequently influence the MFC performance in terms of power density and coulombic efficiency (Kim *et al.*, 2006; Jung & Regan, 2007; Ha, Tae & Chang, 2008; Liu *et al.*, 2009; Chae *et al.*, 2009).

A wide range of substrates from pure compounds to complex mixtures of organic matter has been used in MFC studies. Pant *et al.* (2010) reported that simple compounds such as acetate and butyrate are easier to degrade in MFCs thus tend to improve the power output whereas complex substrates are favoured by diverse and electrochemically active bacterial communities. However various target compounds still need to be investigated in MFCs. For example, human urine which showed a great potential in terms of power generation and sanitation improvement (Ieropoulos, Greenman & Melhuish, 2012), has not been much explored.

The relationship between substrate concentration and MFC current generation usually follows Monod's equation if there are no other limitations for the anodic biofilm to function (Borole *et al.*, 2011). Therefore increasing substrate concentration leads to higher power

output up to a certain level (Park & Zeikus, 2002; Moon, Chang & Kim, 2006; Gil *et al.*, 2003). However this is not always the case. Pinto *et al.* (2010) reported that a high organic load could promote methanogenic metabolism, rather than current production when the system is run under non-optimal conditions such as too high external load.

$$\mu = \mu_{max} \frac{S}{K_s + S}$$

where μ is the specific growth rate of the microorganisms, μ_{max} is the maximum specific growth rate of the microorganisms, S is the concentration of the limiting substrate for growth and K_S is the half saturation constant.

Conductivity (ionic strength) and pH of anolyte also have a significant effect on anodic biofilms. Higher conductivity yields higher power output levels since it lowers the R_{INT} of the MFC (Min, Román & Angelidaki, 2008). In the case of anolyte pH, low pH has an advantage for transferring protons to the cathode and minimising proton concentration gradients across the membrane. However many anodophiles that form biofilms are not acidophilic (Borole *et al.*, 2011). Thus many researchers choose neutral pH (close to pH 7) for the anolyte. On the other hand, some studies showed that alkaline anolytes increased power output and anodophiles tolerated relatively high pH values, up to 10 (Yuan *et al.*, 2006; Zhuang *et al.*, 2010b; Yuan *et al.*, 2012). High pH can also be advantageous for the MFC performance by supressing the growth of methanogens.

External Resistance

In electronics, it is well known that the maximum power transfer (MPT) can be achieved when the external resistance (R_{EXT}) is matched with the internal resistance (R_{INT}) of a system, which is known as Jacobi's law. Thus selecting an external resistor corresponding to the R_{INT} is critical when maximising power output. For an MFC using organic matter as a fuel,

external resistance also affects the microbial metabolism in terms of coulombic efficiency (Liu, Cheng & Logan, 2005).

Furthermore, in long-term operations, R_{EXT} affects the structure of the anode biofilm. Several studies have shown that electroactive species could be selected by controlling the R_{EXT} during the maturing period (Lefebvre *et al.*, 2011; Pinto *et al.*, 2010; Zhang *et al.*, 2011a). These studies reported that R_{EXT} has a great influence on the length of maturation, suppression of methanogenic growth, morphology and EPS content of anode biofilm.

Operating Temperature

Operating temperature becomes an important factor to consider when commercialising the MFC technology. Unlike a laboratory environment with a controlled temperature, MFCs in a real world application will be exposed to a wide and variable range of operating temperature thus the effect of this parameter on MFC performance should be investigated. The majority of MFC research has been conducted under ambient temperature and performance reduction was observed when the operating temperature decreased (Wang, Feng & Lee, 2008; Patil *et al.*, 2010; Cheng, Xing & Logan, 2011). On the other hand, increasing the operating temperature had a positive effect on current generation (Min, Román & Angelidaki, 2008; Liu *et al.*, 2010b; Larrosa-Guerrero *et al.*, 2010). However it seems that MFCs can be quite tolerant with temperature variation; a recent study demonstrated that a mixed culture anode biofilm inoculated from wastewater can adapt to temperature fluctuations within a temperature range between 0 °C to 45 °C (Patil *et al.*, 2010).

2.4. Chapter Conclusions

The global demand for sustainable energy and water has been growing continuously since the energy issues of energy security and climate change were recognised. As a result, efforts have intensified for seeking and developing alternative energy sources instead of fossil fuels. Amongst the rising renewable energy technologies, MFCs are a unique technology capable of offering a solution for both sustainable energy and clean water demands. In order to take the MFC technology to a commercial level, more effort has to be spent in order to improve the performance and treatment efficiency; this thesis has therefore concentrated on the majority of the aforementioned parameters, in relation to the MFC anode.

3. General Materials and Methods

3.1. Microbes, Substrates and Catholytes

3.1.1. Procurement and Inoculum

Municipal wastewater and activated sludge were provided from Wessex Water sewage treatment plant which is located in Saltford, UK. Neat (unprocessed) human urine used in this study was donated from consenting individuals (adults with various height and weight) anonymously. The properties of wastewater, activated sludge and urine for each sample in terms of colour, BOD, microbial load and ecology between samples could vary slightly.

The anodes were inoculated with activated sludge or effluent of the previous experimental setups. When activated sewage sludge was used as the inoculum, sludge was mixed with 0.1 M acetate or 1 % tryptone and 0.5 % yeast extract (referred to as TYE) prior to use, resulting in an initial pH level of 7.2 - 7.5, and the same mixture was used as the initial feedstock. There was no artificial alteration such as pH change or genetic modification unless stated.

3.1.2. Feedstock

Municipal wastewater with activated sludge

Wastewater was obtained from the treatment plant at Saltford. It was diluted with tap water with various dilution rates and acetate was sometimes added in order to provide more readily biodegradable carbon source to MFCs. Tap water was used to provide minerals and stored at room temperature for at least 24 hours prior to use. The details are found in each chapter. Prior to use it was stored at 4 °C and left on the bench to let the temperature rise to room temperature before putting into MFCs.

Tryptone yeast extract (TYE)

TYE was used to represent complex feedstock and was prepared by adding 1 % tryptone and 0.5 % yeast extract (both weight percentage) to deionised water (DIW). TYE was also used for maturing MFCs and in this case, the same amount of tryptone and yeast extract was added to activated sludge described above.

Human urine

Urine was donated from male and female individuals of varying height and weight, and diet and was pooled together prior to use. It was used without dilution (full strength) and on the day of donation (unless stated otherwise). When storing was required, it was kept at 4 °C.

Uric salts

Uric salts (also called uric scale or uric sludge) was provided from an operating communal urinal facility run by Whiff- Away Ltd, Slough, UK. It was diluted with tap water with several dilution rates.

Modified 2SPYN medium

The original recipe of 2SPYNG for *Geobacillus* species (Extance, 2012) was modified for the thermophilic MFC experiment (section 5.1) by adding tryptic soy broth (16 g/L), yeast extract (10 g/L) and sodium chloride (5 g/L) to DIW. The pH of solution was adjusted to 7.0 ± 0.5 with 5 M potassium hydroxide then it was autoclaved for sterilisation.

Modified M1 minimal medium

The M1 medium was originally used for *Shewanella* species (Pinchuk *et al.*, 2010; Ledezma, Greenman & Ieropoulos, 2012) and the recipe was modified for this thesis. Details of the chemical composition and preparation can be found in appendix B.

3.1.3. Catholyte

Two types of cathode were used in the study; aqueous cathodes in closed systems and open to air cathodes in open systems. Only the closed cathode system requires catholyte and potassium ferricyanide solution ($K_3Fe(CN)_6$; 0.1M, KH_2PO_4; 0.1 M, pH 7.5) or aerated tap water was used. Carbon veil cathodes of the open cathode system were hydrated on a daily basis whereas hot-pressed activated carbon MPL cathodes of the same system did not require hydration.

3.2. Reactor Construction and Component Materials

3.2.1. MFC Designs

Rectangular MFC (R-MFC)

This MFC design is one of the most common types used by many researchers. The chamber design allows electrodes with large surface areas to be placed closely to the separator and the other electrode, thus preventing high R_{INT}. The R-MFC can be built to accommodate either an open to air cathode or a closed cathodic chamber to hold a liquid electrolyte e.g. water or ferricyanide (Figure 3.1). Although the R-MFC can be used for continuous-flow operation, it is ideally suited for a fed-batch system.

The R-MFCs were used in a variety of experiments particularly prior to the construction of the new continuous-flow design.

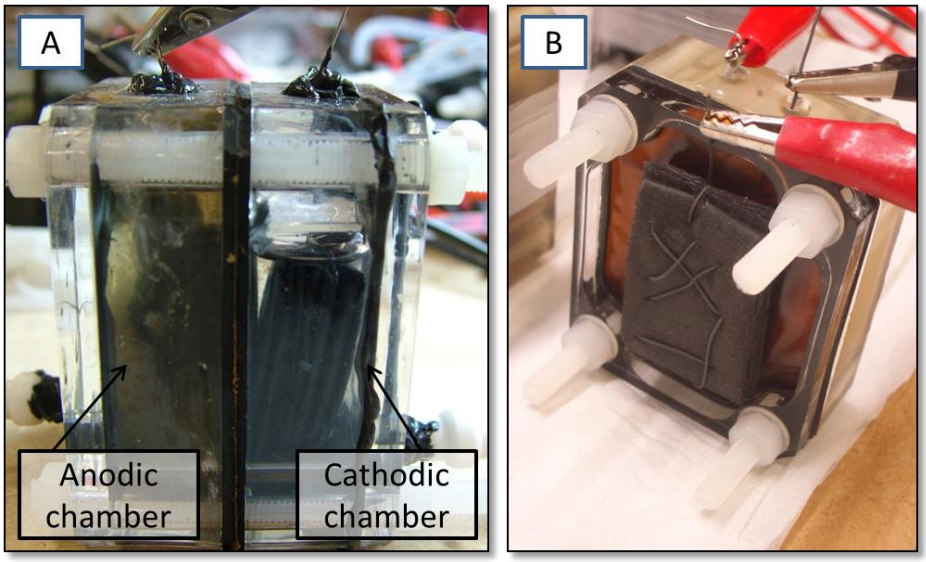

Figure 3.1 Rectangular MFCs; two-chamber MFC (A) and single-chamber MFC with open to air cathode (B)

The R-MFC design was constructed according to the following protocol:

The two-chamber MFCs comprised two (anode and cathode) 25 mL chambers separated by a membrane. Each chamber was made of acrylic material with dimensions of h = 6 cm, w = 5 cm, l = 1.5 cm and the surface area of the membrane was 30 cm^2 (6 x 5 cm). The design of single-chamber MFCs was very similar to the two-chamber MFC apart from they did not have cathode chambers. Cathodes were mounted onto membranes with either parafilm or magnet (Fig. 3.1 B) and exposed to the air directly. Open to air cathodes were wrapped in parafilm to help retain moisture, following cathodic hydration. Both types of MFCs were assembled using rubber gaskets, 5 mm nylon studding, washers and nuts, and were sealed with a non-toxic aquarium sealant (Wet Water Sticky Stuff, Acquatrix, UK). All the experiments using R-MFCs are summarised in appendix A. In all cases, at least two units were used for each condition. Details of specific experiments are described in the relevant sections.

Spherical MFC (S-MFC)

As mentioned in the section 2.2.5, the approach taken in this thesis for scale-up is to build stacks of relatively small sized MFCs connected together electrically. Although fed-batch system is more suitable for some applications such as small volume of wastewater treatment, continuous-flow system has many advantages; it is a better configuration for the treatment of large volumes of waste/watewater and stable power output can be achieved if the constituent of feedstock is consistent.

With this in mind, small scale spherical MFCs (S-MFCs) were designed (Fig. 3.2). S-MFCs consisted of two 0.7 mL hemispherical chambers made of Nanocure® material using the Rapid Prototype technology. Each chamber had an inlet and outlet (d = 2 mm) for continuous feeding. Two chambers were held by clipping both halves together without bolts and nuts which made the assembly simple. Between the two chambers, a circular cation exchange membrane, 15 mm diameter, was placed. S-MFCs were used to investigate effect of using uric salts in the feedstock (section 6.2).

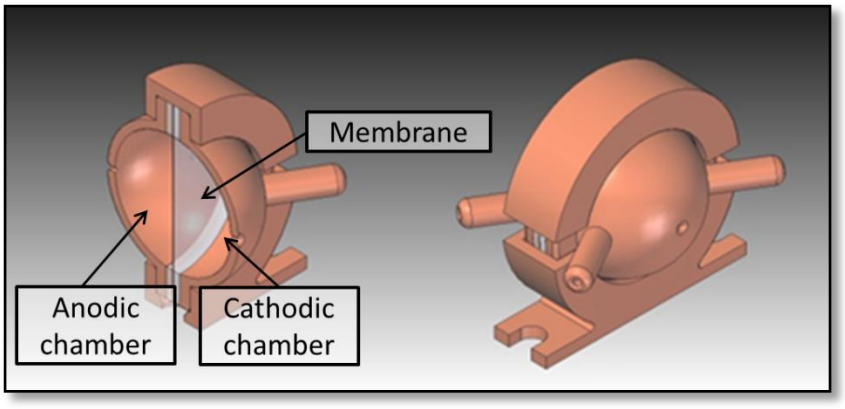

Figure 3.2 3D CAD assembly of S-MFCs

Circular MFC (C-MFC)

Since S-MFCs, more improvements were made in the C-MFC, these improvements enabled continuous feeding operation and accommodating an open to air cathode. C-MFCs had 6.25 mL of anodic chamber and open-to-air cathode. For continuous feeding, the anode compartment had an inlet and outlet (d = 4 mm) on the bottom and the top respectively, which allowed the anolyte to fill up from the bottom and then overflow from the top. They were made of Nanocure® material using the Rapid Prototype technology and assembled by screwing two compartments together. In this way, assembling became handy and quick. A circular membrane, 25 mm diameter, was placed between two electrodes.

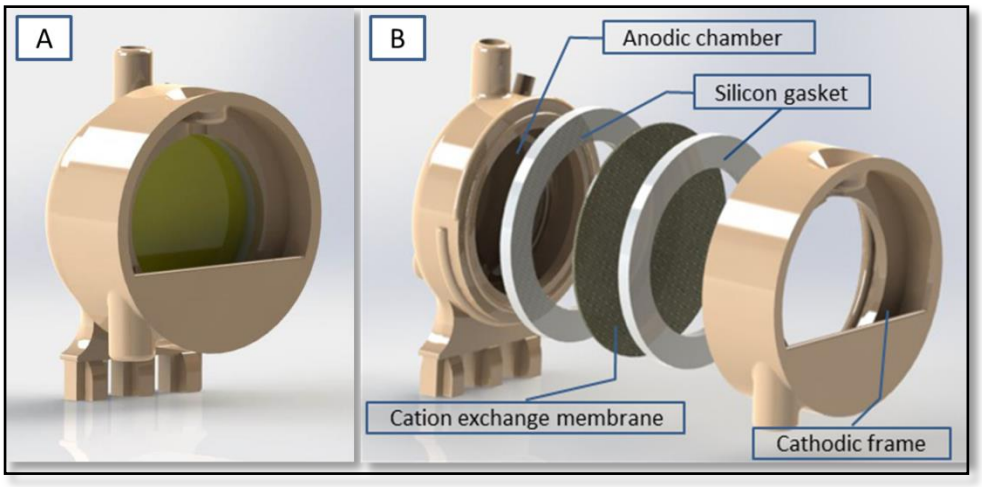

Figure 3.3 Circular MFC design; assembled figure (A) and exploded assembly (B)

Various materials could be used for the cathode electrodes with this design. The open side of cathodic frame was covered with an acrylic sheet to minimise the cathode becoming completely dry when the MPL cathodes, which did not require periodic hydration, were used.

3.2.2. Anode

For the R-MFCs and S-MFCs, plain carbon fibre veil (20 g/m^2 of carbon loading; PRF Composite Materials Poole, Dorset, UK) with a total surface area of 270 cm^2 (w = 30 cm, l = 9 cm) and 28 cm^2 (w = 7 cm, l = 4 cm) respectively, were folded in order to fit into the anodic chambers. The same plain carbon fibre veil with more carbon loading (30 g/m^2) was used for the C-MFCs. Different anode electrode sizes were used over the course of the study and the details are described in the relevant sections.

For anode material comparison (section 4.3), five types of anode material were tested in the C-MFCs. Plain carbon fibre veil (CV) electrodes with different amounts of carbon loading (20 g/m^2 and 30 g/m^2) and untreated (non-wet proofed) carbon cloth (CC) electrodes (FuelCellEarth, Massachusetts, USA) were compared. Microporous layer (MPL) modification was applied onto the plain carbon fibre veil (20 g/m^2) and carbon cloth electrodes. Each material was cut into a rectangular piece (w = 2.2 cm, l = 1.9 cm) and 16 pieces were layered on top of each other. These pieces were fixed by piercing a nickel-chromium wire (0.45 mm thickness) through for connection and current collection, which resulted in the total surface area of an anode being 67.5 cm^2. The MPL modification was prepared at the Center Clean Energy Engineering, University of Connecticut, USA (Santoro *et al.*, 2012). The preparation procedure was as follows; 0.7 g of nano-size carbon black particles (Vulcan XC-72R, FuelCellStore, Texas, USA), 9.1 mL of distilled water and 21.5 mL of non-ionic surfactant (Triton X100, Sigma–Aldrich) were mixed for 1 hour. Then 1 g of PTFE (60 % emulsion, Sigma–Aldrich) was added and mixed for another 30 minutes. This mixture was placed in an ultrasonic bath for 15 min for removing air bubbles in the mixture, followed by 5 min of mixing. This step was repeated twice. After adding 2.75 g of carbon black particles, the mixture was blended for 1 hour which resulted in a form of paste (20 % wt solid). Once this paste was applied onto the base material either CV or CC using the silk screen technique, it was then heated in the middle of two hot plates for 30 min at

280 °C to evaporate the non-ionic surfactant. After all the water and non-ionic surfactant was evaporated from the initial heating, the temperature was increased to 343 °C in order to melt PTFE (polytetrafluoroethylene, melting point of PTFE: 327 °C). The second heating process lasted for 2.5 hours. This solution can coat a base material (carbon cloth or carbon veil) of about 0.19 m^2 size, therefore it is assumed that roughly 18.4 g/m^2 of carbon was added by the MPL treatment.

Table 3.1 Details of anode materials tested in the study

Abbreviation	Composition	Original carbon content (g/m^2)	Total carbon content (g/m^2)
CV20	Unmodified carbon veil	20	20
CV30	Unmodified carbon veil	30	30
CV20-MPL	Modified carbon veil with MPL	20	38
CC	Unmodified carbon cloth	115	115
CC-MPL	Modified carbon cloth with MPL	115	133

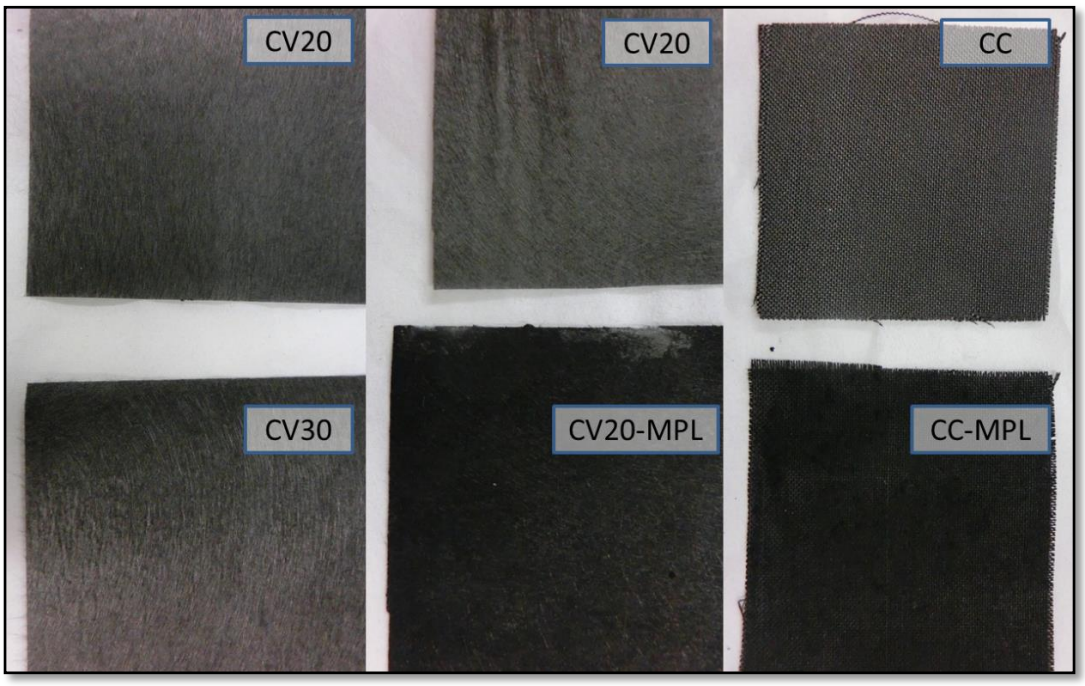

Figure 3.4 Photo of prepared anode materials

3.2.3. Cathode

For the R-MFCs and S-MFCs, plain carbon fibre veil (20 g/m^2 carbon loading) of the same size of each anode (270 cm^2 for the R-MFCs, 28 cm^2 for the S-MFCs) was folded and used as a cathode. This type of cathode had no catalyst or any other modification.

The MPL cathodes were applied in the C-MFCs. The preparation process was as follows; 10 mL of PTFE solution (60 %, Sigma-Aldrich) was diluted with 10 mL of distilled water and this solution was used to coat both sides of the plain carbon veil sheet (1,260 cm^2; 42 cm x 30 cm). The sheet was left to dry at room temperature. Once the coated sheet became dry, 20 g of PTFE and 120 mL of distilled water were mixed in a beaker then 80 g of activated carbon powder (G Baldwin, London, UK) was added into the solution. The mixture soon thickened, turning into a paste. The paste was applied onto the PTFE coated carbon veil sheet prepared earlier; it was then hot-pressed at 200 °C until it became completely dry. This cathode material was cut into a 4.9 cm^2 circular shape (diameter: 25 mm) and the same size of stainless steel mesh was attached onto it with a nickel-chromium wire in order to collect

current more efficiently. Unlike the plain carbon veil cathode, this cathode did not require periodic hydration.

3.2.4. Ion Exchange Membrane

Five AEMs and four CEMs were tested for comparison in the R-MFCs in triplicates. These will be referred to as VWR-C, VWR-A, MI-C, MI-A, FT-C, FT-A, AGC-C, AGC-A and MEGA-A, hereafter. The letter "C" and "A" stand for "cation" and "anion" respectively. Details of each membrane are found in Table 3.2. The total membrane size was 25 cm^2 and the membrane window was 18 cm^2. All membranes were pre-treated and stored in line with the manufactures' guidelines.

After the membrane comparison test, the MI-C membrane was used for the rest of experiments. Size of the MI-C membrane used for the S-MFC and C-MFC was 1.8 cm^2 (d = 15 mm) and 4.9 cm^2 (d = 25 mm) respectively.

Table 3.2 Membrane types tested

Abbreviation	Type	Model name	Manufacturer	Thickness(μm)
VWR-C	CEM	551652U	BDH- Prolabo, VWR, UK	Not provided (measured: 0.10)
VWR-A	AEM	551642S	BDH- Prolabo, VWR, UK	Not provided (measured: 0.10)
MI-C	CEM	CMI-7000	Membranes International Inc., USA	0.45 ± 0.025
MI-A	AEM	AMI-7001	Membranes International Inc., USA	0.45 ± 0.025
FT-C	CEM	Fumasep FKE	FuMa- Tech GmbH, Germany	0.05 - 0.07
FT-A	AEM	Fumasep FAD	FuMa- Tech GmbH, Germany	0.08 - 0.10
AGC-C	CEM	Selemion ™HSV	Ashahi Glass Co., Japan	0.15
AGC-A	AEM	Selemion ™ASV	Ashahi Glass Co., Japan	0.13
MEGA-A	AEM	Ralex®AM-PP	MEGA a. S., Czech Republic	0.45

3.3. Operating Conditions

3.3.1. Feeding Continuity

Batch Feed

Early studies with the R-MFCs were run in batch feeding mode. MFCs were fed once or twice a week and each time 5 mL of old anolyte was taken out before putting 5 mL of fresh feedstock into the reactors. During the feeding process, anolyte in the anodic chambers was fully agitated to ensure homogeneity.

For experiments with the S-MFCs, feedstock solution was recirculated. This is considered as batch fed system since depletion of organic matter in the feedstock occurred which resulted in MFC power decrease thus required replacement of the feedstock.

Continuous Feed

All continuous feeding system experiments were carried out using multi-channel, high accuracy peristaltic pumps (Watson Marlow 205U, Falmouth, England). Before each experiment, the flow rates in mL/h were calibrated according to the pump speed in RPM (revolutions per minute). Figure 3.5 shows an example of the calibration processes. Flow rates varied depending on the requirements of different experiments and are detailed in the relevant section.

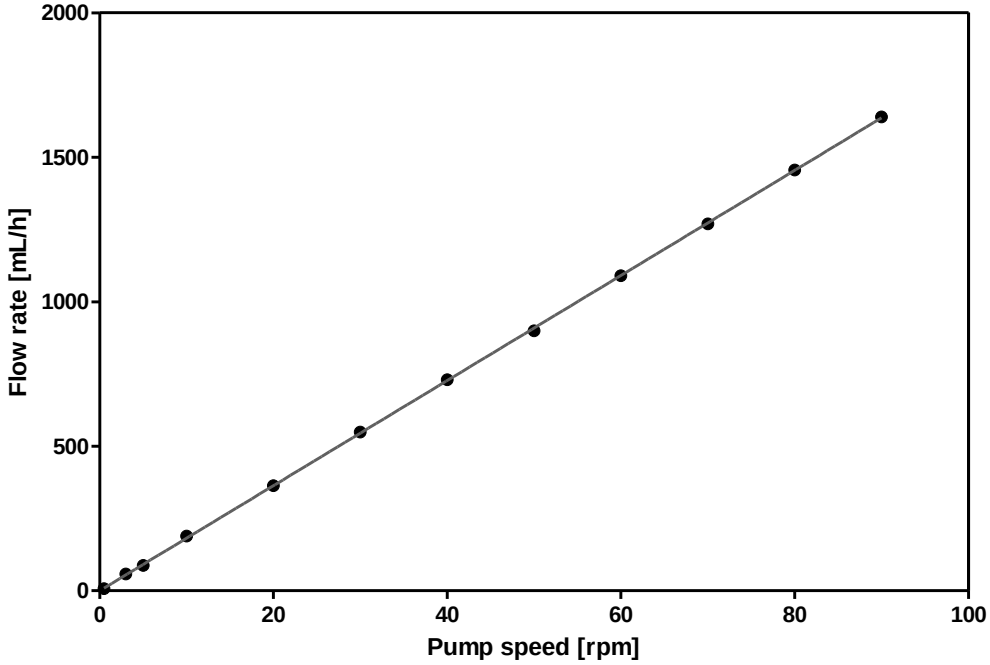

Figure 3.5 Flow rate in relation to speed of the peristaltic pump used in this work

3.3.2. MFC Unit Arrangement

For most of this thesis work, MFC units were fed individually. On the other hand, for the MFC stack system (section 6.4), MFC units were placed vertically and groups of MFCs had a common feeding source point. In this cascade system, substrate solution filled up from the bottom of the anodic chamber of the first MFC then overflowed from the top of the anodic chamber to the MFCs below, and so on. All the MFCs used in the work were hydraulically isolated.

3.3.3. Operating Temperature

All the work except the experiment with thermophiles (section 5.2) was carried out in a temperature controlled laboratory, at 22 ± 2 °C. The experimental setup with thermophiles was placed in an incubator at 60 ± 5 °C.

3.4. Testing Procedures and Instruments

3.4.1. Chemical and Physical Analysis

Conductivity, pH and ORP

The conductivity of water samples was measured by a hand-held conductivity meter (470 Cond Meter, Jenway). Both pH and ORP (oxidation reduction potential) of influent and effluent anolyte, and catholyte were measured with a bench-top pH/ORP meter (pH290, Hanna Instruments). When dilution was required, distilled water was used.

Microscopic Analysis

A scanning electron microscope (SEM, model name-XL30, Philips) was used to examine shapes and structures of the unmodified/modified anode material surfaces. Around 0.5 cm^2 of each material was cut and mounted on an aluminium mount using contact adhesive. Samples were prepared for microscopy by sputter coating in gold using an Emscope SC500 sputter coating unit before being observed.

Digital microscopic images of precipitates (section 6.4) were taken by a digital microscope (KH-7700, Hirox, Japan).

X-ray Diffraction

The crystal characterization of the dried precipitates from the struvite precipitation stage described in section 6.4.1 was identified by X-ray diffraction (XRD) (D8 Advance Diffractometer, Bruker, UK) and the result was analysed using EVA software package (Bruker, UK). The precipitates were filtered through 0.45 μm filters (Millex, UK), and then dried at 40 ºC prior to analysis.

Water-soluble Element Analysis

For measuring soluble elements such as COD, NH_4^+–N and PO_4^{3-}–P, urine samples were filtered through 0.45 µm filters (Millex, UK) then analysed according to the standard methods of the American Public Health Association (Clesceri, 1998) using test kits (Camlab, UK).

Four-wire Resistance Measurement

In order to measure electrical conductivity of the tested anode materials, 4-wire resistance measurement was carried out with a digital multimeter (M-3850D, METEX, Korea) and bench power supply (PSM-3004, GW INSTEK, Taiwan). A small piece of each material (15 mm x 15 mm) was placed between two clamps. Voltage drop between the two points was measured when constant current was supplied to the material from the power supply. This method is considered more accurate than the 2-wire method for low resistance measurements since it reduces the effect of test lead resistance.

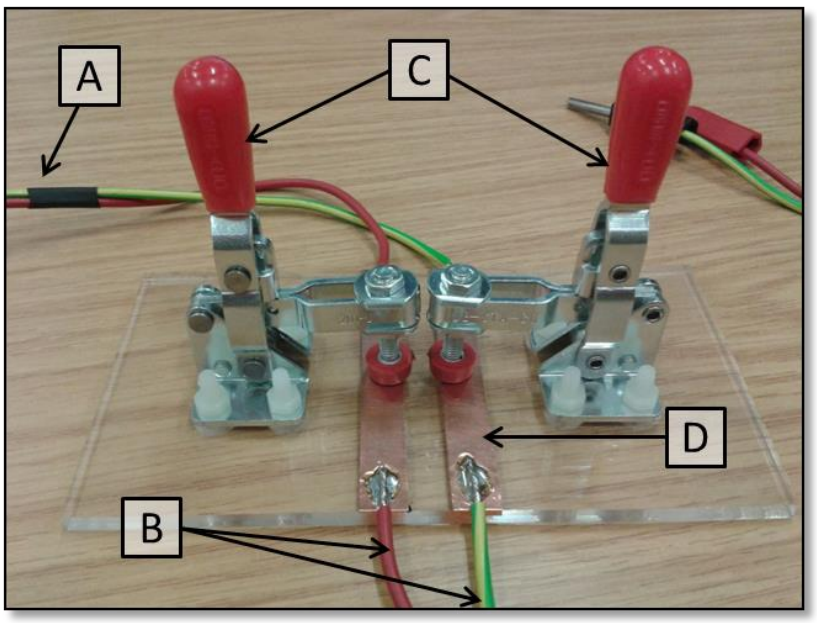

Figure 3.6 Apparatus used for four-wire resistance measurement: (A) cables connected to power supply set for constant current; (B) cables connected to voltmeter; (C) clamps to hold tested material; (D) copper tape

3.4.2. Microbiological Analysis

Direct Cell Counting

For the hemocytometric cell number measurements, 0.1 mm deep Neubauer-improved hemocytometers were used (Marienfeld-superior, Germany). The two independent consecutive measurements were performed using the two different sides of each hemocytometer. The raw effluent was diluted 10-20 times with phosphate buffered saline (PBS). The bacterial cell population was determined by counting individual cells using a grid-field.

Indirect Cell Counting

Viable counts were performed on non-selective nutrient agar (Oxoid, Basingstoke, UK) and the number of colony forming units per sample (cfu/mL for effluent and cfu/mm^2 for anodic biofilm) was calculated. A 1 mL volume of each sample was serially diluted to 10^{-6} and 100 µL from sample dilution 10^{-4}, 10^{-5} and 10^{-6} spread onto the non-selective recovery medium. All plates were incubated in an anaerobic cabinet (MK3 anaerobic workstation, Don Whitley, Shipley, UK) at 37 °C for 5 days.

The optical density (OD) at 600 nm wavelength of each undiluted 1 mL sample was measured using a spectrophotometer (model name: 6700, Jenway, Staffordshire, UK).

Community Level Physiological Profiling (CLPP)

For studying biofilm metabolic pathway activity change (section 5.4), community level physiological profiling (CLPP) using Biolog AN plates (Biolog, Hayward, CA, USA) was employed. At the end of each stage, two MFCs from both groups were opened and one layer of the anodes was removed aseptically for the Biolog analysis. The anode sample was transferred into 40 mL of sterile PBS (Sigma-Aldrich, Dorset, UK) solution and re-suspended by rigorous vortex mixing for 3 min. The 96 wells of a Biolog AN plate were

inoculated with 150 µL of each sample per well. Then the microplates were incubated anaerobically (10 % CO_2 in oxygen free N_2) in a portable container at 30 °C to allow utilisation reactions to proceed along with tetrazolium colour changes, and the changes in colour intensity were measured at 590 nm every 24 hours up to 120 h, using a Biolog Microstation in accordance with the Biolog operating protocol.

Average well colour development (AWCD) was calculated according to Garland and Mills (Garland & Mills, 1991), i.e., AWCD = ∑(C − R)/n where C is the optical density of each well measured at 590 nm, R is the absorbance value of the control well (A1), and n is the number of substrates (n = 95). In order to compare a specific carbon source (acetate in this case) utilisation of the two groups at different stages, the raw difference data of the well containing acetic acid was divided by the AWCD of the plate, i.e. (C - R)/AWCD. As a measure of the degree of substrate utilisation (substrate richness) and diversity of extent of particular substrates utilisation (substrate evenness), the Shannon-Wiener index (H) was used: $H = -\sum_{i=1}^{n} p_i(\ln p_i)$ where p_i is the proportional of a microbial activity on a particular substrate (OD_i) to the total microbial activity ($\sum OD_i$) and n is the number of substrates on a plate (Zak *et al.*, 1994; Frąc, Oszust & Lipiec, 2012). Plate readings at 24 h of inoculation were used to calculate AWCD and H.

3.4.3. MFC Performance Analysis

Voltage Data Capture and Power Output Calculation

The MFC output was recorded in real time in volts (V) using an ADC-24 A/D converter computer interface (Pico Technology Ltd., Cambridgeshire, UK) or using a HP Agilent multiplex logging module (34907A, HP). The current (I) in amperes (A) was determined using Ohm's law, I = V/R, where V is the measured voltage in volts (V) and R is the loaded external resistance value in ohms (Ω). Power (P) in watts (W) was calculated by multiplying

voltage with current; P = I×V. Current density (j) and power density (P_D) were calculated in terms of electrode total surface area or anodic volume; j = I/A and P_D = P/A, where A is the total anode electrode surface area in square meters (m^2) or j = I/V and P_D = P/V, where V is the total anodic volume in cubic meters (m^3). R_{INT} was calculated from Kirchhoff's voltage law which states the directed sum of the electrical potential differences (voltage) around any closed network is zero:

$$V_{O/C} - I_L R_{INT} - I_L R_{EXT} = 0$$

where $V_{O/C}$ is the open-circuit value of the MFC which equals to electromotive force (Ɛ), I_L is the current under a given load and R_{EXT} is the value of the load resistor. Thus, R_{INT} is:

$$R_{INT} = \left(\frac{V_{O/C}}{I_L}\right) - R_{EXT}$$

The value of R_{INT} was also validated from the V/I curves of polarisation experiments according to Jacobi's impedance matching law (maximum power transfer law).

Detailed explanation about R_{INT} can be found in appendix C.

Polarisation Measurement

Polarisation experiments were performed periodically by connecting a DR07 decade variable resistor box (ELC, France), between the anode and cathode electrodes by varying the external resistance from 30 kΩ to 10 Ω at time intervals of 5 minutes after the MFCs had established a steady-state open circuit voltage (at least 2 hours of open circuit condition).

Specific materials, substrates, configurations used for each experiment as well as power output of the work are summarised in appendix A.

4. Selection of MFC Materials

4.1. Introduction

Materials and designs of each MFC component need to be selected according to the application. For treating a large volume of wastewater as well as producing a meaningful level of electrical energy, system scale-up is indispensable. As discussed in section 2.2.5, this study aimed to realise the scale-up through building a system consisting of multiple small-sized MFCs under continuous flow. Reducing building cost and minimising environmental impact are also very important as well as increasing system performance and lifespan. This chapter comprises a number of experiments investigating better performing membrane materials, anode/cathode electrodes, and reactor designs for the application.

Parts of this chapter (section 4.3) have been published as You, J., Santoro, C., Greenman, J., Melhuish, C., Cristiani, P., Li, B., and Ieropoulos, I. (2014) Micro-porous layer (MPL)-based anode for microbial fuel cells. International Journal of Hydrogen Energy ***39*** *(36), 21811–21818.*

4.2. Membrane Comparison

It has been widely agreed that a form of separator is necessary to ensure efficient MFC operation. Various types of membranes including CEMs, AEMs, polymer/composite membranes and porous membranes have been employed in MFCs (He, Minteer & Angenent, 2005; Ieropoulos, Greenman & Melhuish, 2010; Kim *et al.*, 2007; Zuo, Cheng & Logan, 2008; Biffinger *et al.*, 2007b; Fan, Hu & Liu, 2007; Walter, Greenman & Ieropoulos, 2014). Although still many of MFC researchers employ Nafion® due to its highly selective permeability of protons and relatively lower internal resistance compared with other types of membrane separators, it is one of the expensive components, alongside platinum as cathodic catalyst, that brings up the MFC building cost significantly. As discussed in section 2.2.2 (IEM part), IEMs or other separators need to be selected according to the final applications.

Since this thesis focuses on waste and wastewater utilisation, seeking low cost but still well performing materials is very important. A simple comparison of the various membranes in MFC systems from the literature review is not feasible since different operating systems under different conditions have been used. Therefore nine different commercially available membranes (both CEMs and AEMs) were examined in order to find suitable ones for the thesis work. This work was carried out in collaboration with Iwona Gajda. The specific methods used for this experiment are detailed in the following section.

4.2.1. Methods Specific to Experiments

As detailed in section 3.2.4, five AEMs and four CEMs were tested for comparison in the R-MFCs (section 3.2.1) in duplicate. MFCs were fed with activated sludge and 0.1M acetate as a carbon source (pH 6.5 – 7.2) without addition of buffer in batch cycles when the produced voltage started decreasing and the cycle was usually every 3-5 days. Cathodes were periodically hydrated with tap water (pH 7) on a daily basis. The experiment was carried out in two parts. For the first part of the work, R-MFCs with four membranes, FT-C, AGC-C, AGC-A and MEGA-A were set and run for 5 weeks including a week for allowing microorganisms to attach and settle on the anode electrode. During the settlement period, anolyte was replaced every 2 days and MFCs were left in open circuit condition until a resistance of 8 kΩ was connected on each MFC. After the first part, the R-MFCs were disassembled and cleaned before replacing with new anodes and membranes. In the second part, the remaining five membranes, VWR-C, VWR-A, MI-C, MI-A and FT-A were tested in the repeated running condition. The total running time for the second part was also 5 weeks. Power output and polarisation data for comparing the all nine membranes, was collected from last 2 weeks of each part of work.

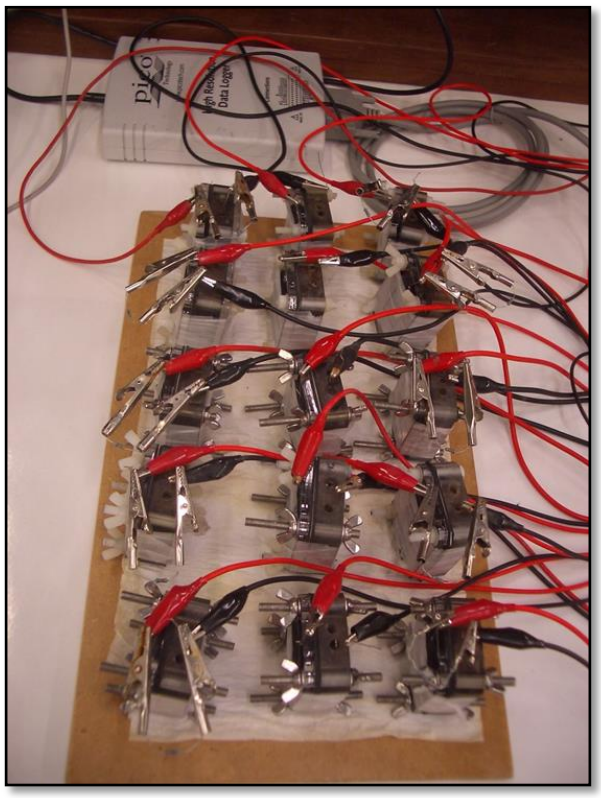

Figure 4.1 Photo of R-MFCs used in the work

4.2.2. Average Performance Comparison of CEMs and AEMs

The average power output for 2 weeks (after anodic biofilm maturation) produced by the MFCs with the 9 different membranes are shown in Fig. 4.2. VWR-C membrane showed the highest power output, 18.4 µW (0.68 mW/m^2), followed by MI-C and FT-C which had 17.0 µW (0.63 mW/m^2) and 14.3 µW (0.53 mW/m^2) respectively. Within the same manufacturing line, CEMs performed better than AEMs. In general, CEM-MFCs generated higher power than AEM-MFCs with the exception of MI-A which produced 15.4 µW (0.57 mW/m^2).

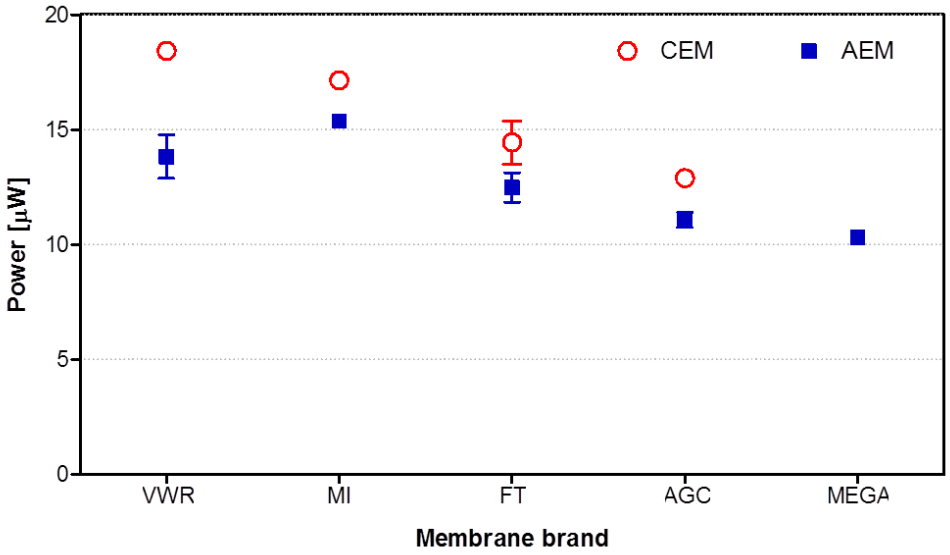

Figure 4.2 Power production of MFCs with different membranes
* Average power output for the last 2 weeks of experiment (n=3).

These findings are in contrast with previous studies (Kim *et al.*, 2007; Rozendal *et al.*, 2008; Mo *et al.*, 2009) reporting AEMs outperformed CEMs. This difference is thought to be due to the lack of additional buffer in this work. The AEMs in the previous studies facilitated proton transfer with the help of phosphate or carbonate as the proton carrier and pH buffer. However, for a practical application designed for minimum human intervention or large scale wastewater treatment, the use of a buffer is undesirable and therefore studies investigating the performance of AEMs without any chemical buffers should be pursued.

The lower performance of AEMs is also explained by sharp reduction of performance during the batch cycle. Figure 4.3 shows results of polarisation measurement carried out on 3rd and 5th days after anolyte replacement. P_{MAX} of MI-A dropped by 46.7 % in 2 days while MI-C showed only 14.7 % decrease in P_{MAX}. The same pattern was observed in all pairs of AEM and CEM from the same brand. Therefore CEMs seem more suitable for this configuration especially when batch fed.

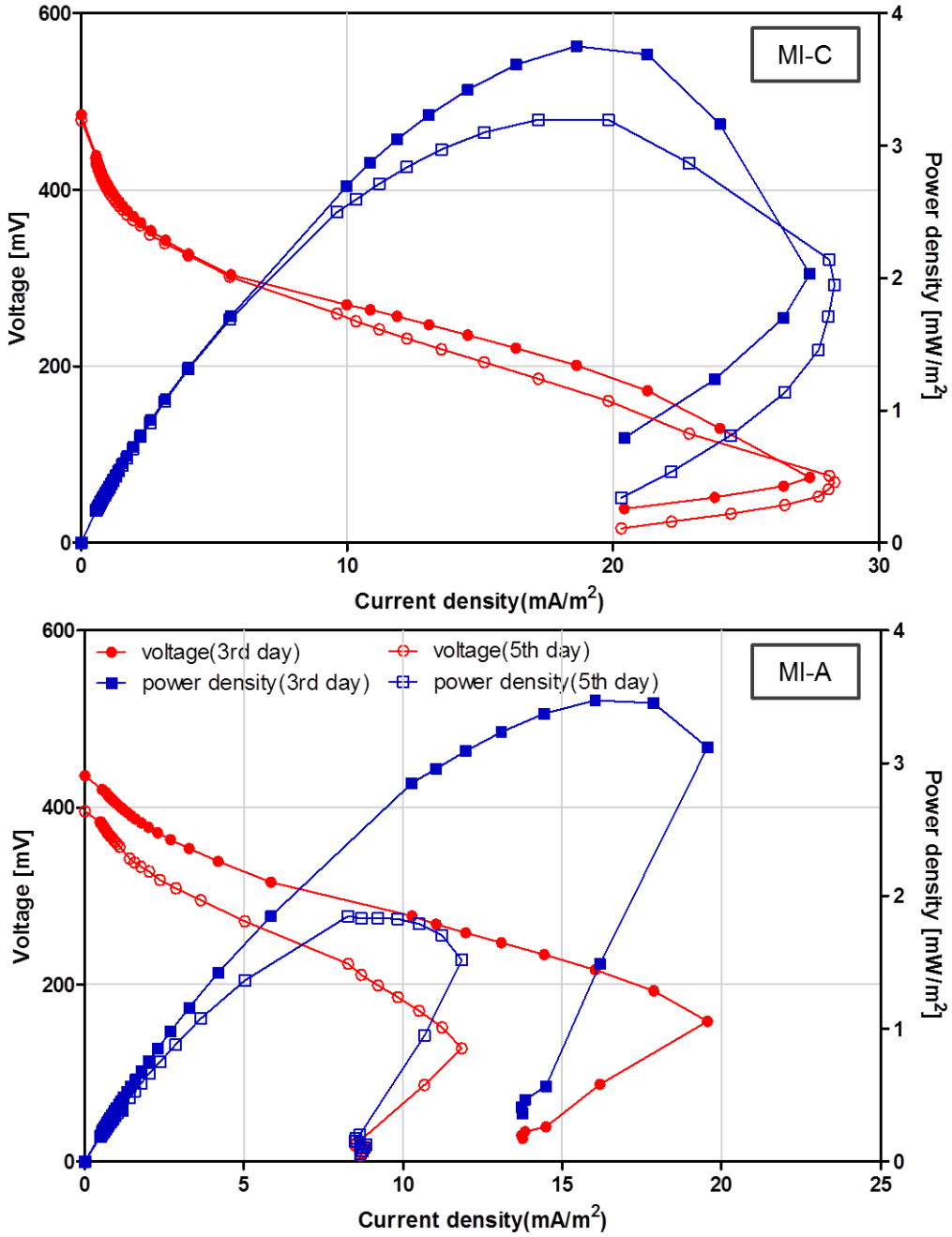

Figure 4.3 Performance reduction comparison between MI-C and MI-A on 3rd day and 5th day after anolyte replacement

4.2.3. Polarisation Measurements of CEMs and AEMs

The better performance of CEMs than AEMs was also verified by polarisation measurements. Polarisation results (Fig.4.4) show that every CEM was superior to AEMs in

this configuration in terms of R_{INT} and potential power generation. The R_{INT} values calculated from the power curves showed that CEMs had lower R_{INT} than AEMs. This lower R_{INT} attributed to the higher P_{MAX} of CEMs. The best performing CEM, FT-C's P_{MAX} was 116.1 µW (4.3 mW/m^2) which was 2.3 fold higher than the best performing AEM, MI_A, 51.3 µW (1.9 mW/m^2).

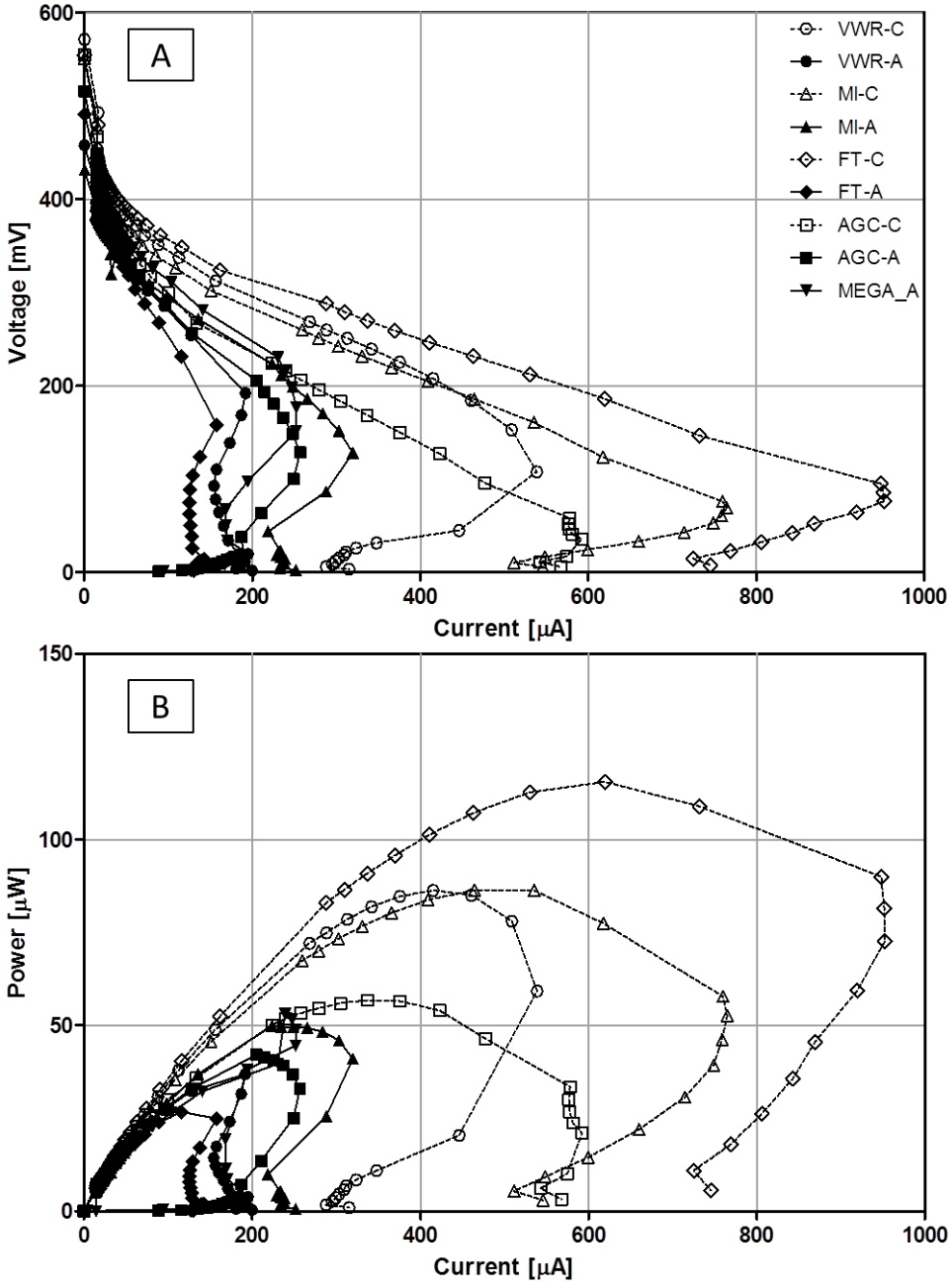

Figure 4.4 Polarisation curves (A) and power curves (B) of the tested membranes

4.2.4. Economic Considerations

For any practical applications to be considered viable, the manufacturing and running cost must be kept low. The same is true for the MFC technology especially when developed into stacks for powering real world applications utilising waste/wastewater.

Table 4.2 compares the maximum power generated by MFCs with different membranes based on the actual membrane purchasing cost. The power generation of MFCs with nine membranes ranged from 0.46 mW/$100 to 20.72 mW/$100. Although some AEMs such as MEGA-A showed lower power performance compared to CEMs, they nevertheless appeared to be better value for money. This would render them more suitable for a larger stack involving a higher number of MFC units and continuous flow of feedstock.

Table 4.1 Performance/cost comparison of MFCs with different membranes

CEMs	P_{MAX}[a] per membrane cost (mW/$100)	AEMs	P_{MAX} per membrane cost (mW/$100)
VWR-C	1.11	VWR-A	0.46
MI-C	20.72	MI-A	11.97
FT-C	6.39	FT-A	1.48
AGC-C	1.39	AGC-A	1.38
		MEGA-A	14.71

[a]P_{MAX}: based on the membrane size

One thing needs to remind is that this is comparison of performance to purchasing costs thus cost performance for long-term operation could be different. After this experiment, MI-C membrane was chosen and used for the rest of thesis work due to its high cost performance.

Although membrane performance change during long-term operation was not investigated in this experiment, MFCs with the MI-C membrane showed good durability in many cases.

4.3. MPL Based Anode

As discussed in section 2.2.2, good material for the MFC anodes needs to meet several requirements; biocompatibility, conductivity, chemical stability, mechanical strength and low cost. For bacterial attachment, high surface area and surface roughness are also important. Micro-porous layer (MPL) has been widely used as a cathode material for hydrogen fuel cells (Weber & Newman, 2005; Wang *et al.*, 2006; Cho & Mench, 2012) and more recently, microbial fuel cells (Santoro *et al.*, 2011; Papaharalabos *et al.*, 2013). In a cathode half-cell, MPL is usually placed between the gas diffusion layer (GDL) and the catalyst layer (CL). The function of MPL in this configuration is to provide sufficient porosity and hydrophobicity to allow better oxygen and water transport, as well as to reduce the electrical contact-resistance between the GDL and the adjacent CL. Hydrophobicity is not normally considered appropriate for anodes of MFCs but high porosity with good electrical conductivity are in fact desired properties in anodic materials. Therefore a hypothesis was formulated that the MPL could also work for MFC anodes.

In this study, carbon fibre veil (CV) and carbon cloth (CC) electrodes were modified with carbon powder, in order to introduce a MPL of improved surface area and conductivity. The main objectives of the study were to test electrode modification with MPL, in order to evaluate its performance as an anode and investigate the feasibility of using MPL modified anodes in terms of power production, surface morphology, biocompatibility, electrical conductivity, long-term stability and production costs.

4.3.1. Methods Specific to Experiments

Five different types of anode materials including two MPL modified materials were tested in C-MFCs (as described in section 3.2.2). MFCs were fed continuously with a flow rate of 11.5 mL/h. For the cathode electrodes, which were identical for all 15 MFCs, hot-pressed activated carbon onto untreated carbon cloth was made and its total surface area was 4.9 cm^2.

Following the inoculation of the MFCs and the maturing of the biofilm communities on the anodes for two weeks (referred as 'initial period'), untreated human urine was used as the sole energy source. For maximising power output in the long term, different external resistance values, which matched the internal resistance values of MFCs for the different anode materials, were connected throughout the work.

For comparing performance of each material in long term operation, the experiment was running for 7 months. The initial 2 weeks period when anode biofilm was formed and settled on the electrodes is referred as 'initial stage' and the next 4 months period when power output was relatively stable is referred as 'middle stage'. After these two stages, the performance decrease became apparent with time. Thus the last 2.5 months are referred as 'late stage'. Thus the division of each time stage was based on MFC performance, not a consistent time interval. Each experimental condition was tested in triplicate.

4.3.2. Performance of the MPL Modified Anodes

The MPL modification improved the MFC performance significantly when compared with the unmodified anode materials as shown in Fig. 4.5. From the beginning, the MPL modified anodes showed higher power performance than the plain ones, which was consistent throughout the entire line of work. During the middle stage, when the biofilm on the anodes was considered to be mature, the MFCs performed their best. The best

performing anode material, CV20-MPL, produced a maximum power of 304.3 μW (60.7 mW/m^2 normalised to the anode total surface area, mean value 290 μW ± 13), which was 1.2 fold higher than the second best performing anode material, CC-MPL with a maximum power of 253.9 μW (50.6 mW/m^2, mean value 249 μW ± 8). The maximum power produced by the unmodified electrodes, CV20, CV30 and CC, was 140.0 μW (27.9 mW/m^2, mean value 130 μW ± 10), 180.7 μW (36.0 mW/m^2, mean value 171 μW ± 10) and 143.4 μW (28.6 mW/m^2, mean value 137 μW ± 6), respectively. Polarisation curves revealed how MPL modification increased performance. Although electrochemical characteristic change through MPL modification made $V_{O/C}$ values of modified materials lower than plain materials, it significantly lowered activation losses and ohmic losses. The difference between modified materials and plain ones in terms of activation and ohmic losses from polarisation measurement data was distinct from the initial stage of work and became bigger during the middle stage when all MFCs were running in their best condition. In the late stage, MPL modified materials showed far less deterioration in these two types of loss compared to plain ones. This demonstrates that the MPL modification can result in significant anode improvements.

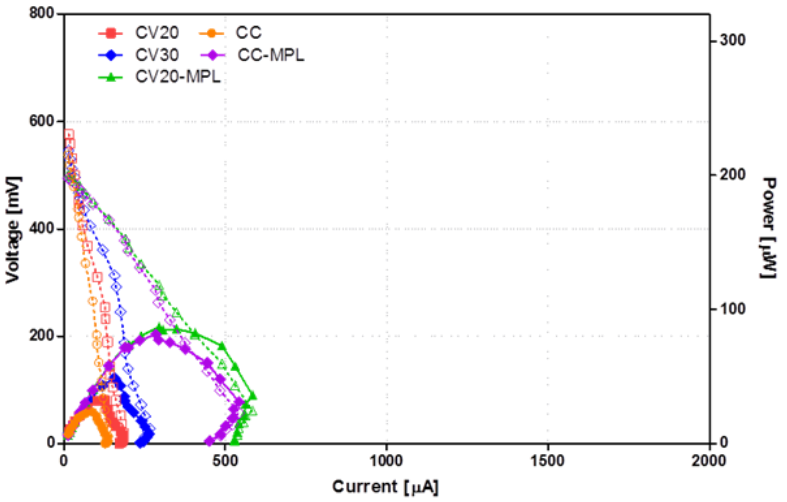

< Initial stage >

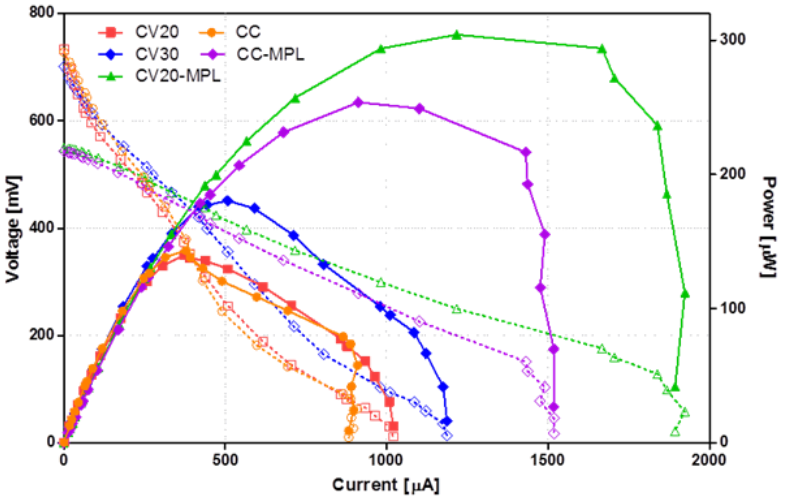

< Middle stage >

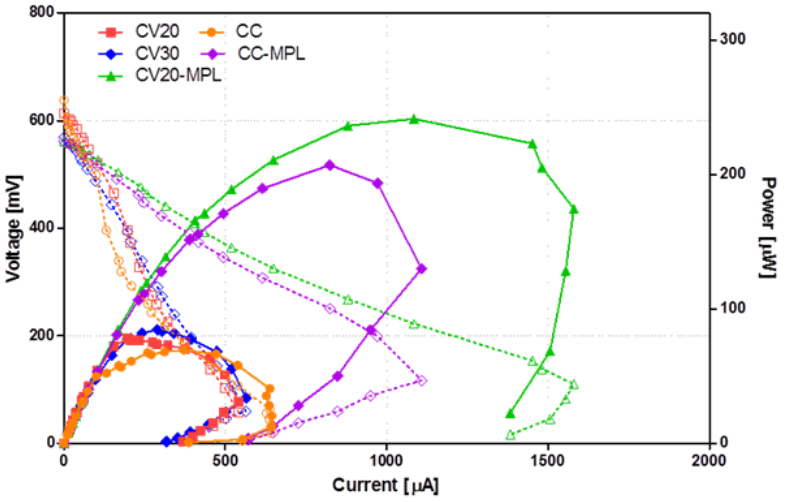

< Late stage >

Figure 4.5 Power and polarisation data of anode materials at each stage of experiment

* The closed and open symbols represent polarisation curves and power curves respectively.

* For the definition of each stage, refer to section 4.3.1.

The resulting 2.2 and 1.8 fold higher power was achieved by modifying the plain CV with 20 g/m^2 of carbon loading and CC carbon materials, which is also supported by the improved performance from the off-the-shelf higher-loading carbon (30 g/m^2), compared to the unmodified electrodes. It is therefore valid to assume that the higher carbon content from the MPL modification contributed - to a degree - to the higher power generation of MFCs. Although this was expected, it could not have been the only reason for the improved anode performance. The maximum power output of each anode material during the middle stage was compared (Table 4.3). For the specific power density, presented as the power output per 1 g of anode carbon, the same amount of carbon did not result in the same level of increase in the output, especially for the CC based materials, where specific power density was far lower than the CV based materials.

Table 4.2 Maximum power output during the middle stage

Electrode	Absolute power (μW)	Power density (mW/m^2)	Specific power density (mW/g)
CV20	140.0	27.9	1.40
CV30	180.7	36.0	1.20
CV20-MPL	304.3	60.7	1.60
CC	143.4	28.6	0.25
CC-MPL	253.9	50.6	0.38

4.3.3. Surface Morphology

Another possible explanation for the performance enhancement with MPL modification may be its surface characteristics. The SEM images of the sterile CV and CC anodes (Fig. 4.6(a)-(c)) showed that the MPL covered the anode surface as well as the gaps between

carbon fibres (Fig. 4.6(d) and (e)). With higher magnification, the MPL surface seems uneven and more porous, which could result in better and higher surface area for bacterial attachment (Fig. 4.6(f)).

The SEM images could explain why CC based materials did not perform as well as CV based materials, even though they had higher carbon content. Carbon fibres of the CC were densely woven (Fig. 4.6(c)), so that even though bacteria could penetrate deep into the strata, fuel supply from percolation would have been uneven at those inner layers, which is not the case for the less dense CV. Uneven and decreasing concentrations of fuel would have inevitably resulted in an eroding inner CC biofilm core.

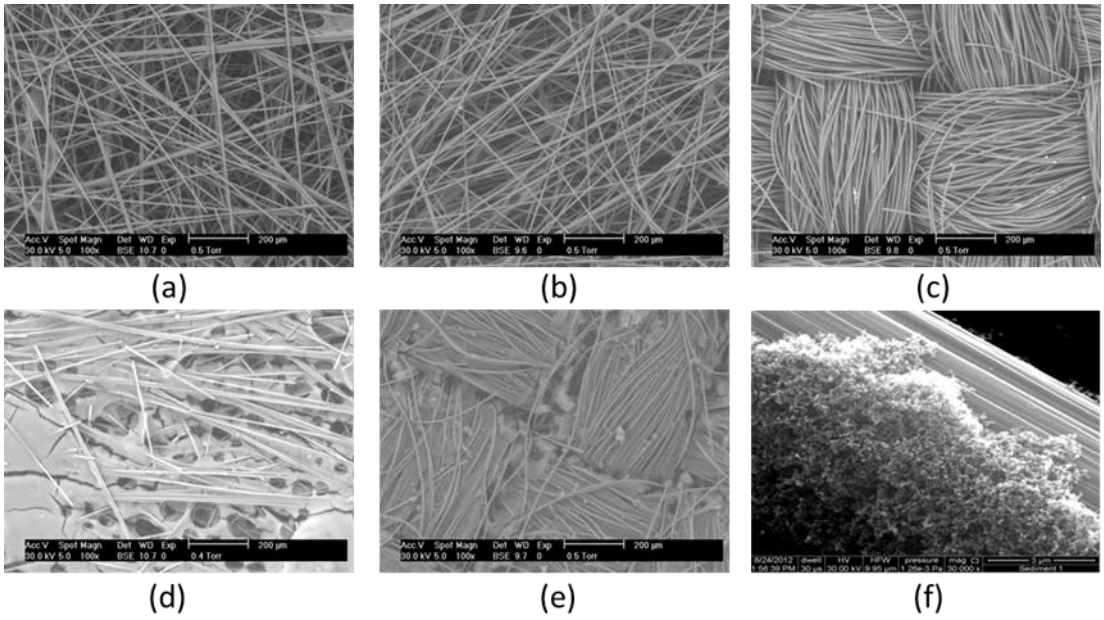

Figure 4.6 SEM images of tested anode electrodes at different magnifications (100X for (a)-(e), 30,000X for (f); (a) CV20; (b) CV30; (c) CC; (d) CV20-MPL; (e) CC-MPL; (f) MPL structure on CC-MPL

4.3.4. Biocompatibility

In order to address whether the increased anode surface through MPL modification was beneficial for the growth of anodophilic bacteria, the bacterial production rate from the

effluent of all MFCs was measured over a 2-month operational period, which allowed MFCs to run in various conditions.

With the direct cell counting method, all the suspended cells in the anolyte, both living and dead, were non-selectively counted (including non electro-active species). Nevertheless, a relationship between bacterial cell production and power output could be drawn from the results shown in Fig. 4.7. Although the relation between the two was not directly proportional, higher bacterial populations tended to contribute to higher power output levels. Therefore a conclusion could be drawn that higher anodic surface area, through MPL modification, had positive influence on bacterial growth on the anodes, increasing the anodic load of attached cells from which daughter cells are derived or increasing the growth rate of the attached biofilm layers, thus producing higher numbers of shed daughter cells in the perfusate.

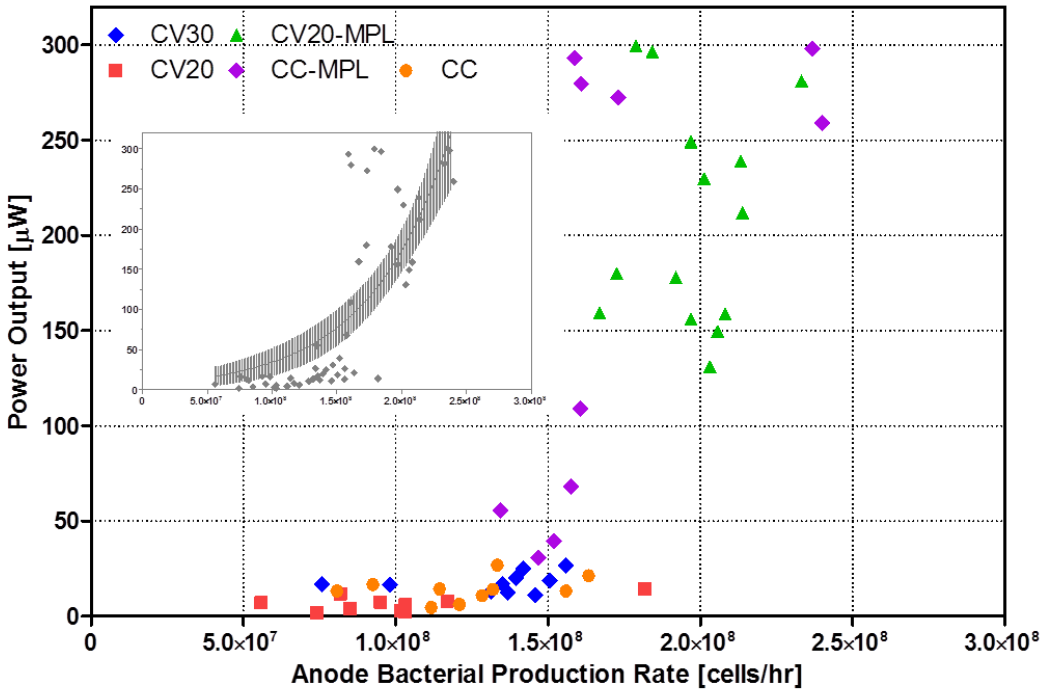

Figure 4.7 Relation between power output and bacterial production rate from the effluent of MFCs with different anode materials

* Inset shows the non-linear regression fit of the data with 95 % CI.

The relationship between bacterial cell production rate and power output might indicate that the portion of anodophiles constituting the whole microcosm population was larger in the MFCs with modified anodes due to the change brought about by the anode modification. In this case, it may be assumed that MPL modification is selective to anodophiles. In-depth bacterial analysis would need to be carried out to investigate this.

Cathodic MPL modification is traditionally performed with PTFE, which is used for making the layer hydrophobic as well as binding carbon powder and current collection (e.g. CV or CC). This hydrophobic characteristic appeared in the modified anodes. When MPL modification was completed, the water-uptake element of the MPL modified anodes was low. However this did not seem to have a significant negative effect on bacterial growth, at least over the long-term. The mixed number of attachment points with different surface hydrophilic/hydrophobic properties (carbon or PTFE) may result in greater diversity of surfaces and therefore greater diversity of types of bacteria that can attach. Bacteria can actually colonise pure PTFE surfaces, which is problematic in protecting medical equipment from bacterial contamination (Malaisrie, Malekzadeh & Biedlingmaier, 1998; Treter & Macedo, 2011), and the results derived from bacterial population counting are consistent with this, showing that the MPL modified anodes (with PTFE) were biocompatible.

4.3.5. Electrical Conductivity

Another possible downside predicted for using PTFE in anodic materials, was the decrease in the anodic electrical conductivity. According to the manufacturer of PTFE, volume resistivity of PTFE at 20 °C is more than 10^{18} Ωm (DuPont). Thus PTFE could work as an insulator in the modified materials due to its high resistivity.

Electrical conductivity of anodes is an essential feature because it greatly affects ohmic losses in MFC systems; since conductivity is the reciprocal of resistivity, the former can be

derived by measuring the latter. Electrical resistivity (volume resistivity) of each anode material was measured at room temperature (22 ± 2 °C) (Fig. 4.8).

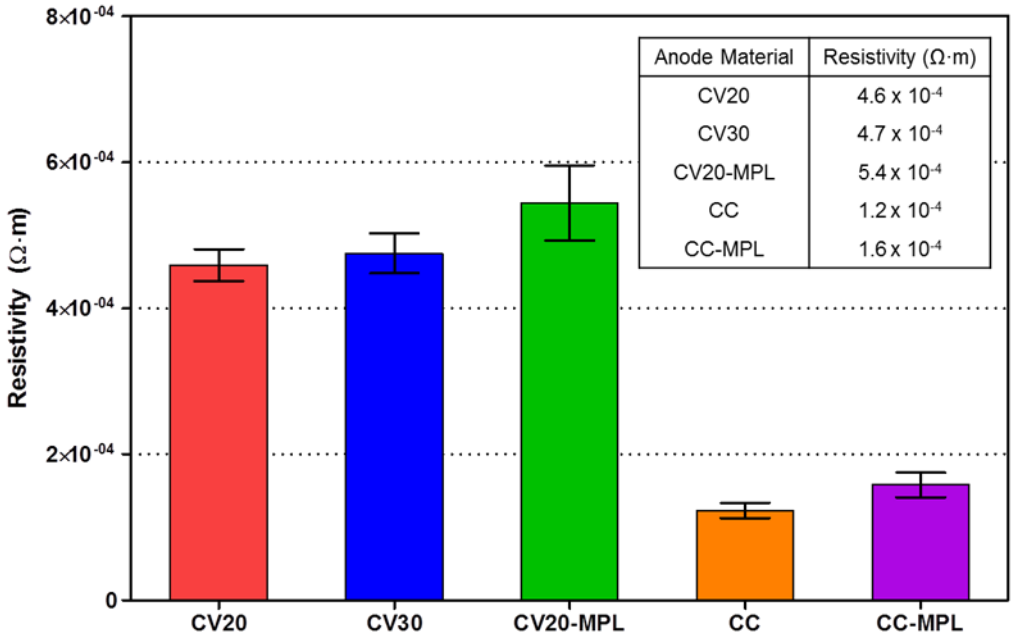

Figure 4.8 Electrical resistivity of each anode material (n = 3)

Although all the tested anode materials consisted of the same carbon base, the resistivity varied due to the particle size, aggregate structure and porosity (Polley & Boonstra, 1957). As a result, electrical resistivity slightly increased both in CV and CC through the MPL modification, which might be the result of the PTFE addition. In this particular case, and even though the differences in resistivity were small, it is clear that the PTFE loading was counteracting the increase in surface area, achieved from the MPL modification. It can also be noted that the resistivity of the off-the-shelf unmodified electrodes was much lower for the under-performing CC than the CV20 or CV30, and this may be attributed to the higher carbon loading. Since micro-structure and characteristics of MPL changes with different PTFE loadings (Paganin, Ticianelli & Gonzalez, 1996; Giorgi *et al.*, 1998), the amount of PTFE needs to be carefully selected for an optimum modification.

It should be noted that unlike resistance, resistivity is an intrinsic property thus resistivity value of a specific material is a ‘material constant’ and is independent of the dimensions of the sample. Resistance of the anodes used in the test could vary based on their shape and size. In this study, the same surface size was used for all materials but the volume of anodes was different, due to different thicknesses of the anode materials.

4.3.6. Long-term Operation

Durability is critical for long term MFC operation. The MPL modified anodes were operated for 7 months to investigate the long term stability. Good MFC anodes are expected to have a low level of fouling, however meeting this requirement is not trivial since a high void volume consisting of fine spaces for sustaining the microbial growth and multiplication, is essential. In an ideal continuous-fed system with the optimum flow rate, this could be avoided or minimised since clogging is a result of slow flow and poor hydrodynamic control. Even though the MFC systems were under continuous flow conditions, anode chamber clogging due to urine precipitation was observed, which would have been accompanied by membrane ageing (Fig 4.9). During the 7-month operational period, MFCs were opened 3 times, in order to clear the precipitation that was accumulating on the membranes and anode chambers. There might have also been an element of an accumulating biofilm on the anode electrodes. After cleaning the MFCs, performance of all units dropped but then quickly recovered to their previous performance levels.

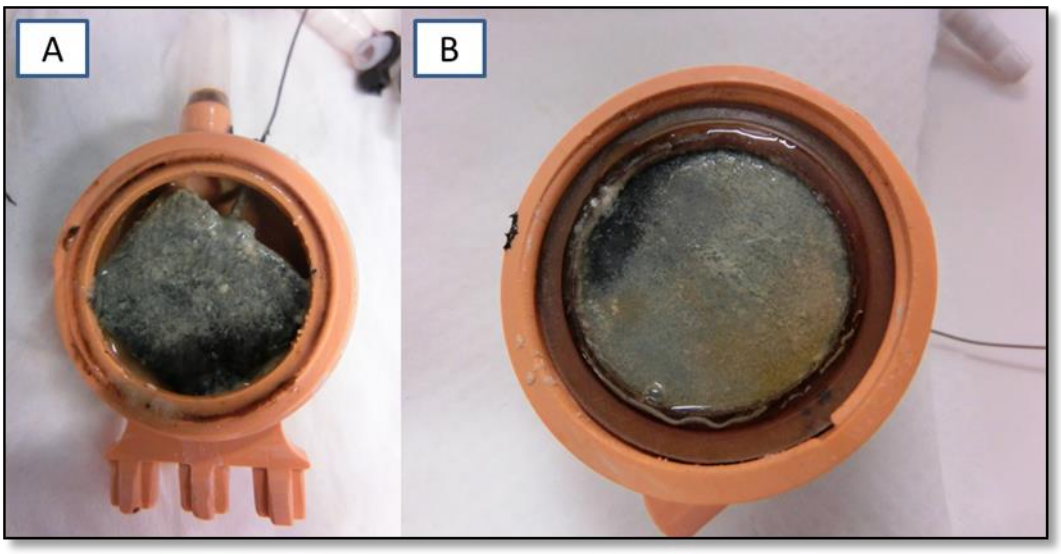

Figure 4.9 Photos of anode (A) and membrane to the anode side (B) when an anodic chamber was opened for cleaning

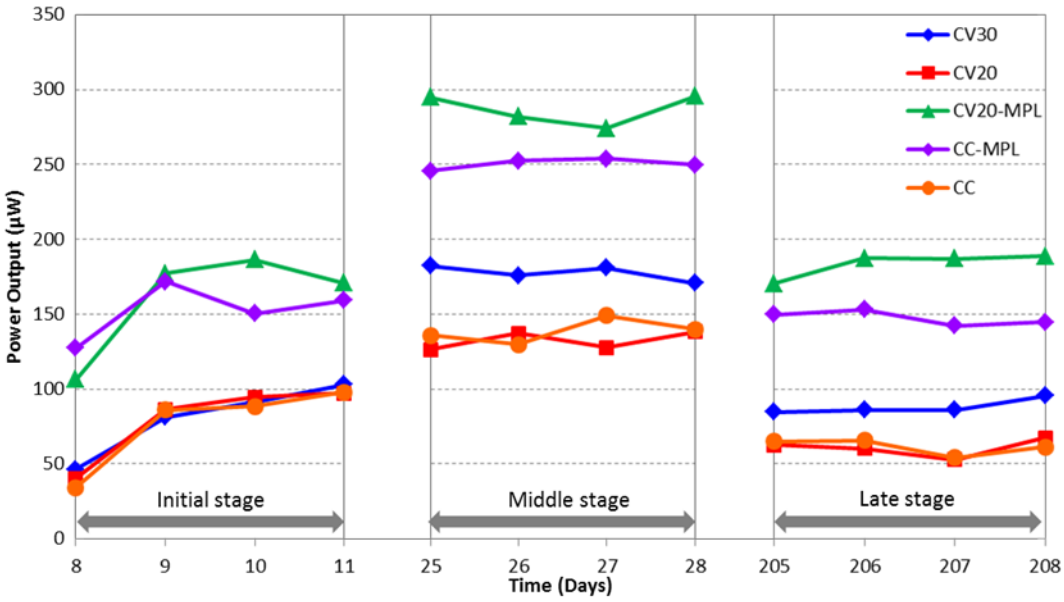

Figure 4.10 Power production from MFCs with different anode materials in each stage of the work; temporal profile

Figure 4.10 shows the power generating performance profile of tested anode materials at different stages of the experimental period. All MFCs showed a similar pattern: performance increased in the early stages and then decreased in the later stages. In the 2nd week, power output increased gradually as MFC anodes matured. After 1 month (referred to as middle stage), the power output of all MFCs improved significantly, which implied that biofilms on the anodes were fully established. After nearly 7 months, power output of all of the anodes declined compared to their output in middle stage. However, the extent of performance decline differed for each anode material. Over 50 % of the decline in performance occurred in unmodified CV30, CV20 and CC (50.4 ± 6 %, 54.1 ± 3 %, and 55.6 ± 1 %, respectively), whereas only 36.0 ± 5 % (CV20-MPL) and 41.2 ± 4 % (CC-MPL) of performance reduced in the MPL modified anodes. Their power performance change is also verified in the polarisation curves (Fig. 4.6). Maximum power output decreased by only 20.7 % and 18.5 % for the CV20-MPL and CC-MPL respectively, whilst 53.2 %, 43.9 % and 51.5 % reduction was recorded for CV30, CV20 and CC between the middle and late stages. Therefore, this result indicated that MPL modification improves anode durability for long-term operation.

Another factor to consider when selecting anode materials for an MFC system is substrate. Urine which was used as a substrate in this work tends to precipitate naturally. If a defined substrate with less insoluble matter is used, a different size of anode cavities or surface morphology may be more desirable. Or urine can be treated to have less precipitation, which would reduce the clogging issue and consequently lengthen the operation period between cleaning cycles. This will be examined in chapter 6.

4.3.7. Economic Evaluation

So far the MPL modified anodes were compared with the unmodified anodes in terms of power production, surface morphology, biocompatibility, electrical conductivity and long term durability. The economical aspect should not be overlooked even though the majority of MFC research is still at laboratory level. When the economical aspect is considered for a MFC system, various elements need to be taken into account. The costs of the anode materials tested were compared (Table 4.3), with respect to the material cost only, but not the cost of fabrication of the MPL modification. The modification of 1 m^2 of two anode materials, required approximately 40 USD. This additional cost gave 220 % and 180 % of performance improvement than unmodified CV and CC anodes, respectively and also enhanced the stability of the MFC systems. This cost could be reduced significantly for mass production. Although it is too early to justify that MPL modification is affordable or competitive in terms of cost, this consideration is important.

Table 4.3 Anode material cost spent in this study and other factors to consider

Anode material	Anode material cost (USD/m^2)	Power per cost (mW/USD)	Performance decline after 7 months of operation (%)
CV20	12.3	2.27	54.1 ± 3
CV30	16.2	2.22	50.4 ± 6
CV20-MPL	52.1	1.17	36.0 ± 5
CC	588.4	0.05	55.6 ± 1
CC-MPL	628.2	0.08	41.2 ± 4

Despite the fact that many researchers studying fuel cells, including hydrogen based fuel cells, claim environmentally friendly advantages of the technology, sustainability in

manufacturing, operating, and discarding of fuel cell systems is often forgotten. Especially for the MFC technology, which is believed to have green energy merits for the future, this is very important. Although a direct comparison of MPL modified anodes to other anode materials is difficult in terms of environmental impact, it is reasonable to assume that the extent of pollution did not increase much by the modification since no toxic chemical or heavy metal was used.

4.4. Improvement of Cathode Performance

As the thesis work progressed, the design and material of cathodes had been continuously changing with improvements. Consequently various types of cathode were explored throughout the work. Although a direct comparison of all the cathodes used in this work was not carried out, since it was outside the scope of this thesis, some details of each cathode type such as their performance, advantages, disadvantages and improvements made, are discussed in this section.

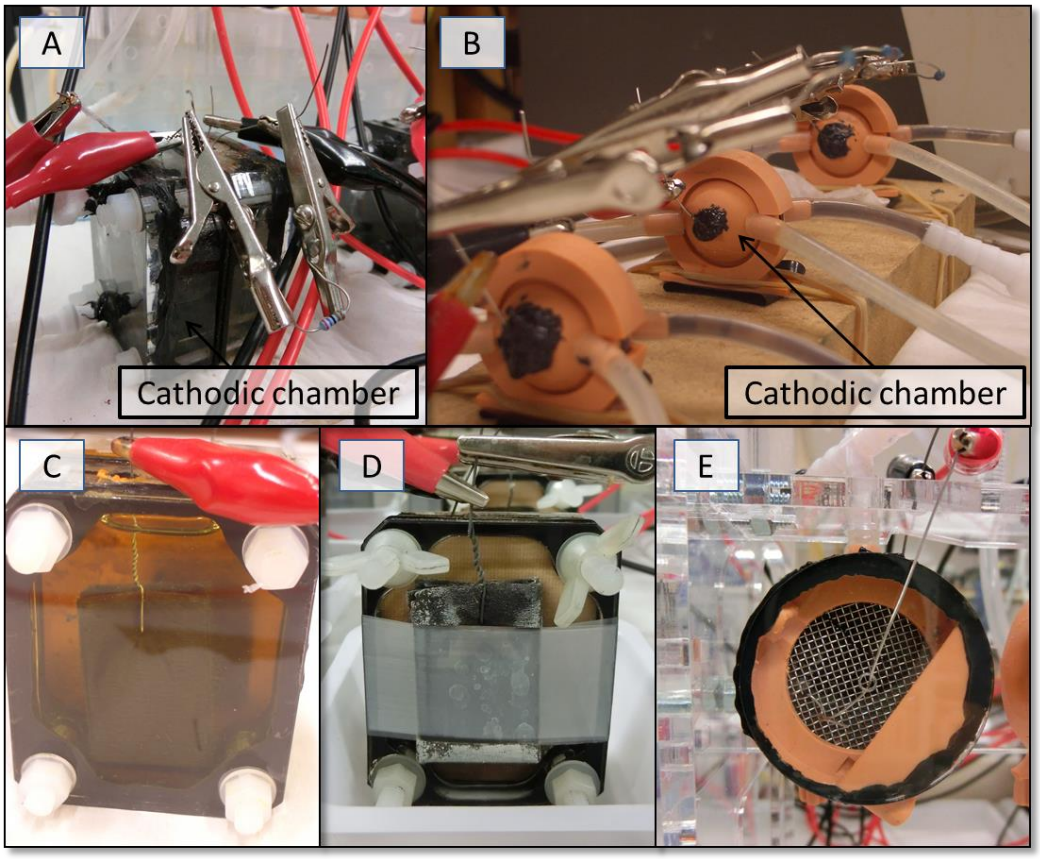

Figure 4.11 Various cathode designs applied in this thesis work
*(A) batch type aquatic cathode; (B) water re-circulating cathode; (C) ferricyanide cathode; (D) carbon veil open-to-air cathode; (E) Hot-pressed activated carbon open-to-air cathode

Batch type aquatic cathode

The earliest type of cathode was water-based for the two-chamber MFCs (Fig. 4.11 - A). The cathode chamber was half-filled with water in order to maintain moisture for proton transfer via the membrane as well as oxygen contact. The cathode, which was made of the same material and size as the anode (carbon fibre veil, surface area of 270 cm^2, 20 g/m^2 carbon loading), was immersed in water. In this design, cathodes use oxygen in the air as a terminal electron acceptor and the water prevents the electrode from drying out. This cathode was used for some preliminary work including additional pin electrode experiment, presented in appendix E.

Water re-circulating cathode

Due to the limited cathode performance of the batch type aquatic cathodes caused by poor oxygen transfer, water (catholyte) was re-circulated for S-MFCs using a peristaltic pump. In this design, dissolved oxygen (DO) in the water acts as a final electron acceptor. In order to maintain a certain level of DO, air pumps were attached to the water reservoirs. Because of the additional energy for operating air pumps, this design would not be suitable for scale-up thus new alternatives were required.

Ferricyanide cathode

Experiments used R-MFCs (both two-chamber and single chamber MFCs) and S-MFCs also employed ferricyanide cathodes only when minimising cathode limitations were needed in order to see the effects of each variable more clearly. Ferricyanide is a highly efficient electron acceptor and worked better than the previous two cathodes due to the low overpotential. However, despite the excellent performance, a major drawback of using ferricyanide cathode is its unsustainability since it is a toxic compound and requires replacement once it becomes depleted.

Carbon veil open-to-air cathode

Due to the poor performance or unsustainability of the previous cathodes, new alternatives were needed. Carbon veil open-to-air cathode is easily maintainable and by removing the cathode chamber, system design becomes simple and more favourable to scale-up. However, this type of cathode still underperformed probably again due to slow oxygen transfer from the air to the cathode surface and matrix. Moreover it requires periodic hydration. Although water is formed in the cathode at the end of the series of MFC electron generation reactions, the water formation rate would have been slower than the water evaporation rate in the laboratory environment with the lab ventilation in place, running

continuously. Cathode dehydration hinders oxygen diffusion and causes less physical contact between the membrane and the cathode electrode. Cathode underperformance can be seen in Fig.4.12. When the cathode was hydrated, power output increased instantly and then gradually decreased to the previous level, which implies that the cathode was running under sub-optimal conditions. A similar phenomenon was observed previously (Ieropoulos, Melhuish & Greenman, 2007).

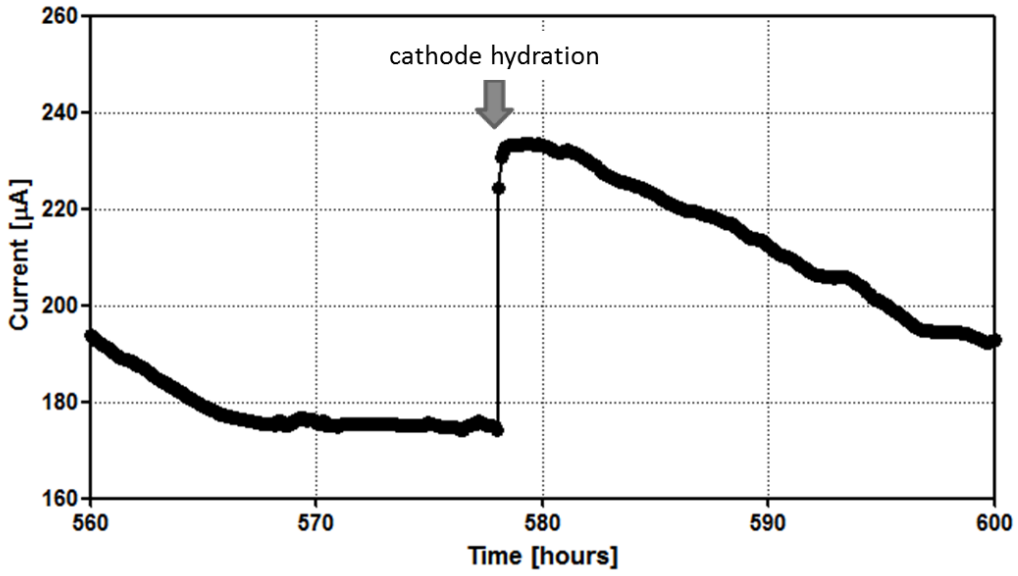

Figure 4.12 Current change when a carbon veil open-to-air cathode hydrated with water

In order to minimise the water evaporation as well as secure the physical contact between the cathode and membrane, this type of cathode was wrapped in parafilm.

Hot-pressed activated carbon open-to-air cathode

The last type of cathode, hot-pressed activated carbon open-to-air cathodes as described in section 3.2.3, showed a significant improvement of performance compared to the carbon veil open-to-air cathodes. Figure 4.13 illustrates power curves of the two MFCs; one with a carbon veil open-to-air cathode (12 layers of CV20, total surface size: 50.2 cm^2) and the

other one with a hot-pressed activated carbon open-to-air cathode (1 layer, total surface size: 4.9 cm^2). Despite the reduced surface size, P_{MAX} rose almost five-fold from 53.0 µW to 257.9 µW with the replacement.

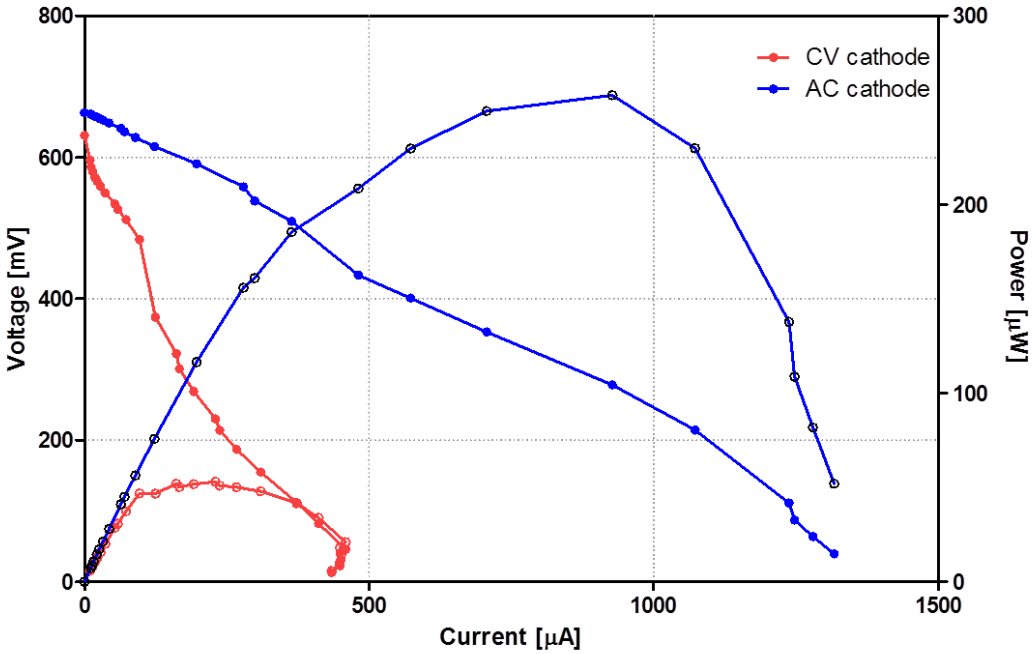

Figure 4.13 Performance comparison of MFCs with a carbon veil open-to-air cathode (CV cathode; red line) and hot-pressed activated carbon open-to-air cathode (AC cathode; blue line)

Another advantage of this type of cathode is that there is no need for cathode hydration, which renders the system maintenance easy. In fact, water formation was observed from MFCs with these cathodes. Furthermore cathode flooding happened as a result of water accumulation, which could be easily solved by minimal design changes of the cathode part. Cathode flooding will be discussed in detail in section 5.4.

4.4 Chapter Conclusions

Depending on the final application of the MFC, different materials and designs of MFCs need to be selected. The final application of this thesis was waste/wastewater clean-up and the approach taken was system scale-up through multiples of relatively small sized MFC units. To achieve this goal, affordable, robust, and environmentally friendly as well as well-performing materials and designs were sought.

In terms of MFC component material and design, different types of membrane, anode and cathode were tested and significant findings were generated as follows;

(1) Within the same manufacturing line, CEMs performed better than AEMs and CEMs were more durable than AEMs against substrate depletion. When considering cost performance, some AEMs could be a better option for scale-up.

(2) The MPL modification of anodes increased power performance, bacterial production rate of anode and MFC stability. Since PTFE caused higher resistivity and hydrophobicity, optimisation of its use in terms of concentration or heating temperature during the MPL making process, or finding an alternative binder that could replace PTFE, needs to be further investigated. This feasibility study indicated that MPL modification for anode materials is desirable.

(3) Throughout the thesis work, continuous improvements had been made in materials and designs of cathodes. Hot-pressed activated carbon open-to-air cathodes showed an excellent cathode performance and potential of easy maintenance.

Three major reactor designs with minor variations were also tested and the last version of reactor design, C-MFC, was capable of facilitating continuous feeding and the open-to-air cathode.

Findings reported in this chapter were employed in the following work.

5. Anodophilic Biofilm

5.1. Introduction

In addition to the system design aspect of MFCs discussed in the previous chapter, understanding the biological aspect of the MFC anode is essential for successful MFC operation. Different running conditions such as temperature, external load and feedstock have a great effect on the condition of anodic biofilms, which in turn could determine the MFC performance. In this chapter, dynamic characteristics of anodophilic microbial communities were investigated.

*Parts of this chapter have been published as You, J., Walter, X.A., Greenman, J., Melhuish, C., and Ieropoulos, I. (2015) Stability and reliability of anodic biofilms under different feedstock conditions: towards microbial fuel cell sensors. Sensing and Bio-Sensing Research **6**, 43-50.*

5.2. Thermophilic Biofilm

Since the microbial metabolic activity rate is likely to increase in thermophilic conditions compared to psychrophilic or mesophilic, thermophilic MFCs had already demonstrated increased current generation (Jong *et al.*, 2006; Min, Román & Angelidaki, 2008; Larrosa-Guerrero *et al.*, 2010). For this reason, and in attempt to investigate the temperature effect in the MFCs of the current study, pure and mixed culture thermophilic MFCs were tested in order to investigate the temperature effect on power generation and microbial behaviour at high temperature with the intention of creating a mixture of well performing electro-active thermophiles which could outperform mesophilic MFCs and potentially demonstrate the breakdown of substrates that is not possible under ambient conditions.

5.2.1. Methods Specific to Experiments

Four different bacterial species were isolated from a previous experiment, which was running under thermophilic conditions (60 °C) in fed-batch mode. The origin of the previous MFCs was activated sludge from Wessex Water sewage treatment plant (Saltford, UK). The isolated species and new activated sludge were then cultivated separately in full strength 2SPYN medium (see section 3.1.2) for 24 hours at 60 °C. The cultivation media was centrifuged for 20 minutes at 4,000 rpm, 20 °C and re-suspended in 2SPYN solution with the OD range between 0.4 - 0.8 for all five culture groups (four pure cultures and one mixed culture as in activated sludge) before being inoculated. Four different species were verified by colony characteristics from three types of agar plates; tryptic soy agar (TSA), brain heart infusion (BHI) agar and cystine lactose electrolyte deficient (CLED) agar. After inoculation, for the first 2 weeks of maturing period, 5-times diluted 1.8 mL of 2SPYN solution was fed on a daily basis. After this period, the same feedstock solution (10 times diluted) was supplied continuously at a flow rate of 5.3 mL/h using a peristaltic pump (Watson Marlow, 205U), which resulted in a HRT of 8 minutes. S-MFCs were used in triplicate. The catholyte, 600 mL of tap water, was re-circulated at a flow rate of 22.5 mL/min in order to provide aqueous oxygen to the cathode. The water was replaced twice a week.

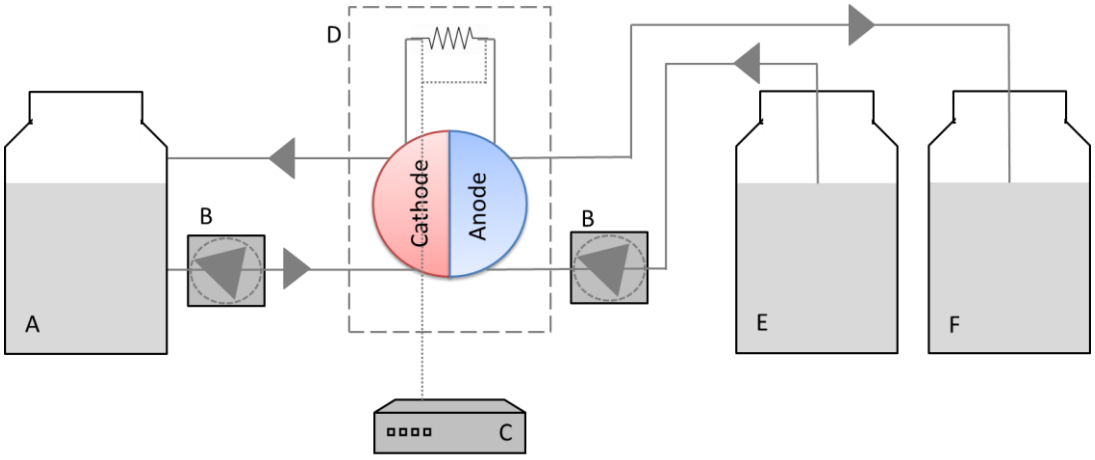

Figure 5.1 Schematic diagram of the experimental set-up: (A) tap water recirculation tank; (B) pumps; (C) data logger; (D) 60 °C temperature controlled container; (E) feedstock bottle; (F) effluent collection tank

In order to prevent the bacteria from growing back from the anode to the feedstock bottle, which may cause cross-contamination among MFCs with different culture groups, anti-bacterial grow-back devices were employed (Figure 5.2). In the middle of the feeding tubes from the feedstock bottle to an MFC, a plastic flow connector with a narrow tip was connected to the end of a 5 mL volume syringe(type 1) or a 5 mL volume syringe inserted in a 50 mL volume syringe(type 2) in order to create an air gap inside the syringe. The air gap provided a disconnection of flow thus the bacterial grow-back was expected to be inhibited.

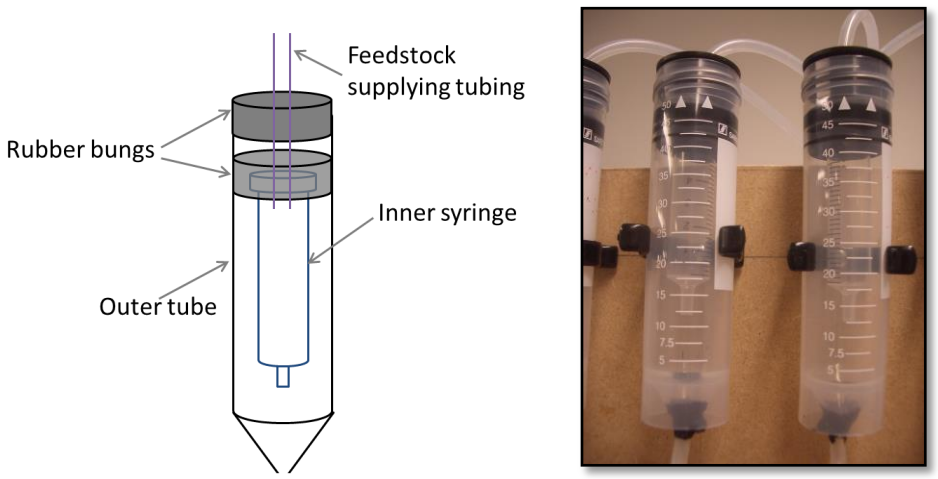

Figure 5.2 Anti-bacterial grow-back device: diagram (left) and photo (right)

On day 36, a substrate flow rate test was performed at flow rates of 5.3, 13.2, 32.4, 78.2 and 153.8 mL/h, to investigate its effect on the MFC performance. Each flow rate was applied for 1 hour and all MFCs reached steady states within the time period.

All MFCs were connected with 12 kΩ resistors from the beginning of experimental running. This experiment was carried out in an incubator at 60 ± 5 °C.

5.2.2. Power Generation of Different Species

Figure 5.3 shows power produced by five cultural groups from the bacterial inoculation to the end of experiment during the first phase. When it was switched to continuous feeding mode on day 13, power output of sample 1 (unknown species) started to increase, which implies that the growth rate of this species was higher than the other cultures. On day 21, sample 1 seemed to have reached a steady state, around 9 mW/m^2 (absolute power: 25 µW, grey arrow and red dashed line in the graph), followed by sample 3 and 4. Once sample 3 reached a steady state, it produced almost the same level of power output as sample 1. Sample 4 seemed to grow faster but it generated less power compared to sample 3. Although sample 2 started to produce a meaningful output earlier than sample 3 and 4, electricity generating performance of the culture was the lowest of all. The active bacterial growth of sample 1 and 3 showed that these two species grow well under the operating conditions and given substrate.

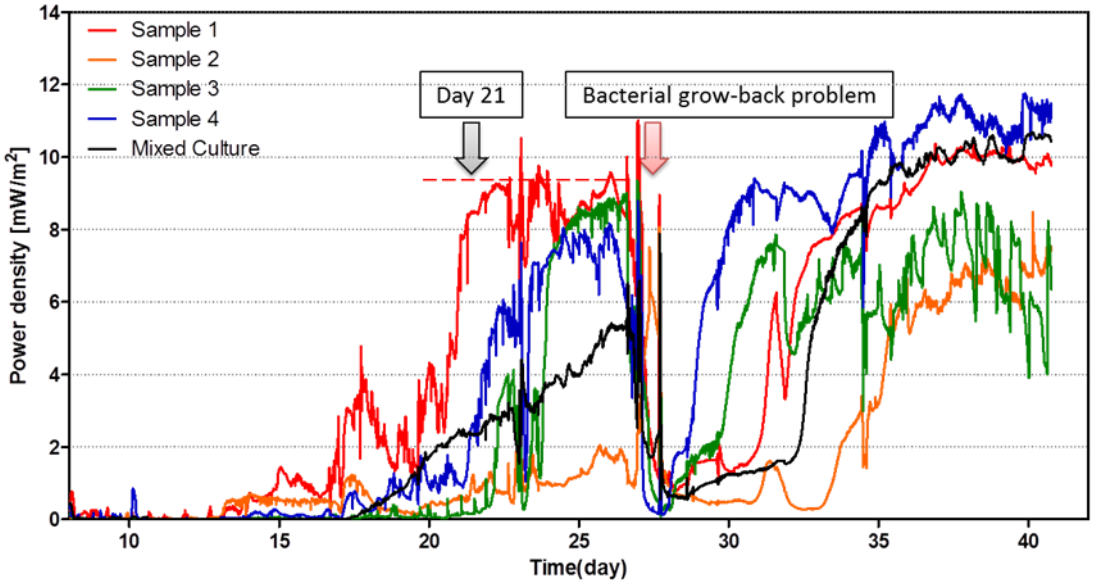

Figure 5.3 Power generating performance of five thermophilic S-MFCs over a 40-day period
* The red arrow indicates when anti-bacterial grow-back devices needed to be replaced due to bacterial grow-back occurrence. (n = 2)

During the experiment, on day 27, the experiment had to stop in order to replace the anti-grow-back devices since cells grew beyond the devices toward the feedstock bottle. Subsequently new anti-grow-back devices with bigger volume (type 2) were applied, but this experiment had to stop because bacterial grow-back across the devices happened once again. Since MFCs shared a common medium solution, bacterial contamination of this feedstock meant that the data would be unreliable. Therefore a new solution for this problem was required. All cultures were affected by the temporary halt, which allowed for several short exposures to a lower temperature and no substrate supply for a day. When the system went back to the original operating condition, it took varying lengths of time for the MFCs to recover. Sample 4 recovered most rapidly followed by sample 3 and 1 which took approximately 3 and 4 days respectively.

Although bacterial species identification was not performed, it can be hypothesised that there were electrochemically active species as well as non-active or less-active species. The

purity of MFC cultures was checked by subculture on agar plates periodically (every 3 - 4 days). Every pure culture kept its original condition except sample 2 and 4 at the end of the experiment. After day 32 when the power output of sample 2 started to rise, subculture results indicated that there were more than 2 species in the cell. Therefore it was assumed that the late power increase that happened in sample 2 and 4 was because of an influx of electrochemically active species from one or some of the other cells. Although this mixing of different species happened accidently, the results are still very interesting since this could verify the following two hypotheses; (1) a mixture of well performing electro-active thermophiles which could outperform a single electrochemically active species, (2) mixed culture perform better than pure culture under certain conditions.

5.2.3. Effect of Flow-rate on MFC Performance

Figure 5.4 shows power output of each MFC at different flow rates. The power density of all five MFCs climbed when the flow rate increased from 5.3 mL/h to 13.2 mL/h. But output of sample 3 and 4 decreased when the flow rate further increased. Overall, the power output of MFCs did not increase to a great extent (less than 10 % of the original values) with flow rate rise. It is likely that the applied flow rates were too fast for the size of S-MFCs since they had a very small anode volume of 0.7 mL. For example the HRT of flow rate 32.4 mL/h was only 1.3 minutes. Higher flow rates result in higher shear forces which could wash off the anodic biofilms. Another reason for the power drop at higher flow rates was an exposure to lower temperature. Since the feedstock solution was placed outside of the 60 °C incubator, there was not enough time to warm up the substrate at high flow rates. Throughout the experiment, thermophilic MFCs seemed very sensitive to temperature change and power output decreased immediately when the temperature inside the incubator dropped.

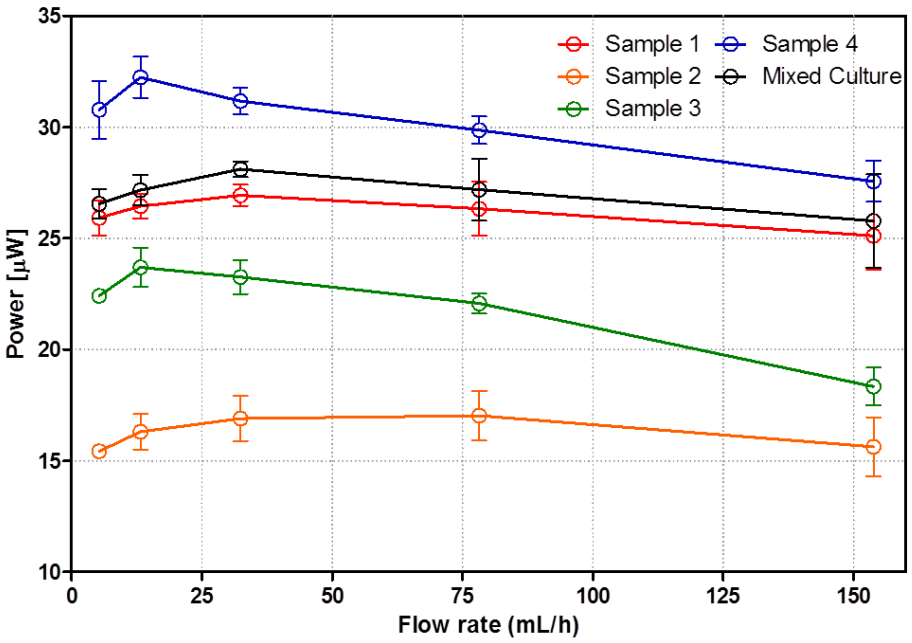

Figure 5.4 Flow rate effect on power generation of thermophilic S-MFCs

5.2.4. Temperature Effect on MFC Performance

Temperature effect on the thermophilic MFC performance was also investigated by changing the incubator temperature. As expected, temperatures lower than the operating temperature, 60 °C, were not preferred by all MFCs. In addition power output dropped at higher temperature, 70 °C. Although the extent of output decline was different, all MFCs showed the same pattern; the highest power output was produced at 60 °C and it decreased as temperature went up and down from this temperature point. Performance decrease with temperature drop was also observed in other studies with MFCs acclimated to a certain operating temperature (Wang, Feng & Lee, 2008; Patil *et al.*, 2010; Cheng, Xing & Logan, 2011) and this is probably mainly due to metabolic activity rate change. The thermophilic MFCs in this study might have not been tolerant to the highest temperature, 70 °C due to enzymatic activity degradation. Also decreased concentration of dissolved oxygen in the catholyte at 70 °C could account for the performance decline.

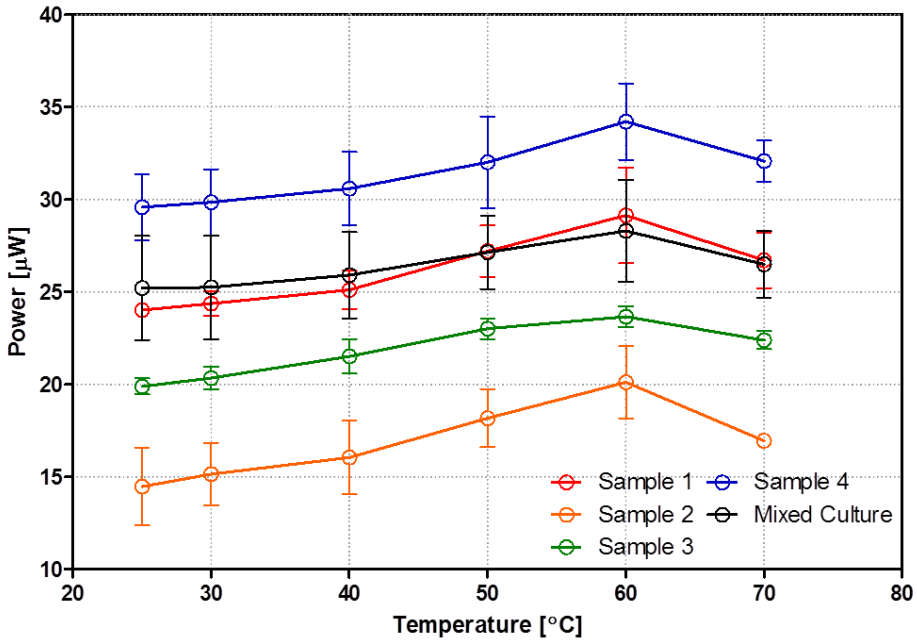

Figure 5.5 Temperature effect on power generation of thermophilic S-MFCs

5.3. Effect of External Resistance on Anodic Biofilm

As discussed in section 2.3.3, there are many parameters that affect the anodic biofilm, the previous section demonstrated the role of temperature, and in this section the importance of external resistance will be investigated. Under a low R_{EXT} (heavy load), there is a bigger demand for electron flow from bacterial cells to the anode. On the other hand, under a high R_{EXT} (light load), anodophiles tend to build up more biomass rather than conveying electrons. Thus it is important to find an optimum R_{EXT} and this depends on the expected outcomes such as maximisation of power output or Coulombic efficiency, or minimising biomass production. Although there have been a few studies looking into the effects of external resistance loading on the length of MFC maturing (Lefebvre *et al.*, 2011; Pinto *et al.*, 2010; Zhang *et al.*, 2011a), there is little information about anode biofilm behaviour after this phase. In this work, therefore, different strategies for anodophile enrichment were employed by loading different resistances to find out the best value which allows maximum power

output or shortens the maturing period. Also the effect of R_{EXT} on the anode biofilm performance after the maturing period was investigated.

5.3.1. Methods Specific to Experiments

For this work, a total of 6 R-MFC with open-to-air cathodes were used. For the first seven days, all MFCs were left in open circuit condition in order to allow bacteria to settle in the environment and grow on the anodes. Then three different external loads, 100 Ω, 1 kΩ and 10 kΩ, were applied onto duplicates from 8th day of the experimental run. On day 33, after nearly 2 weeks of stable power output generation, R_{EXT} values were changed to match R_{INT} values of each MFC in order to see effect of impedance matching on power generating performance. MFCs were fed with 5 mL of neat (untreated) human urine once a week. Cathodes were periodically hydrated with tap water (pH 7) on a daily basis. Polarisation measurement was conducted periodically, usually 3rd day after feedstock replacement, unless otherwise stated. These experiments were performed in ambient temperature (22 ± 2 °C).

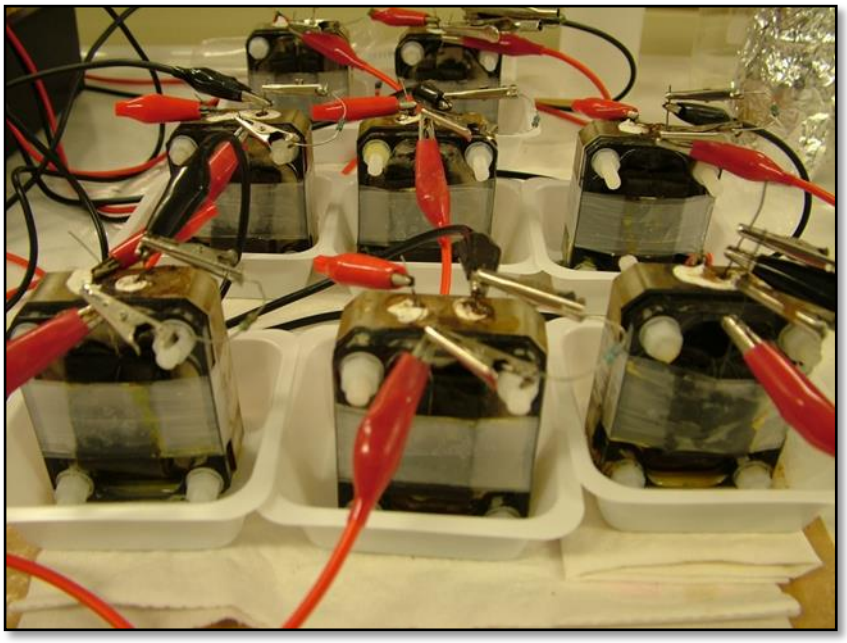

Figure 5.6 Photo of R-MFCs used in the work

5.3.2. Performance Comparison

Figure 5.7 illustrates temporal profiles of voltage, current and power produced by MFCs with different R_{EXT}. The open circuit values for all MFCs increased constantly for the first 4 days and then reached a steady state around 530 – 570 mV. Once the MFCs were loaded, voltage dropped, and then gradually increased over time as the MFCs matured. As expected, the MFCs connected to the highest R_{EXT} (i.e. 10 kΩ) produced the highest voltage around 400 mV when they reached a steady state. The other MFCs with medium and lowest external resistance (i.e. 1 kΩ and 100 Ω) produced about 270 mV and 120 mV respectively in their steady state. This pattern is reversed with current generation; MFCs with lighter loads produced lower current and MFCs with heavier loads produced higher current. For example, MFCs connected to 100 Ω generated up to 1,200 μA while MFCs with 10 kΩ made only 40 μA. In terms of power generation, MFCs with the heaviest load (100 Ω) produced the highest power between 4 mW/m^2 and 6 mW/m^2 (absolute power: 108 – 162 μW). This difference in terms of power generating performance under three different external loads is thought to be due to selectivity of anodic microbial community or metabolic activity. Bacteria community analysis of anodic biofilm could be able to provide a clearer picture on this discussion.

On the other hand, no significant difference in the length of maturing period was observed in this study. Based on power generation (Fig. 5.7) and results of polarisation measurements (Fig. 5.8), all MFCs seemed mature after 20 days of operation. This might be due to the limit of the fed batch system where maintaining constant bacterial metabolic activity is limited.

After the MFCs matured and started producing stable outputs, the value of external resistance was changed to match the internal resistance value of each MFC. 100 Ω, 150 Ω and 1 kΩ were loaded on MFCs that were previously loaded with 100 Ω, 1 kΩ and 10 kΩ in order. This is called impedance matching, and in theory, a fuel cell can produce its maximum

power under this condition (maximum power transfer, MPT). During this period, MFCs started with heavier loads (100 Ω and 1 k Ω) showed similar performance generating about 4 – 6 mW/m^2 (absolute power: 108 – 162 μW) whereas MFCs loaded with 10 kΩ previously, underperformed others.

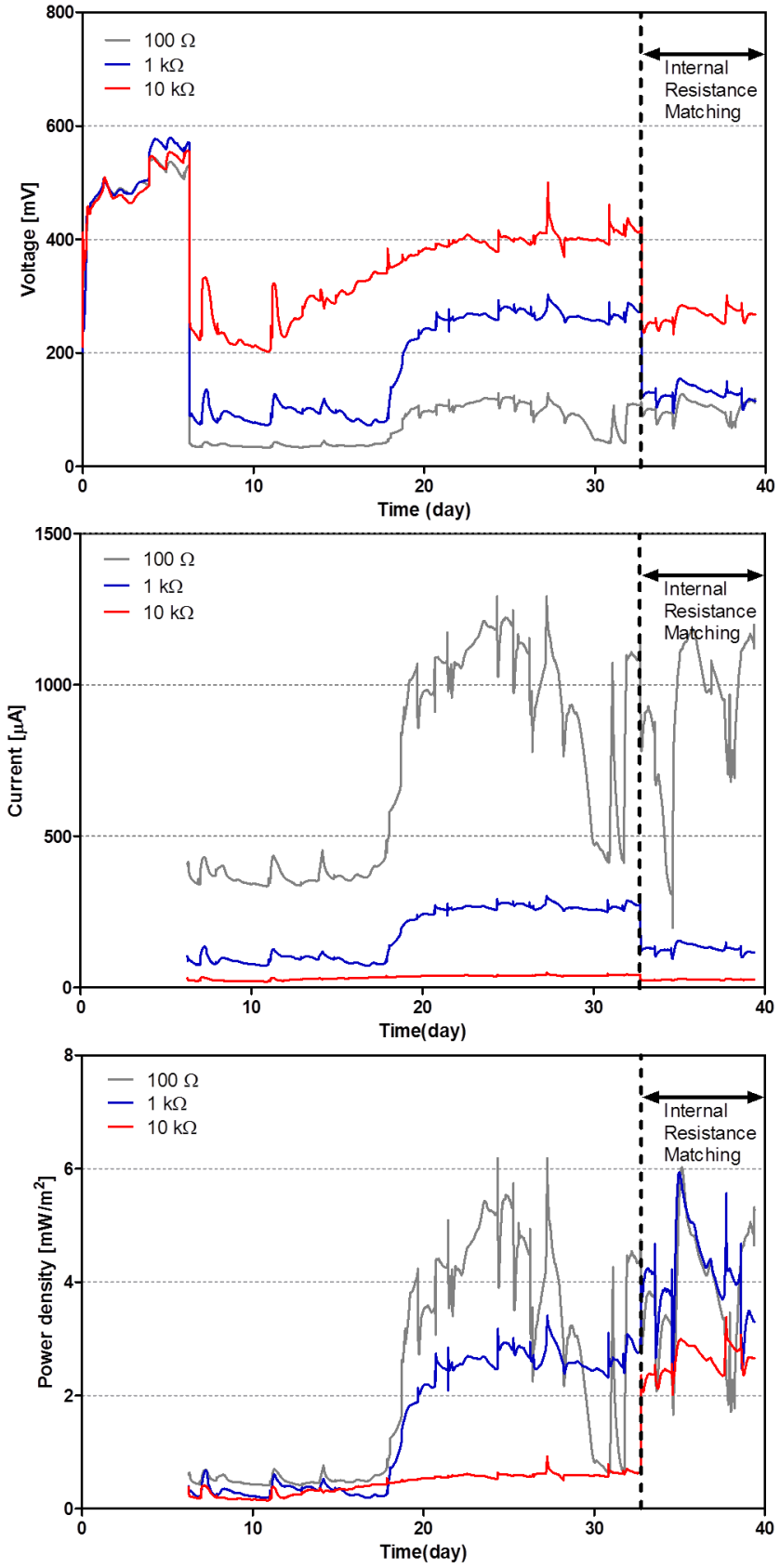

Figure 5.7 Temporal profile of voltage, current and power from MFCs with different R_{EXT}

Polarisation experiments were performed every week in order to understand each MFC properties after MFCs were connected to external resistances. Figure 5.8 shows the maximum power output recorded every week and the calculated R_{INT} values for the MFCs loaded with different R_{EXT}. In the beginning, P_{MAX} values of all MFCs were similar to each other in a range of 28.6 - 39.8 µW (1.1 - 1.5 mW/m^2). In the second week, however, P_{MAX} increased significantly from the first week, apart from the MFCs with 10 k significantly from the first week, apart from the MFC ated and each MFCs and the others. The P_{MAX} of MFCs with 100 Ω and 1 kΩ was 104.9 µW and 112.5 µW (3.9 mW/m^2 and 4.2 mW/m^2) which are nearly twice higher than the value of MFCs with 10 kFC 53.2 µW). In the third week, the difference in power became even bigger. A similar pattern was shown in internal resistance, all MFCs had identical internal resistance values at the beginning but this decreased dramatically a week later with the exception of the MFCs using 10 kΩ loads. These values did not change much in the third week. This suggests that R_{EXT} is one of the factors that determine power generating performance of MFCs. Too light R_{EXT} compared to R_{INT} of a MFC system hinders performance improvement of the system. Therefore the external resistance value is a critical parameter to be considered, when setting-up MFCs.

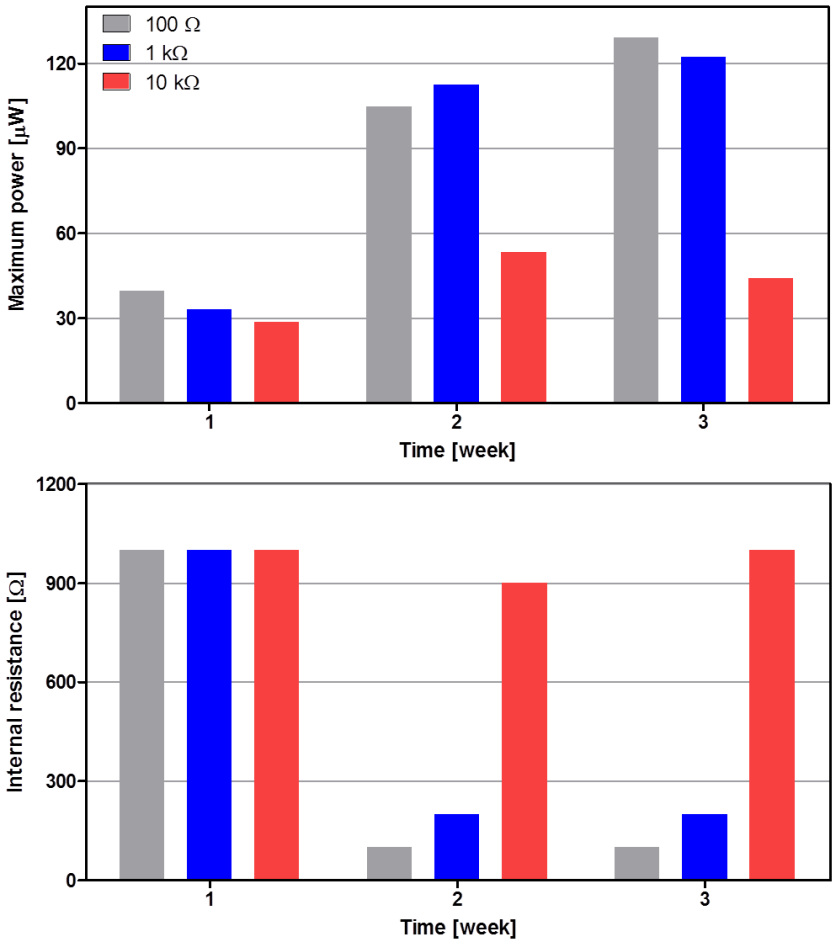

Figure 5.8 Maximum power output and internal resistance of MFCs in each week
* calculated from polarisation curves

5.3.3. Importance of Maximum Power Transfer Point

Generally an MFC is considered to be mature when its output reaches a steady level. As shown in Fig. 5.7, after the 3rd week, output of all three types of MFCs stayed relatively stable over 10 days. However, significant performance enhancement of MFCs with 1 kΩ and 10 kΩ was observed when their R_{EXT} values were changed to match the R_{INT} of each MFC. The average power output for 5 days before and after the resistance change increased 65.9 % and 371.4 % respectively. This is why MFCs need to be operated at the maximum power transfer point (MPTP) by impedance matching. Impedance matching does not only bring

maximum power output but also has the potential of changing MFCs properties. A follow-on polarisation experiment shown in Fig. 5.9 illustrates that there was a significant improvement in power generation and internal resistance in MFCs with the lightest load. P_{MAX} increased more than 3 times from 44.3 µW (1.6 mW/m^2) to 157.7 µW (5.8 mW/m^2) and R_{INT} decreased from 1 kΩ to 200 Ω for the same period. Therefore it is a requirement to run MFCs under an R_{EXT} which matches or is close to their internal resistance in order to maximise their power generating potential.

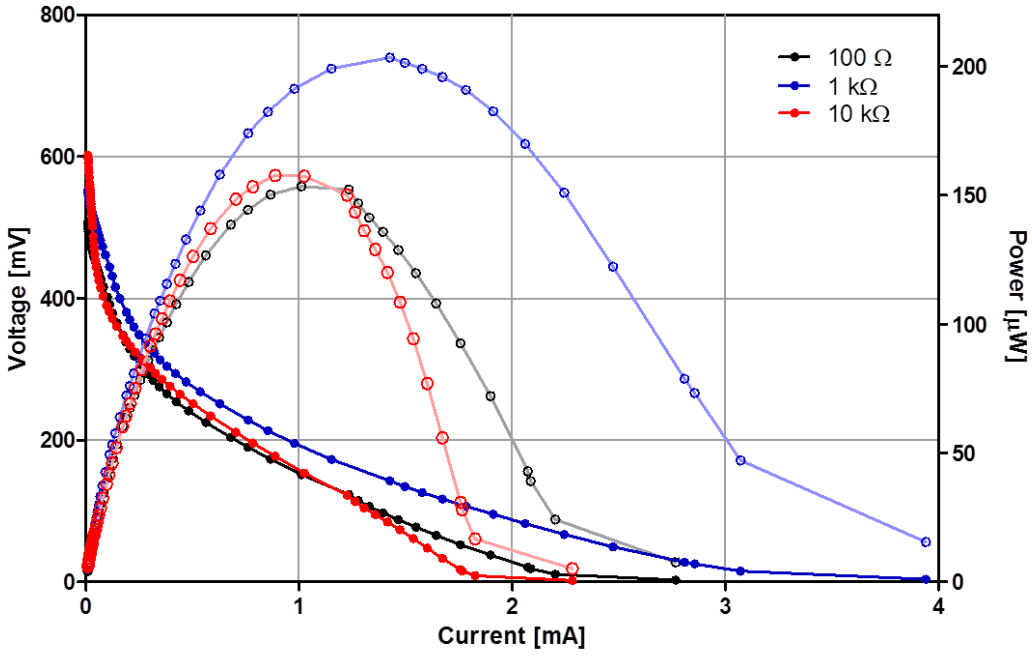

Figure 5.9 Polarisation and power curves of MFCs after running under impedance matching condition

Also the R_{INT} of MFCs should be monitored continuously since MFCs are bio-systems in which anode biofilms change their metabolic activity constantly according to the environmental conditions thus R_{INT} can vary during the operation. This can be done by a periodic polarisation measurement or connecting different resistors to find the R_{EXT} giving half the OCV after measuring the OCV as described in section 2.2.4. However these methods

involve inevitable disruption of the MFC operation because both require disconnecting the load. Another method is to predict the R_{INT} using a simulation model (Pinto *et al.*, 2010). Furthermore a novel way of monitoring the OCV of a MFC, which could facilitate continuous impedance matching by employing the pin method, was tested in this thesis and the results are presented in appendix E.

5.4. Stability and Variability of Anodic Biofilm

As discussed in section 2.3.3, different substrates can have an impact on the structure and composition of the microbial community, which subsequently influences MFC performance. Furthermore, in addition to performance in terms of power generation and coulombic efficiency, the integral composition of the bacterial community enriched under a specific feedstock condition has the potential to acclimate to other substrates depending on the substrate type (Chae *et al.*, 2009; Zhang *et al.*, 2011b). Although previous studies have emphasised the importance of initial feedstock for MFC operation, bacterial cell metabolic adaptation would happen after repeated changes with exposure to a new substrate for prolonged periods, which could diminish the effect of initial carbon sources. A question still remains about how this transition would proceed in terms of biofilm metabolic activity and its power generating performance. The objective of this study was therefore to (1) demonstrate the change of biofilm metabolic activity and power generating performance under different feedstock conditions, and (2) investigate the feasibility of obtaining stability and reliability of MFC anodic biofilms during the feedstock changes. For this study, MFCs were fed continuously with two different substrates, acetate (carboxylic acid, monomer, non-fermentable) and casein (protein, polymer, hydrolysed into monomers).

5.4.1. Methods Specific to Experiments

A total of 16 C-MFCs were used in two groups (group A and B) for this work. Anodes were made of CV30 material with 10 layers of 1 cm^2 (width: 1 cm, length: 1 cm). A hot-pressed activated carbon open-to-air cathode with a total surface area of 4.9 cm^2 was pushed on to the membrane. The cathode window was sealed with a punched circular Perspex sheet with 25 mm diameter in order to prevent the cathode from drying but still enabling oxygen contact from air. Stainless steel mesh was attached on the cathode to enhance current collection.

Modified M1 minimal media with different sole carbon sources (acetate, casein, glutamine or glucose, equivalent COD value of 1150 ppm) were fed to the MFCs continuously at a flow rate of 1.89 mL/hr. When the MFCs produced over 20 μW under an external load of 3 kΩ, the external load was changed to 1 kΩ and stayed the same throughout the study.

Occasional cleaning of the anode chambers was required when blockage in the anodic chamber inlets or outlets occurred due to bacterial overgrowth. Blockage was removed manually, after opening the MFC chambers, or was washed off by switching the media flow to a high rate (580 mL/hr) for 2-3 minutes.

The experiment mainly consisted of three steps; (1) two groups of anodic biofilm from the same inoculum but matured with different substrates (acetate for group A and casein for group B) (2) once MFCs reached steady states in terms of power output and bacterial cell population (monitored in the perfusate), the two substrates were swapped (3) once new steady states were reached, the MFCs were switched back again to their original substrates, to monitor the microbial community response. Additionally a 3^{rd} and 4^{th} substrate, glutamin and glucose, were provided to both groups for 3 days each at the end of the study.

Community level physiological profiling measurements using Biolog were carried out in duplicate at the end of each step. The rest of all chemical, biological and electrical measurements were conducted at least in triplicate.

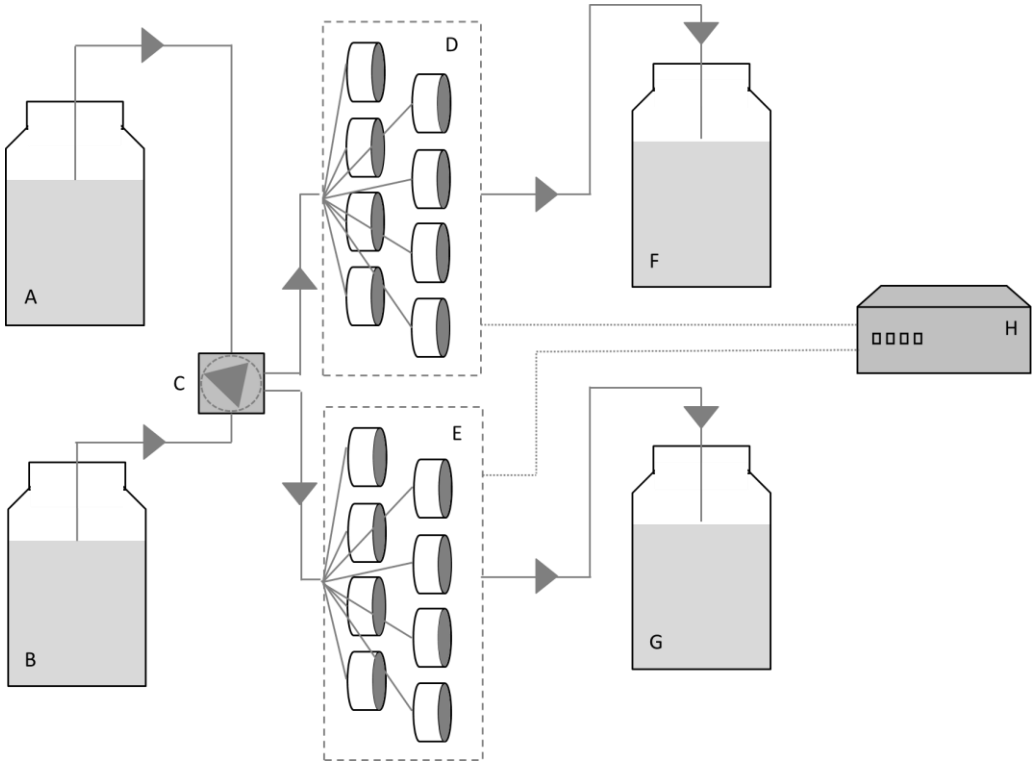

Figure 5.10 Schematic representation of the experimental set-up: (A) feedstock-acetate based; (B) feedstock-casein based; (C) peristaltic pump; (D) group A MFCs; (E) group B MFCs; (F) effluent collection tank no.1; (G) effluent collection tank no.2; (H) data logger

* All the MFCs were fed individually

5.4.2. Main Contributors for MFC Power Generation

As can be seen in Fig 5.11, once the MFCs had matured and showed stable performance under the given feedstock, blockage in the anodic chamber inlets or outlets was observed occasionally mainly due to the overgrowth of bacteria attached inside the anode chamber wall, suspended in the anolyte and the consequent increase of extracellular polymeric substance (EPS), which required periodic cleaning of the anodic chambers. Figure 5.12 shows bacterial population changes of effluent and current generation during one cleaning

cycle (8 days in this case). After cleaning, suspended cell numbers measured in OD_{600} and CFU initially dropped, then rose following an exponential curve whereas current production did not seem to be affected by the cleaning. Therefore suspended cells, which consisted of daughter cells from the anode electrode biofilm, daughter cells from the anode chamber wall biofilm, and planktonic cells did not have a great effect on electricity generation of the MFCs used in this work. This also suggests that the anodic biofilm on the electrode was relatively stable.

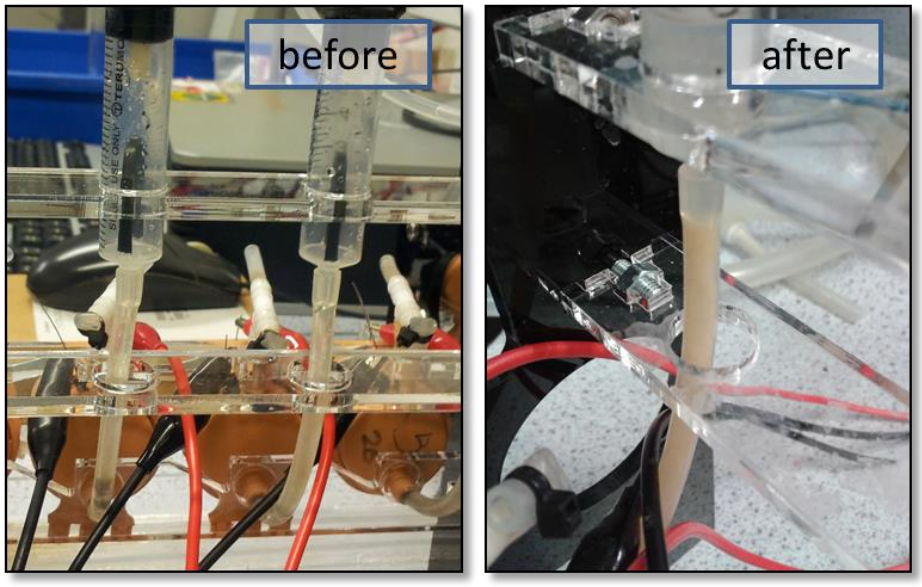

Figure 5.11 Bacterial growth inside substrate supplying tubing

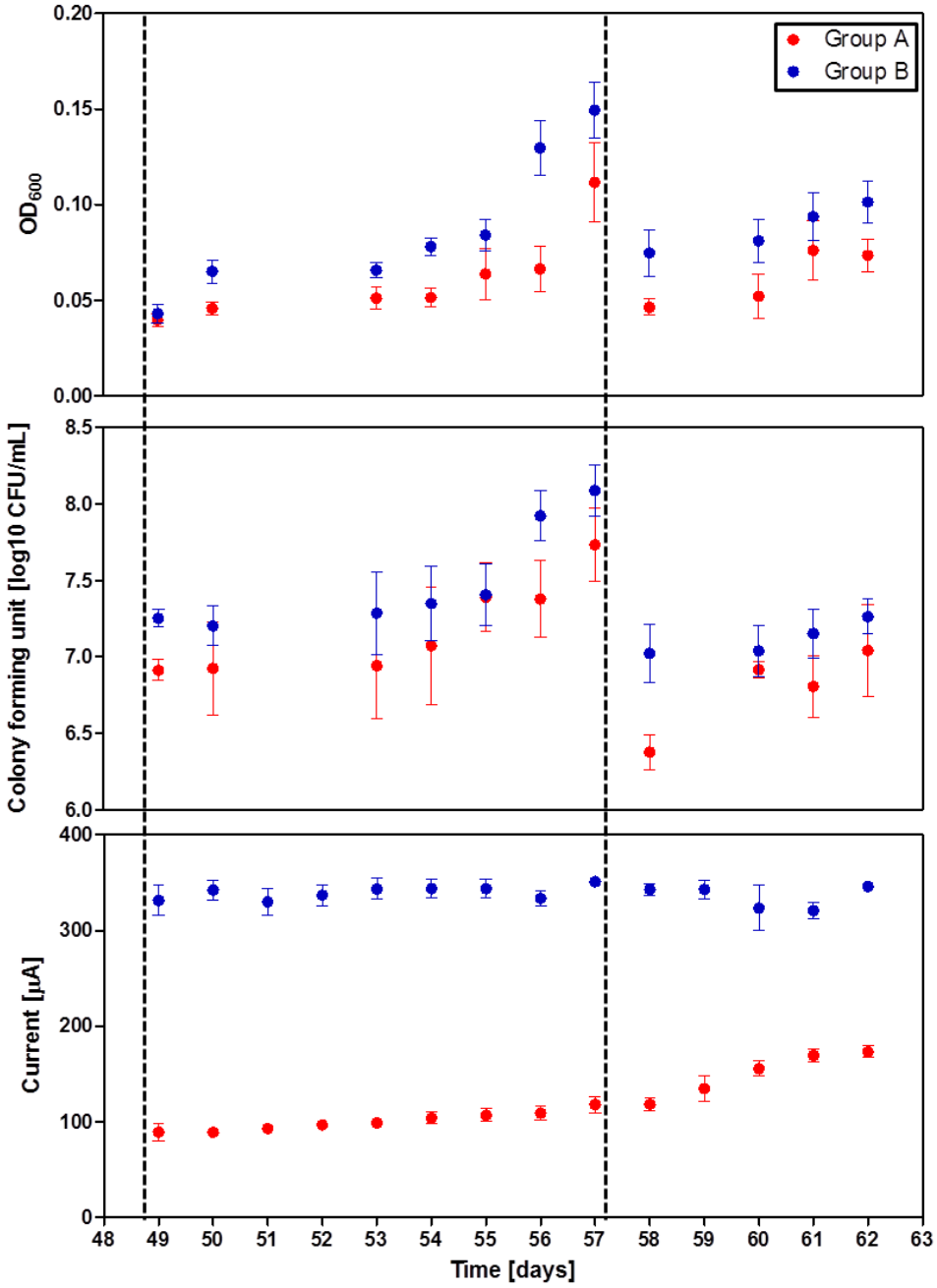

Figure 5.12 OD_{600} and CFU of group A (acetate enriched group) and group B (casein enriched group) perfusate as bacterial population indicators and current generation of the two groups over the same period (n=3)

* The dotted lines indicate when anodic chamber cleaning was carried out.

Voltage change measured every 5 min during the cleaning to remove build-up, which lasted for about 30 min, also supported this finding (Fig. 5.13). When the anolyte including suspended bacteria was removed by cleaning, the voltage output returned rapidly within 20-35 min to the levels observed before removing the planktonic bacteria.

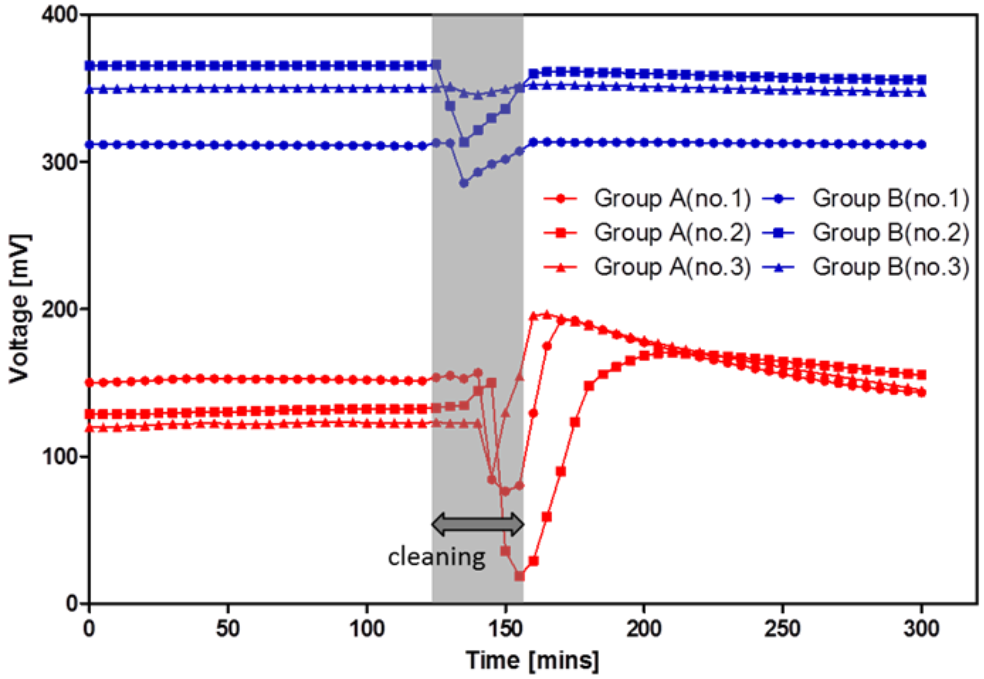

Figure 5.13 Voltage change during anodic chamber cleaning and after
* The grey area is when anodic chambers were cleaned.
* Data presented are from the 3 MFCs of each group separately.

As discussed in section 2.3.1, it is generally accepted that two types of anodic electron transfer mechanisms exist in MFCs; direct electron transfer (DET) and mediated electron transfer (MET) (Rabaey *et al.*, 2007; Schröder, 2007). Unlike DET that requires physical contact of bacterial cells to an anode electrode or other cells, MET can take place from a longer distance with the help of mobile electron shuttling compounds. In this case, even non-anodophiles existing within and/or outside of the anodic biofilm, can contribute to electricity

generation of MFCs by producing endogenous redox mediators through their metabolic pathways.

Unlike batch fed MFCs with relatively large anolyte volume and small size anodes, this system had a small anolyte volume (5.75 mL) and fast feedstock supply rate for the reactor (1.89 mL/hr; HRT = 3 hours). Thus the proportion of suspended cells to anode attached cells was expected to be relatively small. Suspended cells could therefore either have a positive or a negative effect on current generation. If they produce extracellular mediators, this aids anodophiles to transfer electrons from the substrate to the anode. Or some could break substrates down into smaller molecules that can be used by anodophiles to produce electricity, which is unlikely in the case of acetate since it is already a simple structured substrate. On the other hand, their consumption of substrate could result in deficiency of available substrate for anodophiles, which is again unlikely in this work, since the COD of feedstocks was relatively high. If the two scenarios co-exist, then the two opposite effects offset each other. In any case, these results indicated the absence of soluble electron mediators from the suspended cells or their negligible contribution to current generation. Overall it is safe to assume that the cells within the anodic biofilm matrix - rather than suspended bacteria or electron mediators produced by the bacteria - were the main contributors for the power generation in this system.

5.4.3. Power Response to Substrate Change

Figure 5.14 shows the power output profile of the two groups at each stage. At the first stage, group A fed with sodium acetate and group B fed with casein reached steady states 20-25 days after inoculation. Group A showed higher power generation (80-87 µW) than group B (20-29 µW) and this performance lasted for 3 weeks until the two substrates were swapped. Since casein requires digestive hydrolysis, the low performance of casein fed MFCs could

imply its consumption by non-electroactive species. Moreover, for most microorganisms, it would be harder to utilise casein due to the complex molecular structure and composition, which needs to be broken down into monomers first. When the two groups of MFCs were supplied with different feedstocks, group B responded to the substrate change and reached the new steady state more quickly than group A, probably due to the readily biodegradable nature of acetate. Also group B produced higher power than group A when fed with acetate. This could be anticipated since similar responses have been observed by other researchers, where MFCs enriched with a more complex structured carbon source, showed better substrate versatility than when a simpler structured carbon source was provided (Chae *et al.*, 2009). The power output of group A steadily increased and reached a new steady state in the 3rd week after the first substrate swap. The slow power increase indicated that the group A biofilm needed to acclimate to casein by producing peptidolytic enzymes or encouraging other types of proteolytic bacteria. At the second steady state, it reached a similar power output level to that of group B when fed with casein, and this signified that group A was able to utilise casein to a similar extent to group B. Hence it was demonstrated that in a continuous flow system, MFCs could adapt to achieve the same level of utilisation as more complex carbon source enriched MFCs with time, even though they were adapted to metabolise a relatively simple carbon source from the maturing period. This suggests that the metabolic activity of anodic biofilm microbial communities changes dynamically with changes in nutrient conditions.

Another meaningful observation was the stable performance of the anodic biofilm in terms of power production (inset graph, Fig 5.14). Continuous flow of substrates facilitates steady states and when steady states were reached, power output was very stable (100.9 ± 2.3 μW and 101.2 ± 2.2 μW for a week) until feedstock conditions were changed.

Three weeks later, when the two substrates were swapped again, the power output from both groups went back to their previous level within a week, which shows the resilience of

the anodic biofilm. Again the group switched to acetate from casein responded faster than the other group, but this time group B reached a stable power production very close to the previous level in a much shorter period compared to the previous times for both group B and A. This result implies that the microbial community of the anodic biofilm ‘acquired’ the ability to utilise different carbon sources through exposure to different substrates.

Unlike single species, which switch their metabolic pathways by producing different enzymes under different feedstock conditions, a more complex response is expected when a large community of diverse microorganisms is involved. When changing the main carbon source in a feedstock, a single bacterial cell would switch its metabolic pathway by activating different enzymes if at all possible. Some cells may be inactive if they lack suitable enzymes for metabolising the given feedstock. In this case, other species that can utilise the given feedstock will dominate, and in a microbial community, these shifts can take place simultaneously. However, from a higher level of complexity, the anodic biofilm community seemed to be able to acclimate to a new environment with a new substrate and this acclimation can be accelerated by exposure to diverse carbon sources.

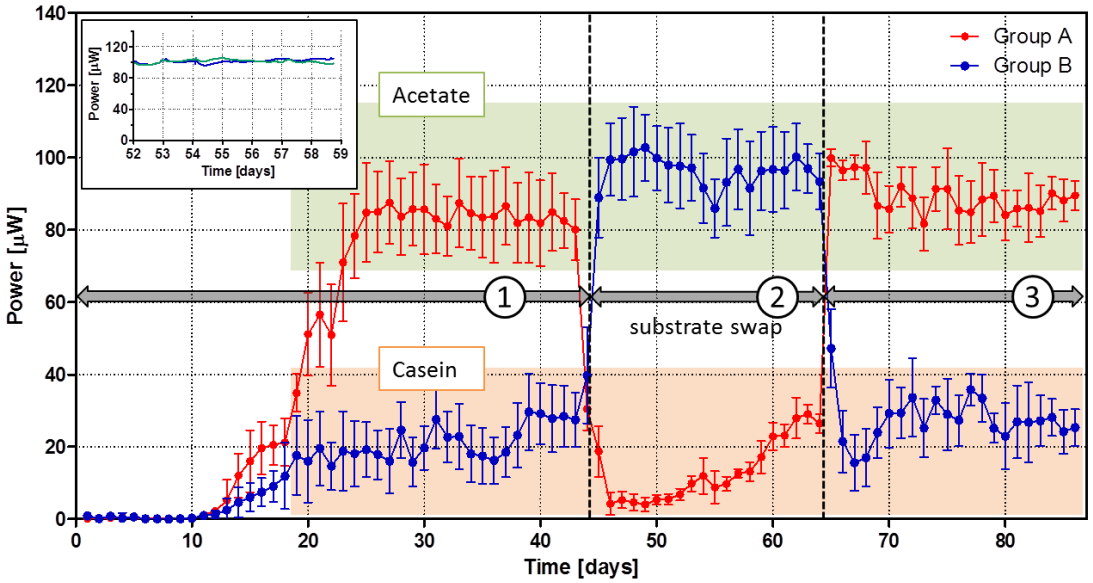

Figure 5.14 Temporal profile of power generation from both groups at each experimental stage

* Numbers in circles indicate the stage and stage 2 is when the two initial substrates were swapped.
* Data presented as average values of 6 cells of each group.
* Inset graph: Example of steady state power production from two MFCs of group B over a week (from day 52 to day 59).

Substrates had a significant effect on the MFC performance, not only in terms of power output but also in terms of internal resistance, which affected P_{MAX} as depicted in Fig. 5.15. During the 6th week of this experiment, before the first substrate swap, P_{MAX} of an MFC belonging to group A was 215.8 µW then it dropped to 67.7 µW, when the main carbon source in the feedstock was changed from acetate to casein. At the same time, R_{INT} increased to 3 kΩ from 500 Ω. This new performance level returned to the previous level, when it was reverted to its initial carbon source (acetate) during the 10th week. In the case of group B, the opposite behaviour was observed. P_{MAX} rose from 137.5 µW to 242.6 µW, whilst R_{INT} dropped from 1 kΩ to 500 Ω with the first substrate change. As seen in the temporal profile of power generation (Fig 5.14), power curves clearly presented that the power performance of group A improved each week whereas there was no significant change in group B during the second stage (7-9th week).

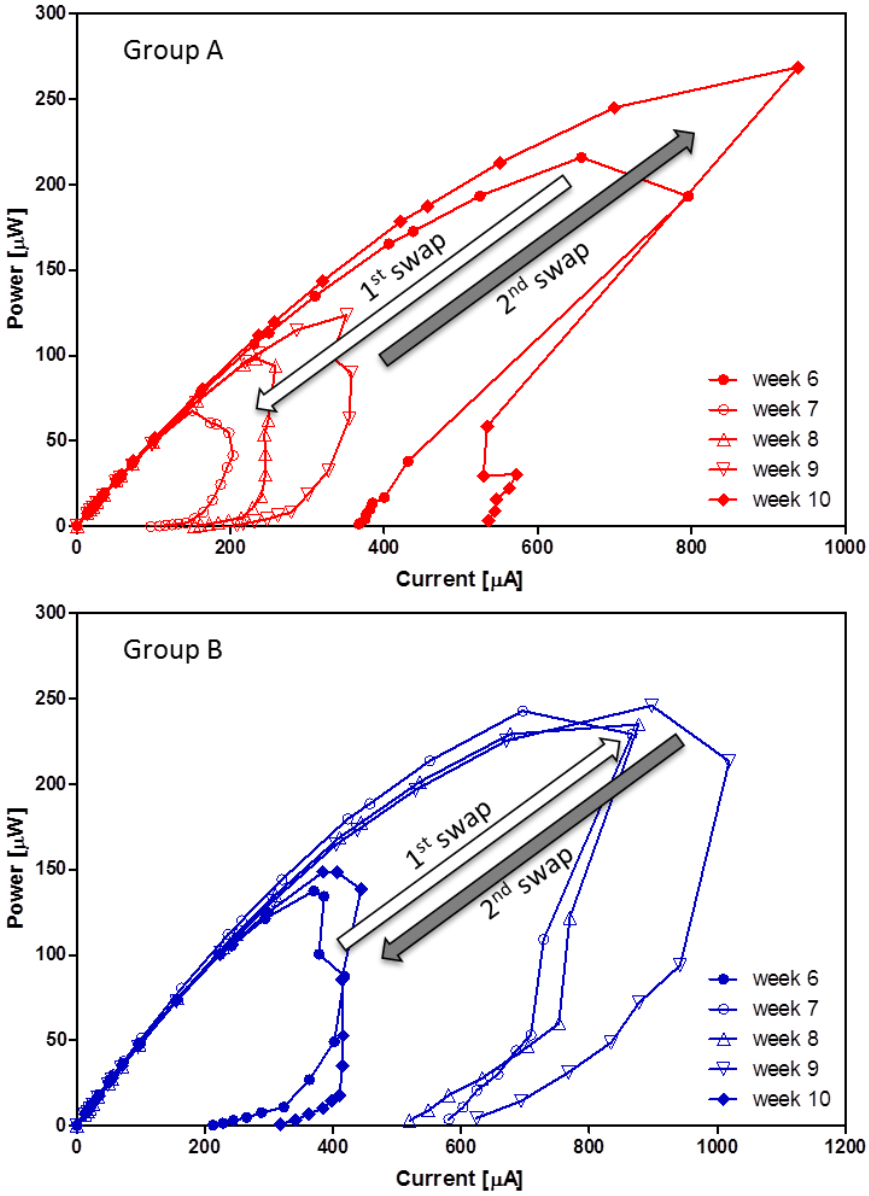

Figure 5.15 Power curves of two individual MFCs of both groups between the 6th and 10th week

* The white and grey arrows indicate the power curve change after the first and second substrate swap respectively.

* A single MFC from each group was chosen instead of average values of multi MFCs for the sake of clarity.

At the end of this line of work, a 3rd and a 4th substrate, glutamine and glucose (both equivalent to COD 1125 ± 31), were supplied to the two groups for 3 days in order to investigate how both groups would respond to a different substrate that was not previously supplied. There was no significant difference between the two groups when they were fed with glutamine (130.9 ± 4.6 μW for group A and 122.5 ± 6.8 μW for group B), however group A showed higher output (78.5 ± 12.4 μW) than group B (56.3 ± 3.8 μW) when glucose was provided. Although the reason for the different substrate specificity is unclear, group A appeared to have a higher affinity to glucose. Considering both groups showed similar level of diverse substrate utilisation (section 5.4.4), it is unlikely that this difference was caused by more complex microbial community consisting of diverse anodophiles or their syntrophic bacteria in group A. On the other hand, the molecular structure of glucose is closer to that of acetate than casein, thus it might have been preferred by group A for the relatively short time of 3 days.

5.4.4. Community Level Physiological Profiling

CLPP, introduced by Garland and Mills (Garland & Mills, 1991), was originally developed for identifying pure cultures of bacteria based on their metabolic properties. This technique has also been used for heterotrophic microbial communities especially for soil bacteria from different habitats (Konopka, Oliver & Jr., 1998; el Fantroussi *et al.*, 1999; Bossio *et al.*, 2005; Frąc, Oszust & Lipiec, 2012) since profiling substrate utilisation provides information on the microbial metabolic capabilities and hence on the functional diversity of a microbial community.

Initially it was expected that there would be a noticeable difference between the two groups, in terms of the number of substrates used (substrate utilisation pattern) after the first stage, once the anodic biofilm had fully matured under different feedstock conditions.

However they both exhibited the ability to utilise a wide range of substrates throughout the study due to the microbial diversity in the inoculum. After 120 hours of incubation, all the wells except E8 (itaconic acid) turned purple, which indicates over 90 substrates on the Biolog AN plate could be utilised by the microbial communities of both anodic biofilms.

Figure 5.16 shows the Shannon-Wiener index (H) of the anodic biofilm samples during different stages of the study. CLPP is sensitive to inoculum density (Konopka, Oliver & Jr., 1998; Viti & Giovannetti, 2005) thus it was suggested to compare different data sets with approximately the same AWCD (Garland, 1996). AWCD values of group A and group B for the same sampling point of H (24 h incubation) were 0.51 ± 0.10 and 0.50 ± 0.06 respectively, which were thought to be valid for statistical analyses. Samples were measured twice at the first stage (stages 1-1 and 1-2 shown in the graph) with 3-week intervals, in order to verify the steady states of the anodic biofilm. The result shows that metabolic functional diversity of both groups increased as the work progressed, which indicates that a wider range of substrates could be utilised in the later stages. Meanwhile, the Shannon-Wiener index of the group B anodic biofilm was slightly higher than group A throughout. This could be explained by the complex mixed consortium of diverse anodophiles and their syntrophic bacteria as a result of the production of various amino acids during the degradation of casein, which resulted in a wider substrate specificity of the group B biofilm than group A. This wider substrate specificity (but lower electricity generating performance of the group B) also supports the possibility of more antagonistic metabolic pathways existing in group B than group A. However, the difference between group B and A was not significant, and the H values of both groups were very close to each other at the 3rd stage. Although it is not possible to observe the anodic biofilm microbial community composition like with other molecular assay based methods, such as denaturing/temperature gradient gel electrophoresis (DGGE/TGGE), CLPP allows full anodic biofilm viewing as a whole, and it showed that potential metabolic diversity had been enhanced. The results demonstrate the

possibility of manipulation of physicochemical conditions, e.g. exposure to different feedstock to encourage biofilm adaptation.

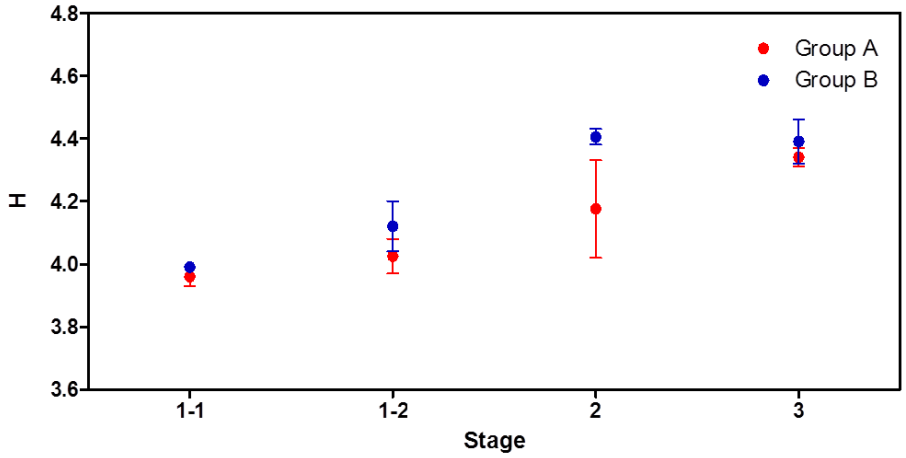

Figure 5.16 Shannon-Wiener index (H) of anodic biofilm samples at different stages (n=2)

Another noteworthy observation is that the affinity to certain substrates could change even after the anodic biofilm has been fully established. Normalised OD values of the Biolog AN plate well, which contained acetic acid, changed at each stage as shown in Figure 5.17. During the biofilm maturation period (stage 1), group A showed higher OD than group B, which signifies higher affinity to acetic acid as a sole carbon source. This was expected, since the anodic biofilm of group A was initially enriched with acetate. At stage 2 when the two main carbon sources were swapped, the substrate affinity of group B to acetic acid increased whereas the affinity of group A declined resulting in a reverse pattern to the previous stage. This pattern change happened again when the substrates were switched back to their original substrate conditions.

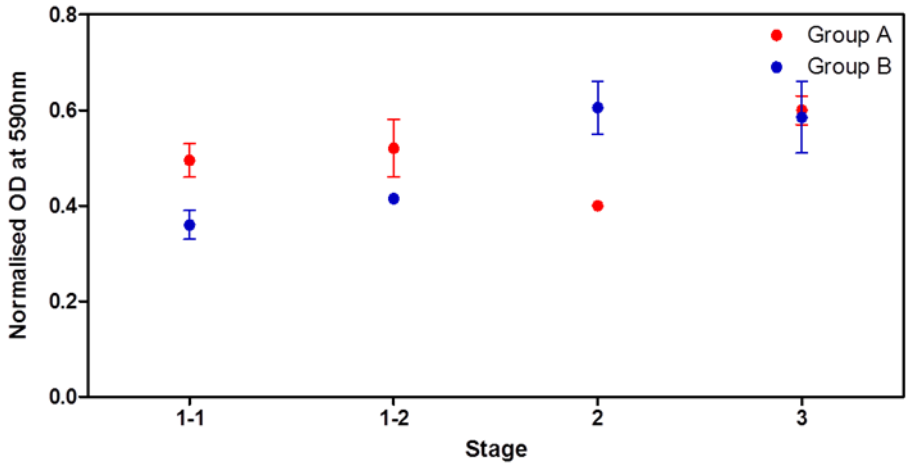

Figure 5.17 Normalised OD values of the Biolog AN plate well containing acetic acid (well no. E2) at different stages (n=2)

5.4.5. Cathode Flooding

Whilst running the 16 MFCs for over 3 months, catholyte accumulation occurred. Catholyte formation on the surface of the cathode electrode was first observed as droplets on the electrode and membrane, and then catholyte accumulated in the cathodic part to the extent that power output started to decrease. It is widely known that water is synthesised by the electrochemical reaction and electro-osmotic drag (Natarajan & Van Nguyen, 2003). Although water is essential for MFC operation, since it enables an electrolyte bridge between anode, membrane and cathode, excessive water that is not appropriately removed is known to cause cathode flooding, which hinders the transfer of oxygen to the reactive site of the cathode (Yu *et al.*, 2009). Similar with other studies reporting catholyte formation in MFC cathodes, cathode flooding had a negative effect on power production (Wilkinson, 2000; Zhang *et al.*, 2012). However it did not seem to significantly affect power generation until a threshold point was reached, as illustrated in Fig 5.18. Water in the cathode formed gradually, but an abrupt voltage reduction was observed only when the water level had reached the very top of the cathodic part. The sudden voltage drop was therefore thought to be due to limited

air exchange through the air holes, thus hindering the oxygen supply. When water was removed, power output instantly returned to its previous level. Alteration of the cathode design, such as with the addition of a drain channel for removing the accumulated water could resolve this.

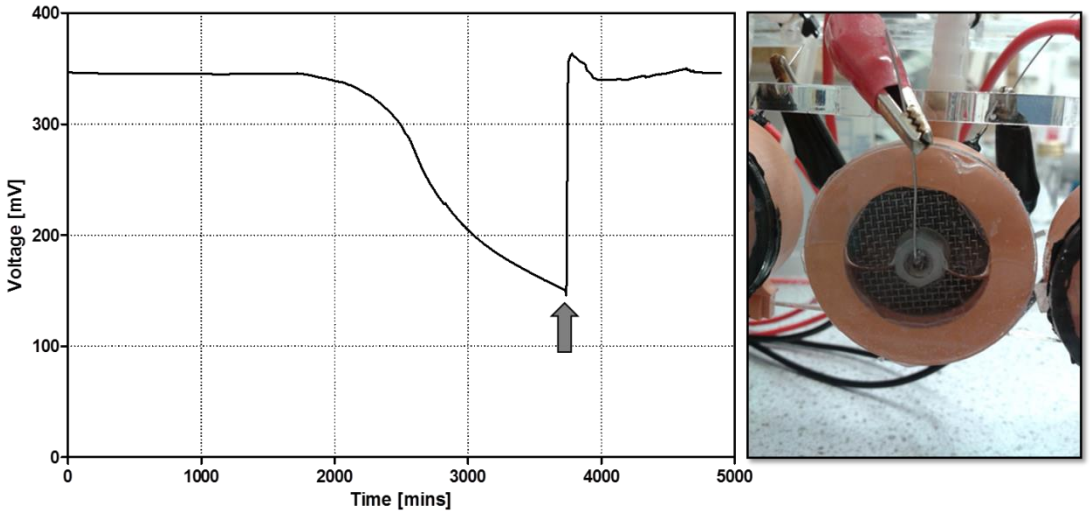

Figure 5.18 Power output change during cathode flooding (left) and photo of the cathodic part with accumulated water (right)
* The gray arrow indicates when water was removed from the cathodic part.

5.5. Chapter Conclusions

In this chapter, three anode biofilm performance factors, including temperature, R_{EXT} and feedstock, were investigated. From the experiments, increasing the MFC power generating performance and substrate utilisation through better understanding of the anodic biofilm were expected. The following conclusions were drawn in these studies.

(1) Although the experiment with thermophilic MFCs was interrupted due to bacterial grow-back and pure culture contamination, this accidental contamination demonstrated the potential for enhancing MFC performance by mixing two or more electrochemically active species.

(2) Impedance matching is a good strategy when an improvement of power generating performance is expected. Also due to the dynamic characteristic of anode biofilms, the MFC performance can increase considerably even after the initial maturing period. Therefore seeking a way to monitor the R_{INT} without MFC system interruption would be extremely beneficial.

(3) The MFCs in continuous feeding mode showed a stable power output once new steady states at all stages. Also they produced a similar level of output when fed with the same feedstock. CLPP results showed the metabolic functional diversity of anodic biofilms increased through exposure to different feedstock conditions. Stability and reliability of the anodic biofilm presented in this study can be very useful for practical implementations of the MFC technology.

6. Waste Clean-up and Resource Recovery

6.1. Introduction

In the previous two chapters, two important aspects of MFC technology, system design and anodophile communities, were looked into. Better materials and designs for each MFC component were selected based on the findings. Consequently, MFC performance was improved by 2.2- and 4.9-fold respectively (based on maximum power -in absolute value- calculated from power curves), when new anode and cathode materials replaced the previous plain carbon veil material. Experiments investigating anodic biofilm affecting factors, revealed dynamic characteristics of anodic biofilms. The study showed that manipulation of anodic biofilm for enhancing MFC performance is possible through controlling operating parameters such as temperature, external load or feedstock. Dynamic steady-states of anodic biofilms under continuous flow of substrate were also successfully demonstrated.

Based on these findings, further work was carried out to put the MFC technology into practice. For this work, two troublesome wastes, urine and uric salts, were chosen. Besides waste treatment and electricity generation using MFCs, resource recovery from urine in the form of struvite was also investigated. At the end of this chapter, a potential practical application of MFC stacks utilising urine, will be demonstrated.

Parts of this chapter (sections 6.2, 6.3 and 6.4) have been published as follows;

Ieropoulos, I., Gajda, I., You, J., and Greenman, J. (2013). Urine—waste or resource? The economic and social aspects. Reviews in Advanced Sciences and Engineering, ***2****(3), 192–199.*

You, J., Greenman, J., Melhuish, C., and Ieropoulos, I. (2014). Small-scale microbial fuel cells utilising uric salts. Sustainable Energy Technologies and Assessments, ***6****, 60–63.*

You, J., Greenman, J., Melhuish, C., and Ieropoulos, I. (2015). Electricity generation and struvite recovery from human urine using microbial fuel cells. Journal of Chemical Technology & Biotechnology, doi:10.1002/jctb.4617.

6.2. Human Urine as a Power Source

In many developed countries with modern sewage systems, human urine is generally considered as waste. Urine makes up less than 1% of municipal wastewater in terms of volume but contains about 50 % of the total phosphorus (P) and 80 % of the total nitrogen (N) in it (Larsen & Gujer, 1996). Phosphorus and nitrogen are the two most problematic elements in wastewater treatment plants (WWTPs) since an accumulation of these can lead to eutrophication. Cultural eutrophication which speeds up natural eutrophication due to human activity is an increasing global issue as the deterioration of water quality and disturbance of ecosystem resulting in significant environmental and societal damages. In addition to this, one individual spends roughly 15,000 L of water to flush faeces and urine away in the modern toilets per year (Quitzau, 2007). It is intensely energy consuming not only to produce this large amount of water but also to treat it in WWTPs. Therefore it is positively necessary to seek for solutions.

In this section, human urine was tested as a power source (substrate) for generating electricity from MFCs. Material and methods used in this work were identical to the ones used in section 5.3.

6.2.1. Response to Urine Addition

Figure 6.1 shows the typical temporal response from two MFCs fed with 5 mL of fresh neat urine (pH 6.4). When the substrate was depleted, the current produced by MFCs was below 150 µA (0.1 mW/m^2), however upon repeated additions of fresh urine, the power output consistently increased to 1 mA (7–8 mW/m^2), with differences being less than 10 % (AUC, Fig. 6.1 inset). The amount of time taken to utilise this volume of urine was approximately 2 days and brought the same level of power output regardless of the length of starvation period. This is particularly important, since it emphasises the robustness of the MFC system, even when it appears that it has reached the end of its lifetime.

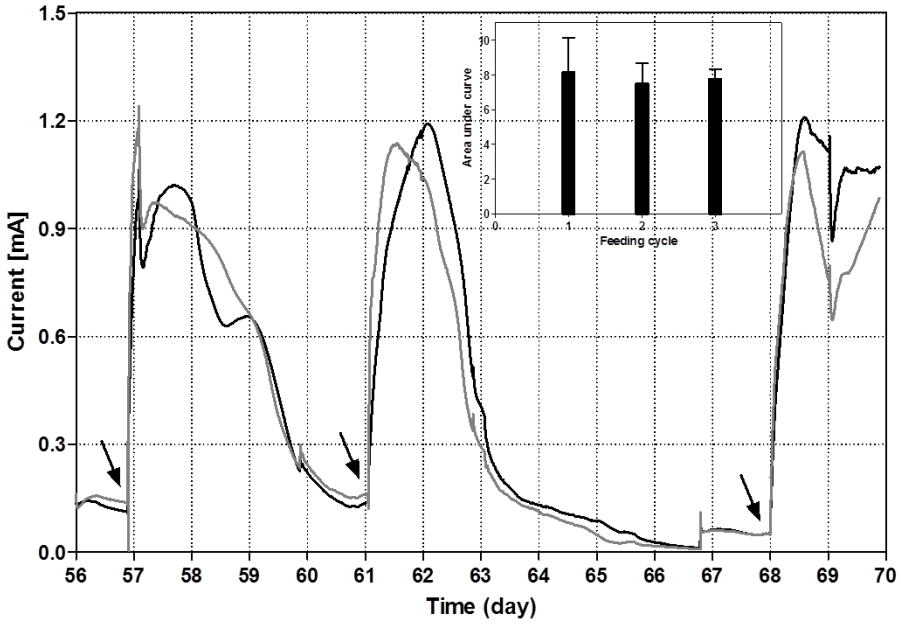

Figure 6.1 Temporal profile of MFC performance when fed with neat urine
* Arrows indicate when 5 mL of urine was provided to MFCs.

6.2.2. Response to Different Urine Volume

As part of this line of work, it was important to capture the response of the biofilm inside the MFCs, to the addition of different volumes of fresh urine. Figure 6.2 depicts the response as a result of decreasing volumes of neat urine. As can be seen, the MFCs responded instantaneously and in proportion to the volume added. The amplitude of the power output was lower than in the previous (Fig. 6.1) experiments, and this can be attributed to the decaying behaviour of a fed-batch system. It is worth noting, that even after 5 months of fed batch operation, and despite the decay in performance, the response from the MFCs was reliably consistent.

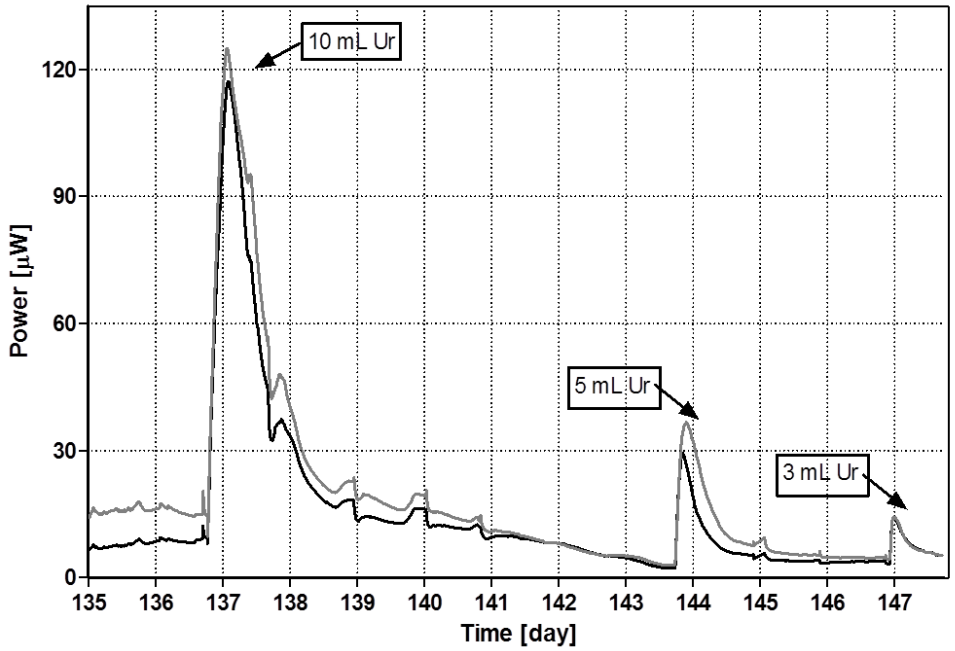

Figure 6.2 Dose response profile with added urine volumes ranging from 3 mL to 10 mL

6.2.3. Comparable Power Generating Performance

The total length of these experiments, from the very beginning, was ca. 1 year. During this time, various other commonly used substrates or growth media were employed as feedstock, under the same experimental conditions. For example, tryptone-yeast extract is normally used at 1 % (tryptone), 0.5 % (yeast extract) and nutrient broth at 25 %, for a standard growth medium, whereas 0.1 M sodium acetate concentration is not uncommon. As can be seen from Fig. 6.3, the P_{MAX} generated by urine was 203.4 μW (7.53 mW/m^2), which was 10 % higher than nutrient both, 55 % higher than TYE and 280 % higher than 0.1 M sodium acetate. In terms of current density, urine generated a two-fold higher output than the second best nutrient broth. Although this was not a direct comparison since the tested substrates had different COD concentrations and length of MFC running, the result indicates that urine possesses the strong potential as a power source for MFCs. And this performance could be boosted by adding extra carbon sources such as acetate or glucose because the elemental composition of urine is C:N:P:K (1:9.5:0.82:1.24), which has a relatively small amount of C and excessive amounts of N, P and K for microbial cell growth (Ieropoulos, Greenman & Melhuish, 2012).

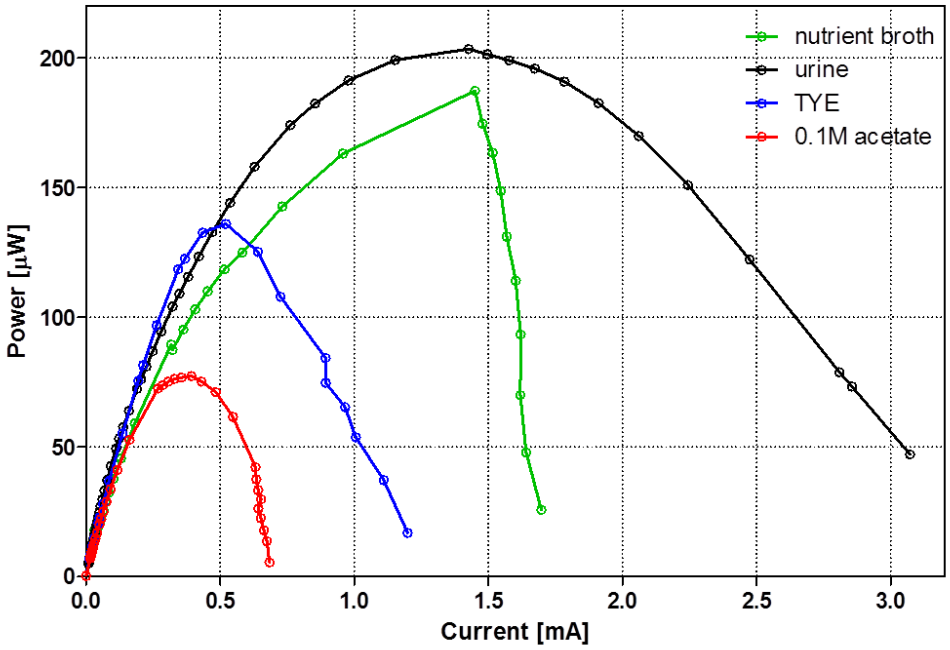

Figure 6.3 Polarisation curves from the same design MFCs fed with different substrates

6.3. Uric Salts Utilisation

The previous work has suggested that the early break down of urine for electricity generation can help remove and lock-away (in the form of new biomass) some of the nitrogen, phosphorous and potassium content in urine, thus having a positive impact on wastewater treatment. However, urine tends to accumulate in the form of uric salts (also called uric salts or uric sludge) especially in communal drainage systems, requiring frequent removal and maintenance. Although the composition of uric salts highly depends on flushing water and individual urine, uric salts typically consists of struvite ($MgNH_4PO_4.6H_2O$), hydroxyapatite (HAP, $Ca_{10}(PO_4)_6(OH)_2$,), calcite ($CaCO_3$), protein, uric acid, polysaccharides and other volatile components (Ohki *et al.*, 2009). Usually strong acidic solutions are used to remove the uric salts, which are not environmentally friendly and bring further problems such as drainage corrosion. With this in mind, this experiment was

designed to investigate the feasibility of utilising uric salts mixed with urine or sludge in MFCs for direct electricity generation.

6.3.1. Methods Specific to Experiments

Uric salts provided by Whiff- Away Ltd, Slough, UK was tested in two types of MFC design; R-MFC (with open-to-air cathode) and S-MFC. For R-MFCs, 5 mL of neat urine (pH 5.56) or uric salts (pH 8.45, 100 times diluted with deionised water) was fed into MFCs for the purpose of substrate comparison after inoculation and maturing for at least 3 weeks. For S-MFCs, cells were fed with uric salts mixed with sewage sludge in batch mode for the first 9 days, in order to let microbial consortia settle and colonise the anode, and then 500 mL of uric salts and sludge mix was re-circulated. As a background solution, sewage sludge was 10 times diluted with tap water (pH 8.74) then uric salts were added at different ratios. Tap water was recirculated with a flow rate of 0.5 mL/min as a catholyte and replaced on a daily basis.

Since the uric salts samples were provided from an operating communal urinal facility, they naturally consisted of a mixture of salts and sludge, which would have been high in impurities and organic carbon. The initial resistor loads used in the experiments were 2.7 kΩ for the R-MFCs, and 12 kΩ for the S-MFCs. These were chosen to match the initial internal resistances of the different MFC types, and were determined by periodic monitoring of the OCV.

6.3.2. Feasibility of Uric Salts as a Substrate

Figure 6.4 shows the temporal profile of power production from the R-MFCs. When MFCs were fed with urine, the power output reached up to13.9 μW (0.5 mW/m^2), and then continuously decreased as urine was depleted. After approximately 12 days, the MFCs produced only 0.8 μW (0.03 mW/m^2), which was the pre-set baseline. At this point, the uric salts solution was injected into the anodes and the power output increased by 10.6 μW (0.39 mW/m^2) before beginning to decrease over the next 3 days. Unlike after the urine feed, this decline did not continue as the power output reached a plateau and remained constant at approximately 6.0 μW (0.2 mW/m^2) for the next 9 days. This suggests that uric salts improved the longevity of continuous power generation, although the peak power was lower than that with urine.

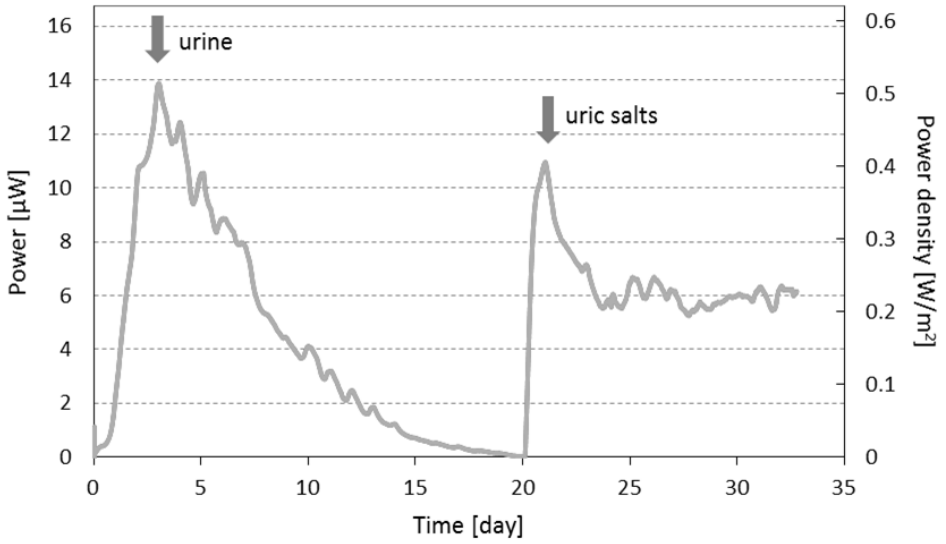

Figure 6.4 Temporal profile of power production from R-MFCs when fed with urine and uric salts

* Arrows indicate when urine (left) or uric salts (right) were fed into the MFCs.

This finding suggests that uric salts can be used as a substrate for direct electricity production by MFCs. Moreover uric salts could improve the longevity when added to other substrates (in this case, urine). This is probably due to the increased organic content from the composition of uric salts, the decreased ohmic resistance of the anolyte due to the high concentration in inorganic salts, as well as the higher pH, which would have buffered any shifts towards acid levels.

6.3.3. Response to Uric Salts Concentration

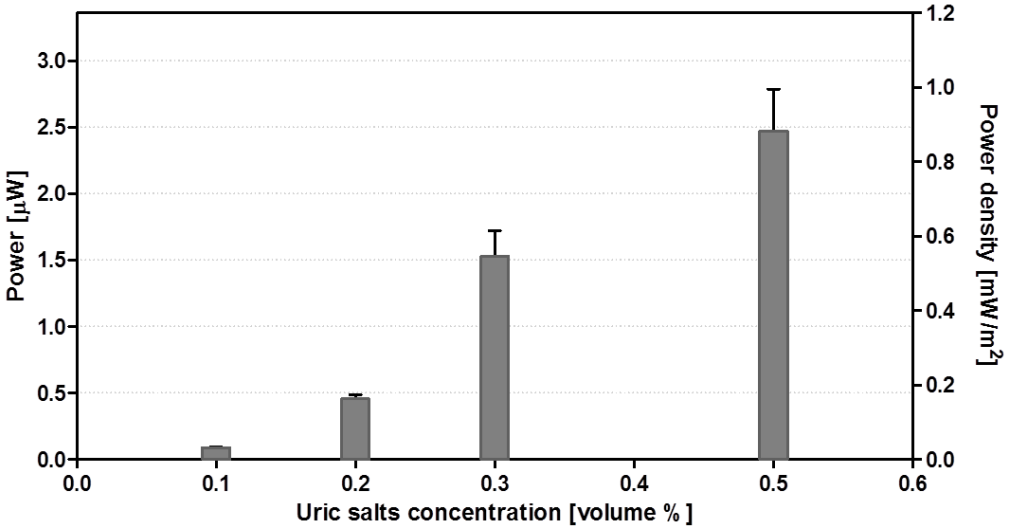

Figure 6.5 Dose response curve of S-MFCs, as a result of substrate concentration (n=2)

From the data shown in Fig. 6.5, when the S-MFCs were fed with 0.1 % uric salts, the average power generated for 7 days was 0.08 µW (0.03 mW/m^2). The average power output increased to 0.45 µW (0.16 mW/m^2, 5-fold increase), 1.54 µW (0.55 mW/m^2) and 2.5 µW (0.89 mW/m^2) respectively, when 0.2 %, 0.3 % and 0.5 % uric salts were provided. The average amount of power produced was proportional to the amount of uric salts added. Also

when the different concentrations of the uric salts mixture were fed to the S-MFCs, the output response was rapid (within 30 min in all cases). It is therefore shown that the S-MFC, which has smaller anodic volume, was more sensitive to the increasing concentration of substrate in comparison to the R-MFC.

Although no performance decline was observed for the entire period of the experiment, the possibility of uric salts deposition on the membrane needs to be considered when a high concentration of uric salts is introduced into the system. The deposition can limit the MFC performance especially in the longer term.

Once again, addition of uric salts to other substrates (in this case, sewage sludge) led to an increase in anolyte pH from pH 8.74 (fresh sewage sludge) to pH 9.27 (uric salts and sludge mix). High pH increases solubility of organic matter in sludge and therefore allows for more substrate to be readily available for uptake. This result is in agreement with previous studies reporting that artificial alkaline treatment of sewage sludge resulted in improved electricity production by MFCs (Yuan *et al.*, 2006, 2012). In the current study the buffering towards the alkaline level is performed naturally by uric salts and this emphasises yet another great advantage of the MFC technology.

6.4. Struvite Recovery from Human Urine

In the 1990s, various European groups started working on the concept of source-separated urine for improving the sustainability of wastewater management (Kirchmann & Pettersson, 1995). Source-separated urine can reduce the operating cost of WWTPs and also contribute to better effluent quality of WWTPs by changing wastewater composition (Larsen & Gujer, 1996). In addition, nitrogen and phosphorus can be recovered and utilised from source points since urine has a high concentration of these elements, and phosphorus recovery through struvite precipitation has received increased attention. Struvite (magnesium

ammonium phosphate, $MgNH_4PO_4 \cdot 6H_2O$) is usually formed in stale urine through the following chemical reaction:

$$Mg^{2+} + NH_4^{+} + PO_4^{3-} + 6H_2O \rightarrow MgNH_4PO_4 \cdot 6H_2O$$

Recovering struvite from urine has two big attractive advantages. First it contains both nitrogen and phosphorus, which renders the simultaneous removal of the two compounds from the main stream of wastewater achievable. In addition, this could also reduce pipe blockage occurrences, which are caused by struvite formation at WWTPs. Once struvite has formed and blocked water pipes, these need to be cleaned or even replaced, and in many cases other elements of WWTPs such as pumps, valves, centrifuges and aerators are also liable to fouling by struvite deposits (Bhattarai, Taiganides & Yap, 1989; Fattah, 2012). These 'undesirable' struvite deposits increase maintenance costs, and reduce the piping system capacity of WWTPs. Second, struvite can be used as a slow-release fertiliser (Nelson, 2000; Münch & Barr, 2001; Ryu *et al.*, 2012), which is not a completely new concept since many communities have used or once used human excretion including urine for growing crops before commercial fertilisers appeared.

Indeed, phosphorus which occurs as phosphate rocks and has to be mined, is a finite resource. Although there is disagreement in estimates of the longevity of phosphate supply, the cost of phosphate rock has doubled over the last 10 years with a price hike event in 2008 (Mew, 2016). Some studies have suggested phosphate production will reach a peak and slow down as the reserves become increasingly expensive and energy intensive to extract (Cordell, Drangert & White, 2009; Walan *et al.*, 2014). Therefore recovery of phosphorus from urine in the form of struvite can be one of the solutions to this issue.

Only recently, recovery of resources while treating waste using bioelectrochemical systems (BES) including MFCs and microbial electrolysis cells (MECs) has begun to gain interest from the scientific community. In the case of resource recovery from urine, nitrogen

recovery in the form of ammonium (both NH_3 and NH_4^+) from the cathode have been attempted using MFCs and MECs (Kuntke *et al.*, 2012, 2014). Zang *et al.* (2012) reported that phosphorus and nitrogen recovery in the form of struvite from stale urine is compatible with MFC operation. However, the current study's thesis is that more effort should be made to better understand the processes and implement the systems especially when dealing with fresh urine such as a MFC system directly connected to urinals.

In order to maximise urine utilisation in this work, a 3-stage MFC/struvite extraction process system that generates electricity while collecting phosphorus and nitrogen in the form of struvite was proposed and its feasibility was tested. With this system, electricity generation is maximised, thus increasing the consumption of organic matter, and high concentrations of nitrogen and phosphorus are recovered through the struvite precipitation process. Furthermore this can be easily integrated with existing source-separated urinals. Therefore, the aim of this study was to combine the MFC electricity production with struvite recovery and investigate whether the two processes can complement each other.

6.4.1. Methods Specific to Experiments

For this work, C-MFCs (as described in section 3.2.1) with hot-pressed activated carbon open-to-air cathodes (refer to section 3.2.3) were used. Neat (untreated without dilution) human urine was used for this work, since the final MFC/struvite extraction process system is envisaged to fit directly into urinals.

Proposed system operation

For a more efficient use of urine with MFCs in terms of power production and nutrient recovery, a system of MFCs which could be fitted into urinals was developed. This proposed system consisted of two MFC groups and each group had four MFC units. In each group,

four MFCs were cascaded with a single flow of substrate, which was provided continuously. The four MFCs were connected in a series/parallel configuration (MFCs 1 and 4, and MFCs 2 and 3 were connected in parallel, and the two pairs were connected in series) in order to produce sufficient power for demonstration of a practical application. An external load of 1 kΩ was applied to both groups.

In the first stage, untreated urine was supplied to Stage 1 (see Fig. 6.6) at a flow rate of 96 mL/h, which resulted in 16 min HRT for all 4 MFCs. Once the effluent was collected, magnesium chloride hexahydrate ($MgCl_2 \cdot 6H_2O$) was added in Stage 2 and mixed using a magnetic stirrer at 100 rpm for 5 min. Following this, the mixing was stopped and the solution was allowed to settle for 45 min before the supernatant was fed into the last stage (Stage 3) of the treatment. The amount of magnesium addition was 1.2 times the phosphate presented in the initial effluent in molar ratio (Morales *et al.*, 2013). In the final stage, the MFCs treated the struvite-deprived effluent (2^{nd} stage effluent) at a flow rate of 42 mL/h (HRT: 38 min). The final effluent was collected for analysis.

Figure 6.6 describes the whole system operation. All experiments were repeated at least three times.

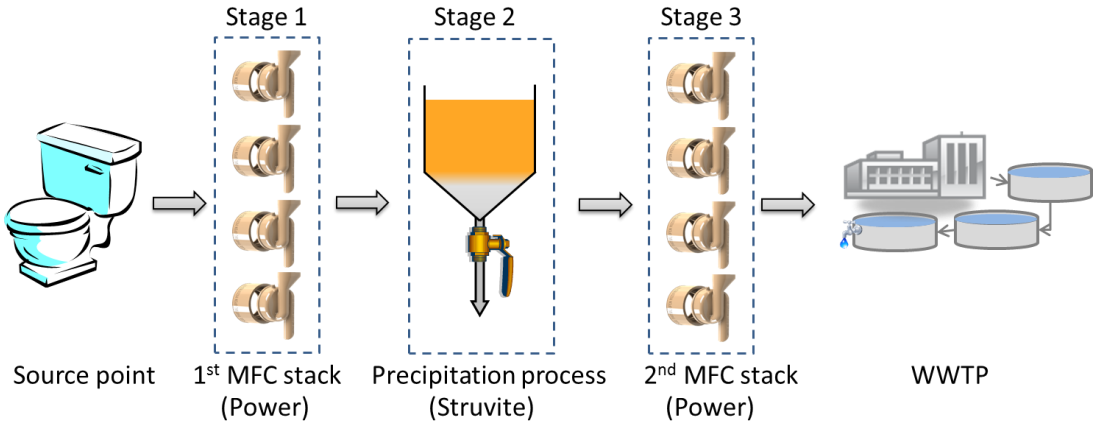

Figure 6.6 Schematic diagram of the 3-stage MFC/struvite extraction process system
* The diagram also illustrates how this can be implemented in real life.

6.4.2. Effect of Struvite Collection on the MFC Performance

Before operating the 3-stage MFC/struvite extraction process system, the effect of struvite collection on the MFC performance was investigated in two steps. First, in order to observe the effect of naturally occurring struvite on MFC performance, untreated neat urine as a fuel was provided to both MFC groups continuously at a flow rate of 21.2 mL/h (HRT: 18 min for individual MFCs) for 5 days. During this period, the MFCs were operated individually without interconnection and the urine was stored at room temperature in an open container. Power performance and struvite precipitation were monitored and are shown in Fig. 6.7. In these 5 days, urine pH rose naturally due to urea hydrolysis, which resulted in increased precipitation. Furthermore, soluble phosphate concentration decreased accordingly since part of it went into the precipitate. Power output from individual MFCs remained relatively stable suggesting that it was not significantly affected by the change of pH or phosphorus concentration in the feedstock. Hence naturally occurring struvite precipitation did not seem to have an effect on MFC performance as long as the same untreated urine was provided.

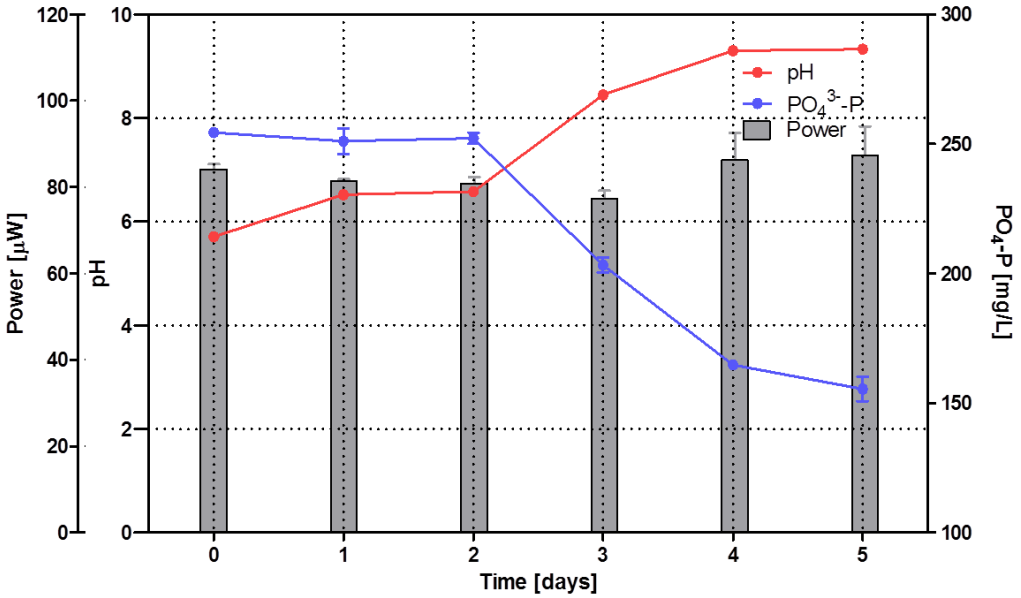

Figure 6.7 Profile of influent pH, soluble phosphate and MFC power output
* Data are based on mean values (n = 2 for PO_4^{3-}–P , n = 4 for power output).

For the second step of this work, rapid struvite precipitation from fresh urine was achieved by manually changing the pH and adding $MgCl_2 \cdot 6H_2O$. Sodium hydroxide (NaOH) pellets were used for increasing the pH to 11 and 0.5 M H_2SO_4 solution was used for bringing the pH back to its initial value after removing the precipitate. The two MFC groups were fed both with untreated freshly collected urine as well as with struvite-deprived urine at a flow rate of 21.2 mL/h. Using this method, 20 % of NH_4^+–N (from 363 mg/L to 290 mg/L) and 82 % of PO_4^{3-}–P (from 202 mg/L to 36 mg/L) were recovered in the form of precipitate (Table 6.1). ORP and conductivity increased while the pH decreased slightly. In both cases of neat- and struvite-removed urine, the change in pH, ORP and conductivity between feedstocks and effluents, demonstrated a similar pattern. The degree of change was proportional to the initial value of the influent. It was also observed that the power output was higher from the struvite-removed urine than from the neat urine. This is thought to be the result of conductivity increase of the anolyte after adding magnesium – $MgCl_2 \cdot 6H_2O$ (molar ratio; Mg^{2-} : PO_4^{3-}–P = 1.2 : 1).

Table 6.1 Comparison of neat urine and struvite-removed urine as a feedstock in terms of pH, ORP, conductivity, NH_4^+–N, PO_4^{3-}–P and power output

	pH	ORP (mV)	Conductivity (mS/cm)	NH_4^+–N (mg/L)	PO_4^{3-}–P (mg/L)	Power (μW)
untreated urine (neat)	6.57	-14	12.3	363 ± 8	202 ± 6	
treated urine from group 1	9.28	-171	23.0	3268 ± 10	254 ± 11	101 ± 7
treated urine from group 2	9.24	-166	22.5	3246 ± 15	244 ± 6	82 ± 3
untreated urine (struvite removed)	6.49	-2	13.5	290 ± 6	36 ± 2	
treated urine from group 1	9.25	-165	24.4	3114 ± 14	36 ± 1	104 ± 6
treated urine from group 2	9.23	-163	24.2	3106 ± 12	36 ± 2	86 ± 4

* Data presented as the mean and error (n = 2 for NH_4^+–N and PO_4^{3-}–P, n = 4 for power output)

Thus from the two tests, it was suggested that a decrease of phosphorus concentration in urine through struvite precipitation did not significantly affect the MFC power performance. This finding can be useful when designing a MFC system that can be connected to urinals. For MFC operation, reducing any insoluble matter in the feedstock solution is preferred for minimising blockages of the anode or membrane. Since the amount of precipitate in urine increases with time, precipitate removal or fresh urine (in both cases of undiluted and diluted urine) is required before adding into MFCs. Relatively high ammonium concentrations of urine have been reported not to hinder the MFC power performance (Kuntke *et al.*, 2012; Zang *et al.*, 2012). However, no published information was found on the inter-relationship between MFC operation and high phosphorus concentration of urine. These findings demonstrate that it is possible to remove the precipitate before the MFC system without negatively affecting the power output.

Struvite removal with Mg addition has the added advantage of higher phosphorus recovery rates in shorter periods of time. Approximately 38 % of PO_4^{3-}–P was removed in 5 days of storage, whereas 82 % of PO_4^{3-}–P was recovered through the Mg addition process, which occurred in less than 1 h. In terms of struvite recovery, struvite precipitation using additional magnesium is a very well established and efficient method of removing phosphorus from urine. A previous study reporting struvite recovery from the cathode electrode observed deterioration of electricity generating performance due to struvite deposition on the cathode and membrane which impedes the mass transfer of ions and oxygen (Hirooka & Ichihashi, 2013). Therefore in the case of utilising urine, which has a high concentration of phosphorus, recovery of this element through the struvite precipitation process seems to be a more convenient and efficient way to pursue.

6.4.3. Urea Hydrolysis Acceleration by Microbial Activity of MFCs

Figure 6.8 shows the general pattern of pH change that takes place in undiluted urine stored on a laboratory bench under ambient temperature conditions. The initial pH of 6.4 did not significantly change during the first 10 h (less than 0.2 pH units), but then increased rapidly over the next 20 h. After 30 h of storage, the pH stabilised at approximately 9.2, which is consistent with previous reports (Liu *et al.*, 2008).

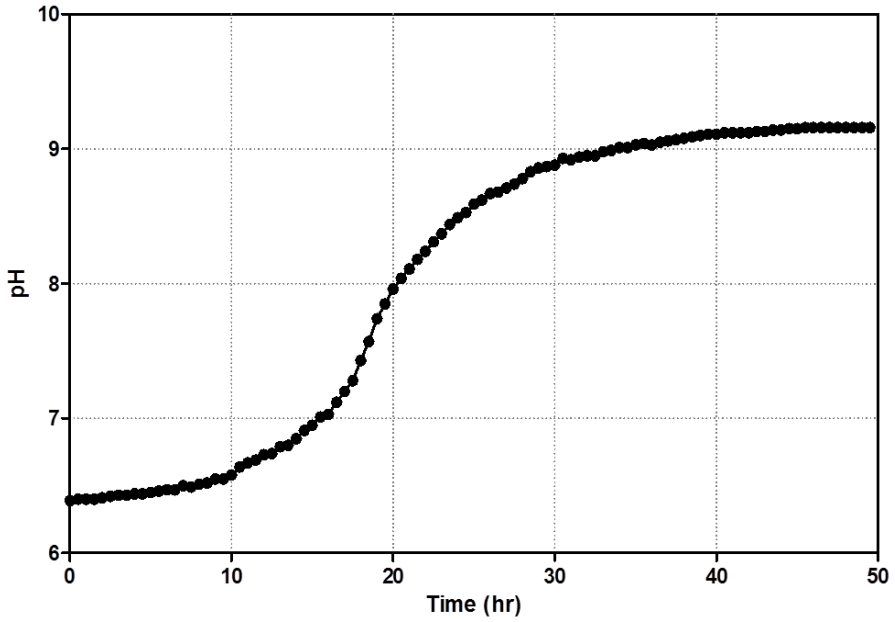

Figure 6.8 Typical pH behaviour of urine when stored in a bottle at room temperature
* pH was measured in situ every 30 min for 50 h.

As shown in Table 6.2., the pH of untreated urine, however, rose to the same level after running through a group of 4 MFCs in only 72 min (HRT of the whole group). This clearly showed that MFCs accelerated urea hydrolysis, which was not attributed solely to the electricity generating activity of microorganisms in the MFCs, since a similar degree of pH increase was also recorded for the same MFCs without an external load (open circuit condition). Therefore the acceleration effect could be the result of urine being exposed to a higher population of microorganisms for a given time.

The pH of urine naturally increases as a result of urea hydrolysis by ubiquitous microorganisms (Udert, Larsen & Gujer, 2003). It is very likely that electricity generating microorganisms existing in MFCs could also hydrolyse urea. Further investigation is needed to confirm if they are the same species as the urease-positive bacteria that hydrolyse urea in urine and if their activity is affected. Nevertheless it seems that introducing fresh urine into MFCs shortens the time for urea hydrolysis thus increasing the pH of urine rapidly.

Previous studies proposed an optimum pH range of 8 – 9 for struvite precipitation (Münch & Barr, 2001; Le Corre *et al.*, 2007; Perera *et al.*, 2007). Since the effluent pH is in this range, no additional NaOH is necessary for pH adjustment. This could be an added advantage when struvite collection is expected from both cases of diluted or undiluted urine. Most studies on struvite recovery from urine used either stored urine to allow the pH of urine to increase naturally or fresh urine but increasing the pH by adding alkalis like NaOH. In both cases, large storage capacity or high cost for pH increase is required, and it seems that operational costs can be significantly reduced, by accelerating the pH increase through MFC systems.

6.4.4. Urine Treatment and Nutrient Recovery

Based on the above findings, a 3-stage MFC/struvite extraction process system was designed. The first stage, running the first group of MFCs, was for generating power and increasing the pH for struvite removal. The second stage centred on the struvite precipitation process by adding Mg. In the third and final stage, the second group of MFCs was fed with the supernatant from Stage 2 at a slower flow rate in order to further reduce COD and generate electricity. Change of pH, conductivity, NH_4^+–N, PO_4^{3-}–P, COD and power output from each stage is shown in Fig. 6.9.

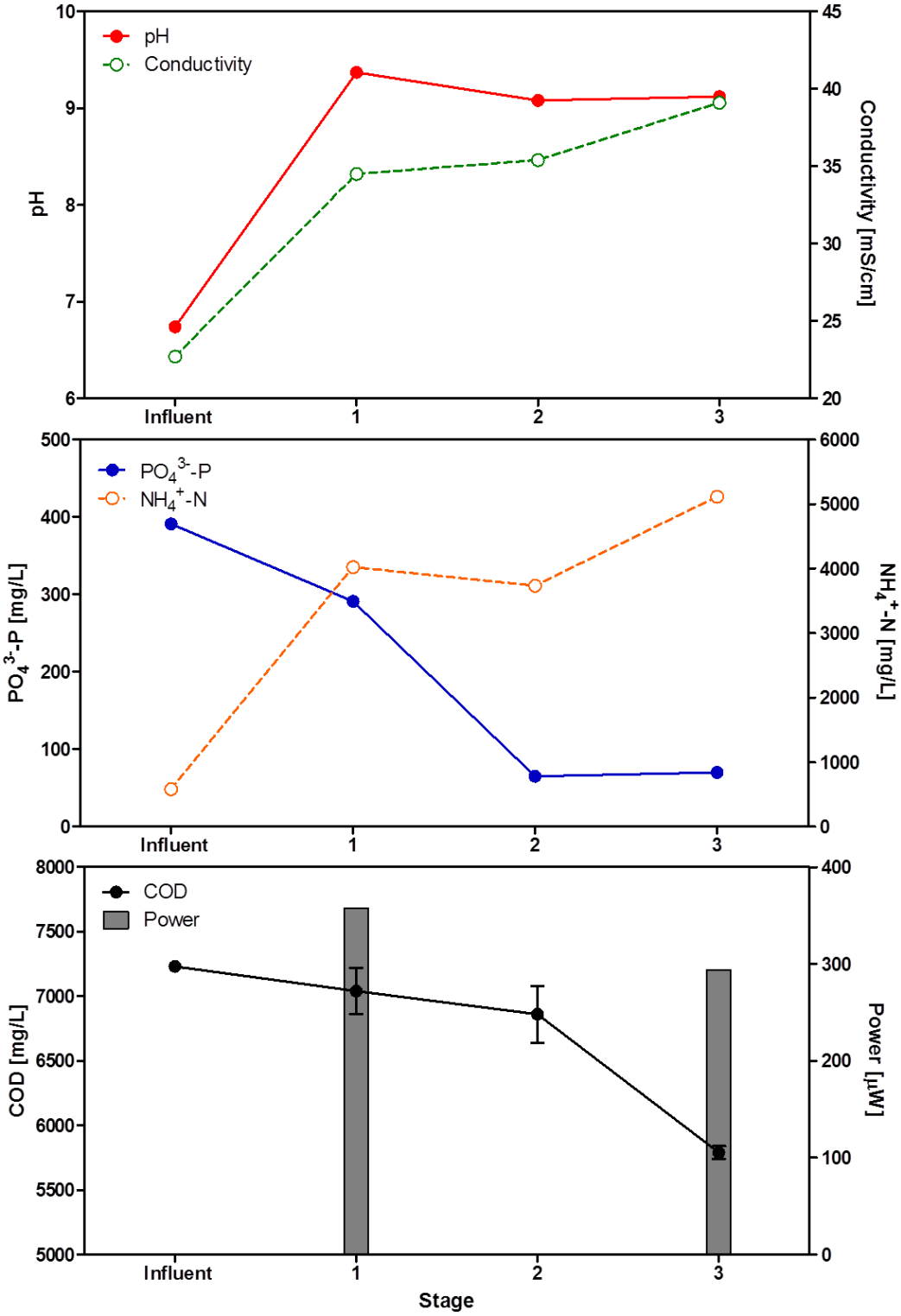

Figure 6.9 Profile of pH, conductivity, PO_4^{3-}–P, NH_4^+–N, COD and power output of each stage (n = 3)

After the first stage of treatment, the pH of urine increased to 9.37 and conductivity rose by 11.8 mS/cm, which implied a considerable amount of urea hydrolysed within 15.6 min of HRT. At the same time, NH_4^+–N concentration increased almost 7-fold while PO_4^{3-}–P concentration decreased by 26 %. Again the increase in NH_4^+–N concentration was a result of urea hydrolysis accelerated by microbial activity in the MFCs and it led to pH increase. The PO_4^{3-}–P concentration reduction could probably be explained by solubility decline of phosphate due to pH increase, and bacterial uptake for growth. Struvite solubility depending on pH value is well described in the literature (Doyle & Parsons, 2002); generally solubility decreases with increasing pH and this results in struvite precipitation within the system. In addition, phosphorus is one of the essential elements for microbial growth thus it could be absorbed by microorganisms in MFCs. However this phosphate behaviour was not consistent in repeated tests as also has been the case in previous reports (Min *et al.*, 2005; Jambeck & Damiano, 2010). The biological phosphorus removal process adopted in modern WWTPs uses specific microbial species, so called polyphosphate accumulating organisms (PAOs) under certain environmental conditions, switched from anaerobic to aerobic (Brdjanovic *et al.*, 1998; Mino, van Loosdrecht & Heijnen, 1998).

Once neat urine was treated in the first stage, magnesium was added without any pH adjustment. This addition brought about a decrease in pH, NH_4^+–N, PO_4^{3-}–P and COD but an increase in conductivity. Since the PO_4^{3-}–P concentration was much lower than NH_4^+–N concentration in the first stage effluent (thus a limiting factor for precipitation), the recovery rate of PO_4^{3-}–P was far higher than the recovery rate of NH_4^+–N. Approximately 7 % of NH_4^+–N and 78 % of PO_4^{3-}–P were recovered by collecting the precipitate.

X-ray diffraction (XRD) analysis showed that this precipitate had a similar pattern to struvite (Fig. 6.10 A). Also a microscopic image (Fig. 6.10 B) showed that the precipitate consisted of mainly transparent rod-like crystals, which is a typical orthorhombic structure of struvite (Le Corre *et al.*, 2007). However, the purity of struvite needs to be investigated

further. In a process like this, besides struvite, other minerals such as montgomeryite ($Ca_4Al_5(PO_4)_6(OH)_5 \cdot 11H_2O$, $Ca_4MgAl_4(PO_4)_6(OH)_4 \cdot 12H_2O$), epsomite ($MgSO_4 \cdot 7H_2O$), and brucite ($Mg(OH)_2$) may also be formed depending on the amounts and availability of other divalent or trivalent metal cations (Lind, Ban & Bydén, 2000).

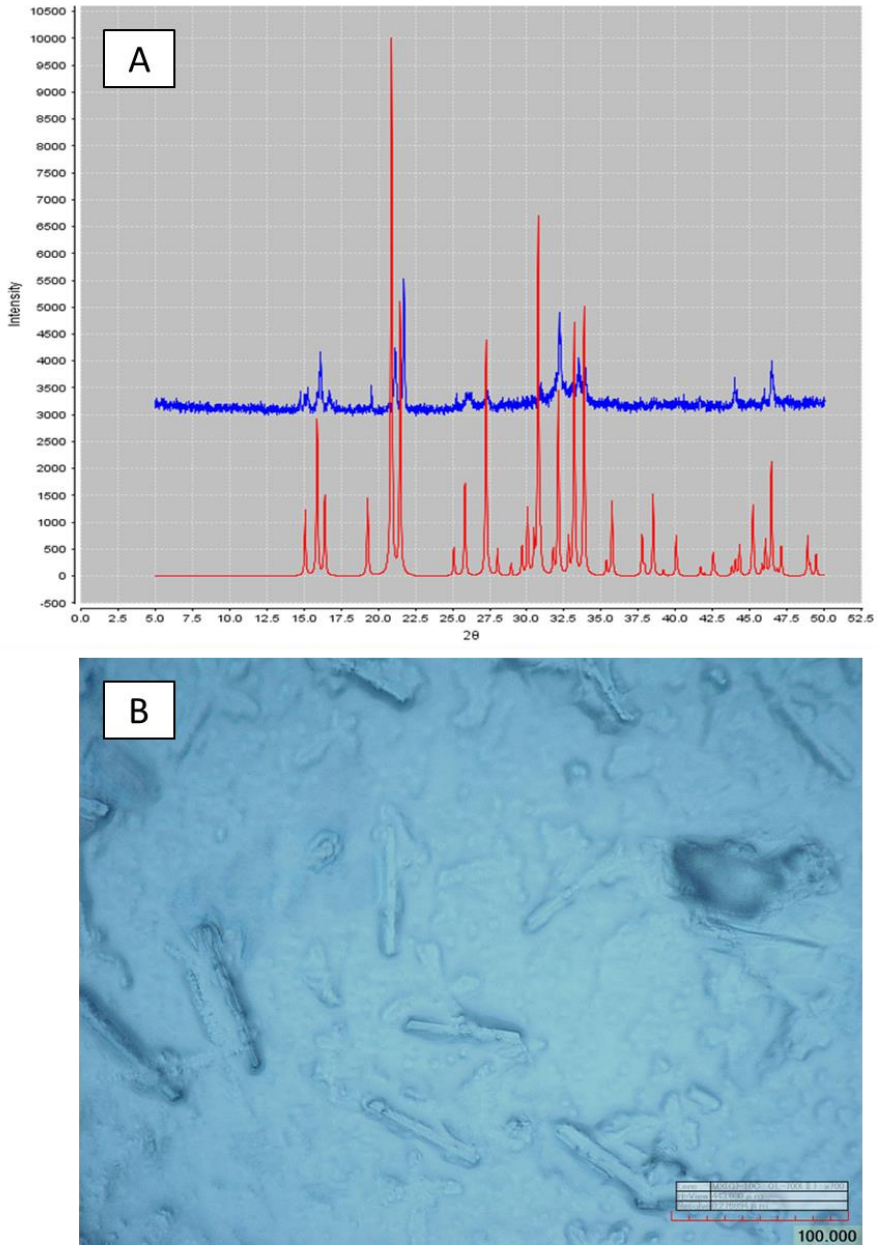

Figure 6.10 Struvite precipitate; XRD analysis (A) and microscopic image (B)
* Red line: standard struvite, blue line: precipitate sample from the second stage

During the final stage of treatment, pH and conductivity slightly increased again due to the hydrolysis of urea that remained from the previous treatment. Consequently NH_4^+–N concentration also increased, which was in contrast to previous studies reporting NH_4^+–N reduction in the anodic chamber of MFCs (Kuntke *et al.*, 2012; Zang *et al.*, 2012). This is thought to be due to different conditions of substrate and MFC operation (fresh neat urine without dilution and continuous feeding mode in this study). Also PO_4^{3-}–P concentration increased slightly this time. However, the phosphate behaviour in the final stage was – as in the first stage – inconsistent. The inconsistent phosphorus behaviour might be attributed to the dynamic physical–chemical reactions and equilibrium conditions of the system as well as bacterial activity. In the case of COD, the highest removal of 15.6 % was achieved at this stage. Longer HRT of the stage was thought to be one of the reasons for the higher COD removal. After the 3-stage system treatment, COD was still relatively high (above 5,000 mg/L), which could easily be tackled by adding more MFC stages to the cascade system. In total, 82 % of PO_4^{3-}–P and 20 % of COD were removed by the 3-stage system.

6.4.5. Electricity Generation

During the first treatment, 358 μW of power (P_D = 14.32 W/m^3) was generated by the first MFC group. The second MFC group produced 294 μW (P_D = 11.76 W/m^3) from the second stage effluent. However, it cannot be concluded that untreated urine always gives higher power than the second stage effluent. In order to evaluate urine as a fuel source at different treatment stages, several factors need to be considered. First, any differences in the microbial community developed at each stage need to be taken into account. In each group, microorganisms had different environmental conditions such as pH, conductivity and salts concentration of the feedstock thus there could have been changes in the abundance and diversity of the complex microbial community in the system. This may have caused differences in the performance between the two MFC groups. In this case, the first group was

better performing than the second group as shown in Fig. 6.11. Therefore the first group was expected to produce higher power than the second group if the same urine was supplied. When the same untreated urine was provided to the second group, the output was 291 μW (P_D = 11.64 W/m^3) which was almost identical to the output generated from the same MFC group fed with the second stage effluent. In repeated tests, the power output from the same group fed with untreated urine was similar or only slightly higher than the second stage effluent. Moreover, when the position of the two groups was swapped, higher power was produced by the first MFC group at the third stage.

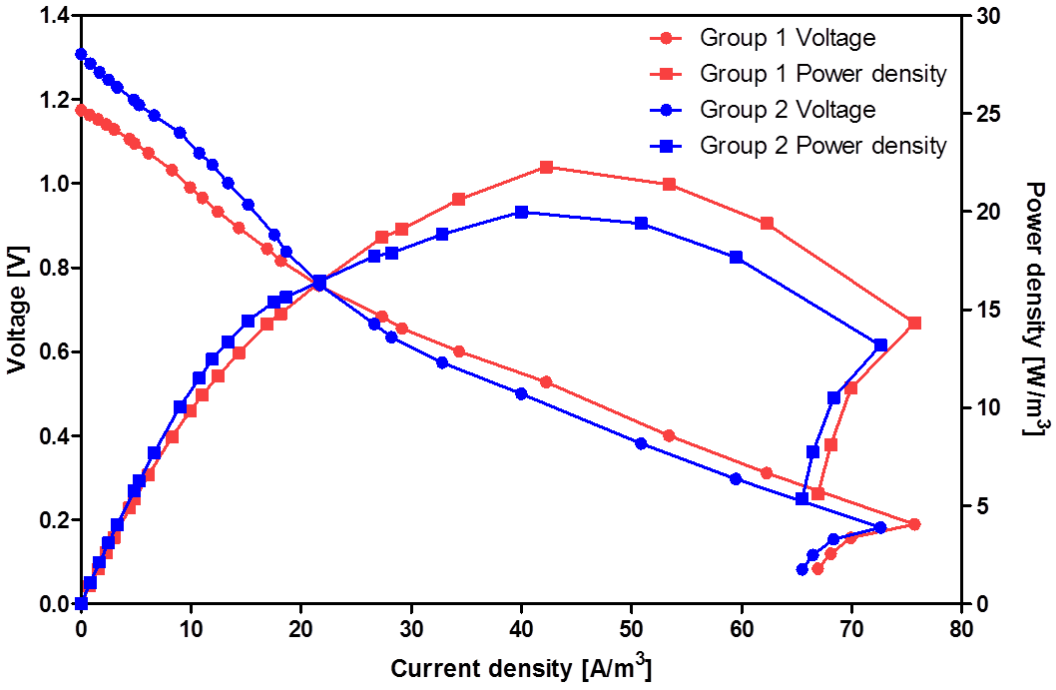

Figure 6.11 Polarisation curves of MFC group 1 and group 2
* Each group consisted of 4 MFC units in cascade.

An important aspect to consider is the flow rate of urine supply resulting in different HRT, and in this study different flow rates were set for the MFC processes. The higher flow rate (96 mL/h) for the first stage was in order to prevent precipitation inside the system but

still result in a good level of power. For operating MFC systems in continuous feeding mode, the flow rate of feedstock needs to be optimised since too low or high flow rate can cause performance decline (Ieropoulos, Winfield & Greenman, 2010). Different flow rates were tested in order to find the optimum flow rate for the system used in this work and with a flow rate of 42 mL/h the system showed maximum power output. Consequently, this was the flow rate used during the final stage. Therefore more power could be expected from the third stage if all other conditions were identical. It is also important to give consideration to the concentration change of readily available organic matter. In most cases, the second MFCs in each group produced higher output than the first units when they were monitored individually. It is likely that the amount of readily available organic matter increased after the first MFC units. In a similar fashion, effluent from the first stage might have had more easily utilisable organic matter than untreated urine. A similar pattern has been witnessed in previous studies using complex feedstocks where the downstream MFCs outperformed the upstream (Gálvez, Greenman & Ieropoulos, 2009; Kim *et al.*, 2010). Therefore the optimum flow rate, HRT, group positioning and amount of magnesium addition need to be chosen accordingly when designing a MFC system for maximising power output and nutrient recovery.

6.4.6. Practical Application

For demonstration purposes, it was attempted to operate a commercially available electronic air freshener with the two groups of 4 MFCs (8 in total) used in this study. The air freshener originally required two D sized batteries to operate. The original circuit board of the automatic air freshener was modified with a 240 mF super-capacitor (Cellergy, Israel) which would allow a maximum voltage of up to 4.2 V. When the charged voltage of the capacitor reached 2.8 V, the air freshener operated the integrated motor, which actuated to press the nozzle of an inserted compressed air spray can. After the firing action, the voltage

of the capacitor decreased to 2.1 V, the system stopped and the capacitor began to charge again. The 4 MFCs within each group were connected as already described above, and the two groups were then connected in series.

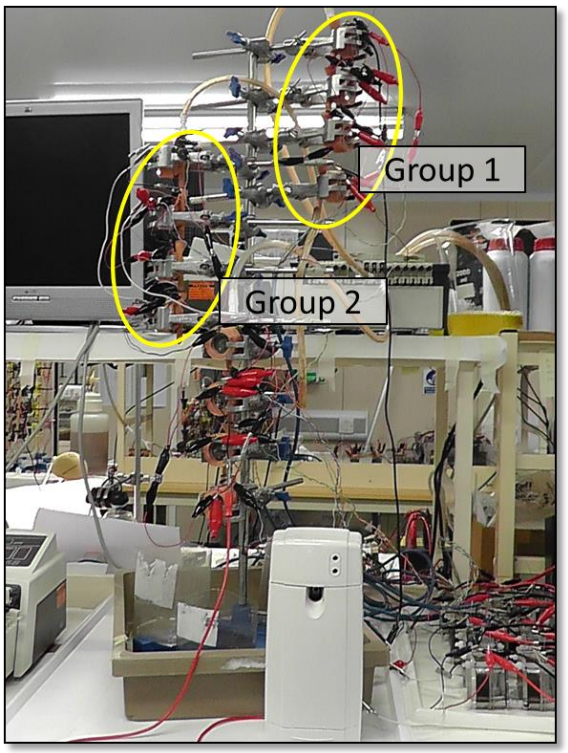

Figure 6.12 Demonstration system set-up
* Top two groups (4 MFCs in each group) in the photo were used for the demonstration.

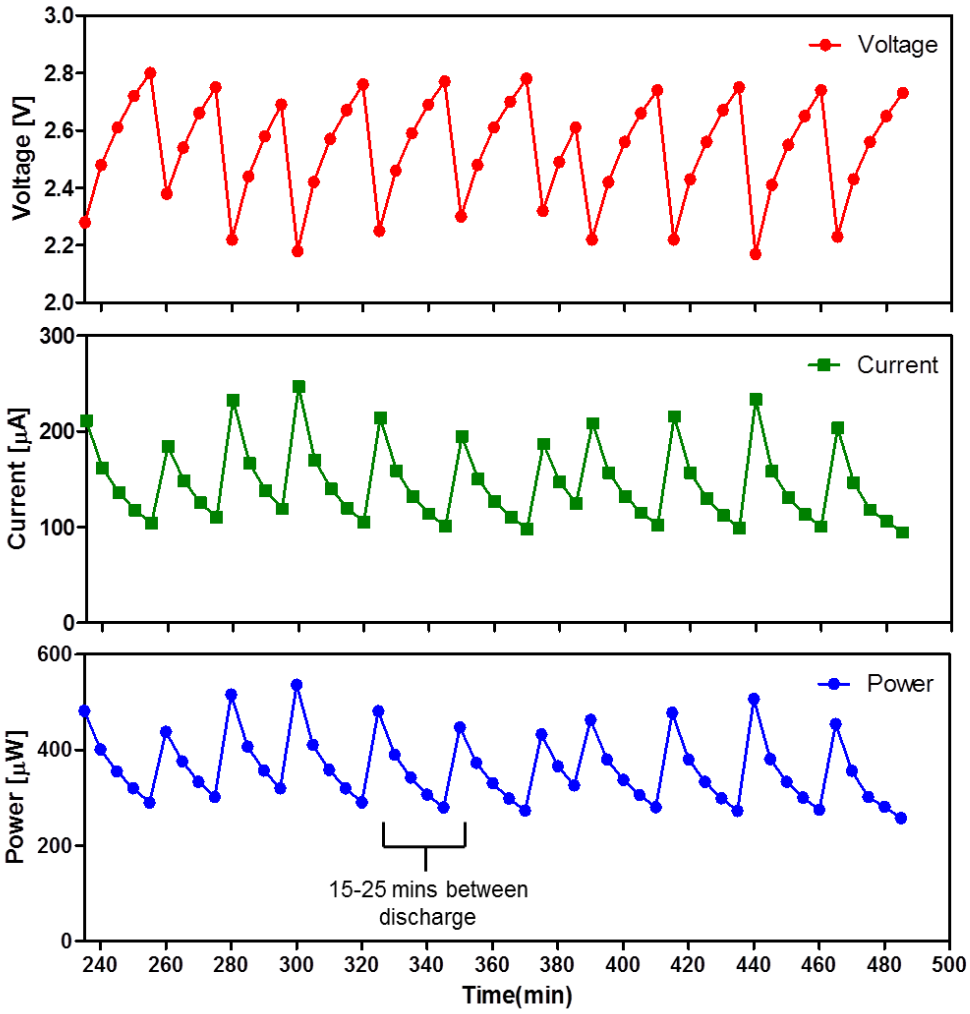

Figure 6.13 Temporal profiles of the MFC stack when connected to a commercial electronic air freshener; charge/discharge cycle in voltage, current and power (from the top).

Figure 6.13 shows the temporal profiles of the MFC stack while operating the automatic air freshener. Each trough and peak represent one charge/discharge cycle where the MFC stack voltage increased as the capacitor was charged. When the capacitor discharged at 2.8 V, the voltage of the stack dropped to 2.1 V then quickly started charging up again. This charge/discharge cycle repeated every 15–25 min for 4 weeks continuously. This exemplar practical application demonstrated successfully the capability of the MFC stack, with only 8 MFCs of 6.25 mL anodic volume each.

6.5. Chapter Conclusions

In this chapter, practical applications of the MFC technology (i.e. waste and wastewater clean-up) were explored based on the findings as shown in the previous chapters. Two troublesome wastes, urine and uric salts showed their great potential for being power sources of electricity generation from MFCs. Furthermore it was successfully demonstrated that operating MFCs can contribute to recovery of resources such as nitrogen and phosphorus in the form of struvite from urine. The suggested 3-stage MFC/struvite extraction process system showed how the MFC technology and struvite precipitation could be beneficially integrated with each other in an attempt to generate energy and recover valuable resources simultaneously. This MFC stack system also proved the capability of the technology by operating a commercial electrical appliance continuously.

7. Overall Conclusions and Future Work

7.1. Conclusions and Summary of Work

The ultimate goal of the thesis was to improve anode performance and waste utilisation. In order to achieve this aim, two main aspects of the MFC anode, system design and biofilm affecting parameters, were investigated. The findings were used to implement the MFC technology for practical applications such as treating difficult wastes and resource recovery as well as producing electrical energy. Each specific objective was accomplished as follows;

(1) To seek better performing components and designs of an MFC reactor

Materials and designs of a MFC system with an intention of building multiple MFC units for waste/wastewater clean-up were explored. CEMs seemed a better choice than AEMs for the pursuing system which would have no need for additional input of compounds as proton carriers. Cost performance is another important aspect when selecting materials, especially for system scale up. Thus the second best performing cation exchange membrane (MI-C) was chosen since it showed the highest performance per unit cost. The MFC performance increased significantly through MPL modification of both anode and cathode (hot-pressed activated carbon open-to-air cathode). By the modification of anode and cathode plain carbon veil material with MPL, 2.2 and 4.9 fold power output improvements were achieved respectively. Although MPL has been used mainly as a cathode material of hydrogen fuel cells, this thesis successfully proved that it can be an excellent material for both anode and cathode of microbial fuel cells. When it was tested as an anode material, various desirable aspects for the MFC anode such as biocompatibility and long-term stability, as well as power producing performance and electrical conductivity were evaluated, which provided in-depth understanding of the material. Furthermore, as a result of steady efforts to make betterment of reactor design, C-MFC was devised to facilitate continuous feeding and the open-to-air cathode.

(2) To evaluate parameters affecting anode biofilms which could lead to ways of manipulating them using these parameters

Experiments investigating the effect of operating temperature, external resistance and feedstock on anode biofilm performance revealed that manipulating anode biofilms towards highly efficient and fast responding initiators of the MFC power generation is possible. Thermophilic anode biofilms running at 60 °C demonstrated their high sensitivity towards operating temperature. This work also proved that the power producing performance of anode biofilm can be improved through mixing two or more electrochemically active species, this came about through an accidental contamination occurring during the work. The performance of anode biofilm can also be controlled by external loads. When maximising power output is expected, keeping the external resistance value close to the internal resistance value is desirable. This is called 'impedance matching' technique which is well known in the field of electronics and this work proved it can be applied in microbial fuel cells as well. This work also highlighted the importance of monitoring open circuit voltage of a running MFC system which could be achieved by the novel way of using the 3rd and 4th pins (refer to appendix E). Under continuous flow condition, MFCs demonstrated their capability of producing stable and reproducible power output according to supplied feedstock. This can be very useful when stable power production is expected or MFC biosensors are considered for practical implementations of the MFC technology. Furthermore this work demonstrated the dynamics of anode biofilm by displaying the importance of not only the initial feedstock but also following feedstocks after the initial period. Through all the experiments, anode biofilms showed their metabolic activity and electricity generating performance can change dynamically according to the external conditions, which implies recovery or reinforcement of biofilm activity is possible even after they are formed on the anodes.

(3) To utilise wastes that have not been tested much in MFCs before and to demonstrate the potential of resource recovery from these wastes

Human urine (both fresh and stale) and uric salts potential was proven as a fuel for MFCs, which have not been explored much in MFC studies before. Especially with urine, MFCs can be integrated with a conventional struvite extraction process not only for recovering electrical energy but also contributing to the existing process by accelerating urea hydrolysis. Unlike other studies investigating struvite recovery from the cathode side of MFCs, this work suggested a separated struvite process is a more practical way to pursue since in this way MFC performance degradation caused by struvite precipitation on membranes and cathodes can be avoided or minimised when treating urine. Through the 3-stage MFC/struvite extraction process system, total 82 % of PO_4^{3-}–P and 20 % of COD of undiluted human urine were removed whilst producing 652 μW.

(4) To build a stack of MFCs operating a commercial electrical appliance as a demonstration of practical applications of the MFC technology

As a completion of the last objective of this thesis, a stack of 8 MFCs used in this work, successfully demonstrated the capability of the MFC technology by operating a commercial electronic air freshener every 15-25 min for 4 weeks continuously. Therefore through the development of a smart design of MFC reactor fitting and electronics such as using super-capacitors or transistors, this can be the first steps to a truly sustainable energy future.

7.2. Original Contributions

This study demonstrated that MFC system performance and waste treatment efficiency can be significantly improved with a better understanding of the anode. The major original contributions of this thesis work are summarised as follows;

The membrane comparison test (chapter 4.2) contributed to the choice of more cost effective ion exchange membrane for the other members work within the Bristol BioEnergy Centre.

The MPL modified electrode (chapter 4.3) was used as an MFC anode for the first time and successfully showed anode performance improvement.

Various designs and materials of an MFC reactor for a relatively small sized MFC unit facilitating continuous supply of feedstock, were devised and tried throughout this study. The last version of reactor design made of Nanocure™ material, C-MFC, met all the requirements for this study. This type of fuel cell design has been used by other members of the research centre.

Dynamic characteristics of anode biofilms corresponding to operating factors such as external load, running temperature and type of feedstock were revealed and novel strategies to manipulate anode biofilms towards specific directions (e.g. power output maximisation, efficiency increase of waste utilisation or recovery of resources) were suggested (chapter 5).

It was the first attempt to use uric salts in MFCs and it was proved that uric salts can be used in MFCs as a source of fuel (chapter 6.3). This work also suggested a solution to the problematic struvite formation whilst operating MFCs with undiluted human urine by recovering struvite separately (chapter 6.4). These studies with urine and uric salts (chapter 6) contributed to ‘Urine-tricity’ research project (funded by the Bill and Melinda Gates Foundation) carried out in the Bristol BioEnergy Centre.

A novel configuration using pin electrodes (appendix E) was investigated and opened up further avenues to explore in terms of pin material, connection/disconnection time or frequency of connections. This work was performed with Iwona Gajda and findings contributed to a patent filing.

7.3. Future Work

Various aspects of the MFC anode were investigated throughout the course of the thesis and opened up further investigation.

In terms of materials and design, seeking affordable and sustainable MFC materials should not stop. For example, ceramic material can be used as a separator or reactor itself. Besides its affordability and sustainability, it showed a good performance in recent work carried out in the Bristol BioEnergy Centre. Optimisation of the MPL modification such as reducing PTFE content or finding an alternative binder can also be performed. In addition to materials, design optimisation for each component needs to be pursued according to the final application. For cascade type MFC stacks, different design of individual MFC units would be required since composition in feedstock might vary throughout the flow. Based on the findings and experience of this thesis, the author is currently involved in an EPSRC funded design mining project (grant no. EP/N005740/1) working on anode and reactor design optimisation using artificial evolution techniques.

The halted work with thermophilic biofilm (chapter 5.2) can be repeated with in depth microbial community analysis and specific target substrates since this could lead to a new venue of MFC technology application. Also modification and improvement of the experimental design will be needed in order to avoid the experienced difficulties. For example, to achieve reliable cathode performance, ferricyanide could be used instead of oxygen dissolved in water and this needs to be stored at the same operating temperature with

the feedstock. Or the activated carbon open-to-air cathode can be another option if MFC reactors are placed in humid or aqueous condition. Thermophilic metabolism has many advantages compared to mesophilic or psychrophilic metabolism due to increases in microbial activity rates. This could contribute to enhancement of waste/wastewater treatment and electricity generation.

There are a lot of interesting paths to take the suggested 3-stage MFC/struvite extraction process system into further study. It would be worth making an attempt to utilise the struvite collected from the system as a fertiliser and compare its efficiency to commercial fertilisers or collected struvite without the MFC operation. Also seeking a cheaper and more sustainable alternative to provide additional magnesium, such as magnesium containing ash from local incineration plants, is worthwhile for practical implementation of the system especially for developing countries. Furthermore since this work was attempting to prove the concept, further improvements and optimisation of the technology need to continue.

The work on 3rd and 4th pin has demonstrated some novel findings, which have formed the basis for a patent filing. The original conception of the idea and preliminary work took place before this thesis, however the experiments carried out and findings generated during this thesis (see appendix E), have helped strengthen the case. There is a significant amount of work that could be done in terms of pin material relative to the working electrode material, pin-driver connection time and frequency of connections, different connectivity between the "working" and "driver" MFCs, as well as the value of the external load, when the pins are engaged. This is a direction that is currently being pursued and could form the basis for a number of new projects in this area alone.

List of Publications

Gajda, I., You, J., Greenman, J., Melhuish, C. and Ieropoulos, I. (2011) "Comparative study of multiple membranes for MFCs", In: Electrochem 2011 conference, 5–6 September, Bath, UK.

You, J., Greenman, J., Melhuish, C. and Ieropoulos, I. (2012) "External resistance effect during MFC maturing period", In: Electrochem 2012 conference, 2–4 September, Dublin, Ireland.

You, J., Greenman, J., Melhuish, C. and Ieropoulos, I. (2012) "Small-scale microbial fuel cells utilising uric salts", In: EmHyTeC - Euro Mediterranean Hydrogen Technologies Conference 11 - 14 September, Hammamet, Tunisia.

Ieropoulos, I., Gajda, I., You, J. and Greenman, J. (2013) "Urine—waste or resource? The economic and social aspects" *Reviews in Advanced Sciences and Engineering*, 2(3), pp. 192–9.

You, J., Santoro, C., Greenman, J., Melhuish, C., Cristiani, P., Li, B. and Ieropoulos, I. (2013) "MPL based anode for improved performance in microbial fuel cells", In: European Fuel Cell Technology & Applications Conference 11–13 December, Rome, Italy.

You, J., Greenman, J., Melhuish, C. and Ieropoulos, I. (2013) "Microbial fuel cell performance improvement through electrodes modification", In: Hydrogen & Fuel Cell SUPERGEN Researcher Conference, 16–18 December, Birmingham, UK.

You, J., Greenman, J., Melhuish, C. and Ieorpoulos, I. (2014) "Small-scale microbial fuel cells utilising uric salts" *Sustainable Energy Technologies and Assessments*, 6, pp. 60–3.

You, J., Greenman, J., Melhuish, C. and Ieorpoulos, I. (2014) "Micro porous layer (MPL)-based anode for microbial fuel cells" *International Journal of Hydrogen Energy*, 39, pp. 21811–8.

You, J., Greenman, J., Melhuish, C. and Ieropoulos, I. (2014) “Electricity generation and struvite recovery from urine using microbial fuel cells”, In: World Renewable Energy Congress, 3–8 August, London, UK.

You, J., Greenman, J., Melhuish, C. and Ieorpoulos, I. (2015) “Electricity generation and struvite recovery from human urine using microbial fuel cells” *Journal of Chemical Technology and Biotechnology*, DOI: 10.1002/jctb.4617.

You, J., Walter, X.A., Greenman, J., Melhuish, C. and Ieropoulos, I. (2015) “Stability and reliability of anodic biofilms under different feedstock conditions: towards microbial fuel cell sensors”, In: 4th International Bio-sensing Technology Conference, 10–13 May, Lisbon, Portugal.

You, J., Walter, X.A., Greenman, J., Melhuish, C. and Ieropoulos, I. (2015) “Stability and reliability of anodic biofilms under different feedstock conditions: towards microbial fuel cell sensors” *Sensing and Bio-Sensing Research*, 6, pp. 43-50..

List of References

Abbas, C.A. & Sibirny, A.A. (2011) Genetic control of biosynthesis and transport of riboflavin and flavin nucleotides and construction of robust biotechnological producers. *Microbiology and Molecular Biology Reviews : MMBR*. 75 (2), pp. 321–360.

Aelterman, P., Rabaey, K., Clauwaert, P. & Verstraete, W. (2006a) Microbial fuel cells for wastewater treatment. *Water Science & Technology*. 54 (8), pp. 9.

Aelterman, P., Rabaey, K., Pham, H.T., Boon, N. & Verstraete, W. (2006b) Continuous electricity generation at high voltages and currents using stacked microbial fuel cells. *Environmental Science & Technology*. 40 (10), pp. 3388–3394.

Aelterman, P., Versichele, M., Marzorati, M., Boon, N. & Verstraete, W. (2008) Loading rate and external resistance control the electricity generation of microbial fuel cells with different three-dimensional anodes. *Bioresource Technology*. 99 (18), pp. 8895–8902.

Aldrovandi, A., Marsili, E., Stante, L., Paganin, P., Tabacchioni, S. & Giordano, A. (2009) Sustainable power production in a membrane-less and mediator-less synthetic wastewater microbial fuel cell. *Bioresource Technology*. 100 (13), pp. 3252–3260.

Allesen-Holm, M., Barken, K.B., Yang, L., Klausen, M., Webb, J.S., Kjelleberg, S., Molin, S., Givskov, M. & Tolker-Nielsen, T. (2006) A characterization of DNA release in Pseudomonas aeruginosa cultures and biofilms. *Molecular Microbiology*. 59 (4), pp. 1114–1128.

Aman, M.M., Solangi, K.H., Hossain, M.S., Badarudin, A., Jasmon, G.B., Mokhlis, H., Bakar, A.H.A. & Kazi, S.. (2015) A review of safety, health and environmental (SHE) issues of solar energy system. *Renewable and Sustainable Energy Reviews*. 41pp. 1190–1204.

Babauta, J., Renslow, R., Lewandowski, Z. & Beyenal, H. (2012) Electrochemically active biofilms: facts and fiction. A review. *Biofouling*. 28 (8), pp. 789–812.

Baidya Roy, S., Pacala, S.W. & Walko, R.L. (2004) Can large wind farms affect local meteorology? *Journal of Geophysical Research*. 109 (D19), pp. D19101.

Bennetto, H.P. (1990) Electricity generation by microorganisms. *Biotechnology Education*. 1 (4), pp. 163–168.

Bennetto, H.P., Delaney, G.M., Mason, J.R., Roller, S.D., Stirling, J.L. & Thurston, C.F. (1985) The sucrose fuel cell: Efficient biomass conversion using a microbial catalyst. *Biotechnology Letters*. 7 (10), pp. 699–704.

Bennetto, H.P., Stirling, J.L., Tanaka, K. & Vega, C.A. (1983) Anodic reactions in microbial fuel cells. *Biotechnology and Bioengineering*. 25 (2), pp. 559–568.

Bhattarai, K.K., Taiganides, E.P. & Yap, B.C. (1989) Struvite deposits in pipes and aerators. *Biological Wastes*. 30 (2), pp. 133–147.

Biffinger, J.C., Pietron, J., Ray, R., Little, B. & Ringeisen, B.R. (2007a) A biofilm enhanced miniature microbial fuel cell using Shewanella oneidensis DSP10 and oxygen reduction cathodes. *Biosensors & Bioelectronics*. 22 (8), pp. 1672–1679.

Biffinger, J.C., Ray, R., Little, B. & Ringeisen, B.R. (2007b) Diversifying biological fuel cell designs by use of nanoporous filters. *Environmental Science & Technology*. 41 (4), pp. 1444–1449.

Bond, D.R. & Lovley, D.R. (2003) Electricity production by Geobacter sulfurreducens attached to electrodes. *Applied and Environmental Microbiology*. 69 (3), pp. 1548–1555.

Bond, D.R. & Lovley, D.R. (2005) Evidence for involvement of an electron shuttle in

electricity generation by Geothrix fermentans. *Applied and Environmental Microbiology*. 71 (4), pp. 2186–2189.

Borole, A.P., Reguera, G., Ringeisen, B., Wang, Z.-W., Feng, Y. & Kim, B.H. (2011) Electroactive biofilms: Current status and future research needs. *Energy & Environmental Science*. 4 (12), pp. 4813.

Bossio, D. a., Girvan, M.S., Verchot, L., Bullimore, J., Borelli, T., Albrecht, a., Scow, K.M., Ball, a. S., Pretty, J.N. & Osborn, a. M. (2005) Soil microbial community response to land use change in an agricultural landscape of western Kenya. *Microbial Ecology*. 49 (1), pp. 50–62.

Brdjanovic, D., Slamet, A., van Loosdrecht, M.C.M., Hooijmans, C.M., Alaerts, G.J. & Heijnen, J.J. (1998) Impact of excessive aeration on biological phosphorus removal from wastewater. *Water Research*. 32 (1), pp. 200–208.

Bullen, R.A., Arnot, T.C., Lakeman, J.B. & Walsh, F.C. (2006) Biofuel cells and their development. *Biosensors & Bioelectronics*. 21 (11), pp. 2015–2045.

Capodaglio, a G., Molognoni, D., Dallago, E., Liberale, A., Cella, R., Longoni, P. & Pantaleoni, L. (2013) Microbial fuel cells for direct electrical energy recovery from urban wastewaters. *The Scientific World Journal*. 2013pp. 8.

Catal, T., Kavanagh, P., O'Flaherty, V. & Leech, D. (2011) Generation of electricity in microbial fuel cells at sub-ambient temperatures. *Journal of Power Sources*. 196 (5), pp. 2676–2681.

Chae, K.J., Choi, M., Ajayi, F.F., Park, W., Chang, I.S. & Kim, I.S. (2008) Mass transport through a proton exchange membrane (nafion) in microbial fuel cells. *Energy & Fuels*. 22 (1), pp. 169–176.

Chae, K.-J., Choi, M.-J., Lee, J.-W., Kim, K.-Y. & Kim, I.S. (2009) Effect of different substrates on the performance, bacterial diversity, and bacterial viability in microbial fuel cells. *Bioresource Technology*. 100 (14), pp. 3518–3525.

Chaudhuri, S.K. & Lovley, D.R. (2003) Electricity generation by direct oxidation of glucose in mediatorless microbial fuel cells. *Nature Biotechnology*. 21 (10), pp. 1229–1232.

Chen, Y.-M., Wang, C.-T., Yang, Y.-C. & Chen, W.-J. (2013) Application of aluminum-alloy mesh composite carbon cloth for the design of anode/cathode electrodes in Escherichia coli microbial fuel cell. *International Journal of Hydrogen Energy*. 38 (25), pp. 11131–11137.

Chen, Z., Li, K., Zhang, P., Pu, L., Zhang, X. & Fu, Z. (2015) The performance of activated carbon treated with H3PO4 at 80°C in the air-cathode microbial fuel cell. *Chemical Engineering Journal*. 259pp. 820–826.

Cheng, S. & Logan, B.E. (2007) Ammonia treatment of carbon cloth anodes to enhance power generation of microbial fuel cells. *Electrochemistry Communications*. 9 (3), pp. 492–496.

Cheng, S., Xing, D. & Logan, B.E. (2011) Electricity generation of single-chamber microbial fuel cells at low temperatures. *Biosensors & Bioelectronics*. 26 (5), pp. 1913–1917.

Cho, K.T. & Mench, M.M. (2012) Investigation of the role of the micro-porous layer in polymer electrolyte fuel cells with hydrogen deuterium contrast neutron radiography. *Physical Chemistry Chemical Physics : PCCP*. 14 (12), pp. 4296–4302.

Clauwaert, P., Aelterman, P., Pham, T.H., De Schamphelaire, L., Carballa, M., Rabaey, K. & Verstraete, W. (2008) Minimizing losses in bio-electrochemical systems: the road to applications. *Applied Microbiology and Biotechnology*. 79 (6), pp. 901–913.

Clesceri, L.S. (1998) *Standard methods for the examination of water and wastewater*. American Public Health Association.

Cohen, B. (1931) The bacterial culture as an electrical half-cell. *Journal of Bacteriology*. 21pp. 18–19.

Cordell, D., Drangert, J.-O. & White, S. (2009) The story of phosphorus: Global food security and food for thought. *Global Environmental Change*. 19 (2), pp. 292–305.

Le Corre, K.S., Valsami-Jones, E., Hobbs, P., Jefferson, B. & Parsons, S.A. (2007) Agglomeration of struvite crystals. *Water Research*. 41 (2), pp. 419–425.

Crittenden, S.R., Sund, C.J. & Sumner, J.J. (2006) Mediating electron transfer from bacteria to a gold electrode via a self-assembled monolayer. *Langmuir : the ACS journal of surfaces and colloids*. 22 (23), pp. 9473–9476.

Davis, F. & Higson, S.P.J. (2007) Biofuel cells-recent advances and applications. *Biosensors & Bioelectronics*. 22 (7), pp. 1224–1235.

Deeke, A., Sleutels, T.H.J.A., Donkers, T.F.W., Hamelers, H.V.M., Buisman, C.J.N. & Ter Heijne, A. (2015) Fluidized capacitive bioanode as a novel reactor concept for the microbial fuel cell. *Environmental Science & Technology*. 49 (3), pp. 1929–1935.

Department of Energy & Climate Change (2014a) *Energy Trends*.

Department of Energy & Climate Change (2014b) *UK energy in brief 2014*.

Donlan, R.M. (2002) Biofilms: Microbial life on surfaces. *Emerging Infectious Diseases*. 8 (9), pp. 881–890.

Doyle, J.D. & Parsons, S.A. (2002) Struvite formation, control and recovery. *Water Research*. 36 (16), pp. 3925–3940.

DuPont (n.d.) *Fluoroplastic Comparison - Typical Properties*. Available from: http://www2.dupont.com/Teflon_Industrial/en_US/tech_info/techinfo_compare.html [Accessed 1 March 2014].

Duteanu, N., Erable, B., Senthil Kumar, S.M., Ghangrekar, M.M. & Scott, K. (2010) Effect of chemically modified Vulcan XC-72R on the performance of air-breathing cathode in a single-chamber microbial fuel cell. *Bioresource Technology*. 101 (14), pp. 5250–5255.

El-Chakhtoura, J., El-Fadel, M., Rao, H.A., Li, D., Ghanimeh, S. & Saikaly, P.E. (2014) Electricity generation and microbial community structure of air-cathode microbial fuel cells powered with the organic fraction of municipal solid waste and inoculated with different seeds. *Biomass and Bioenergy*. 67pp. 24–31.

Extance, J.P. (2012) *Bioethanol Production : Characterisation of a Bifunctional Alcohol Dehydrogenase from Geobacillus thermoglucosidasius*. University of Bath.

Fan, Y., Hu, H. & Liu, H. (2007) Enhanced Coulombic efficiency and power density of air-cathode microbial fuel cells with an improved cell configuration. *Journal of Power Sources*. 171 (2), pp. 348–354.

Fan, Y., Xu, S., Schaller, R., Jiao, J., Chaplen, F. & Liu, H. (2011) Nanoparticle decorated anodes for enhanced current generation in microbial electrochemical cells. *Biosensors & Bioelectronics*. 26 (5), pp. 1908–1912.

el Fantroussi, S., Verschuere, L., Verstraete, W. & Top, E.M. (1999) Effect of phenylurea herbicides on soil microbial communities estimated by analysis of 16S rRNA gene fingerprints and community-level physiological profiles. *Applied and Environmental Microbiology*. 65 (3), pp. 982–988.

Fattah, K.P. (2012) Assessing struvite formation potential at wastewater treatment plants. *International Journal of Environmental Science and Development*. 3 (6), pp. 548–552.

Feng, Y., Yang, Q., Wang, X. & Logan, B.E. (2010) Treatment of carbon fiber brush anodes for improving power generation in air–cathode microbial fuel cells. *Journal of Power Sources*. 195 (7), pp. 1841–1844.

Frąc, M., Oszust, K. & Lipiec, J. (2012) Community level physiological profiles (CLPP), characterization and microbial activity of soil amended with dairy sewage sludge. *Sensors*. 12 (3), pp. 3253–3268.

Freguia, S., Rabaey, K., Yuan, Z. & Keller, J. (2007) Non-catalyzed cathodic oxygen reduction at graphite granules in microbial fuel cells. *Electrochimica Acta*. 53 (2), pp. 598–603.

Gajda, I., Greenman, J., Melhuish, C. & Ieropoulos, I. (2013) Photosynthetic cathodes for microbial fuel cells. *International Journal of Hydrogen Energy*. 38 (26), pp. 11559–11564.

Gajda, I., Greenman, J., Melhuish, C. & Ieropoulos, I. (2015) Simultaneous electricity generation and microbially-assisted electrosynthesis in ceramic MFCs. *Bioelectrochemistry*. 104pp. 58–64.

Gálvez, A., Greenman, J. & Ieropoulos, I. (2009) Landfill leachate treatment with microbial fuel cells; scale-up through plurality. *Bioresource Technology*. 100 (21), pp. 5085–5091.

Garland, J.L. (1996) Analytical approaches to the characterization of samples of microbial communities using patterns of potential C source utilization. *Soil Biology and Biochemistry*. 28 (2), pp. 213–221.

Garland, J.L. & Mills, A.L. (1991) Classification and characterization of heterotrophic microbial communities on the basis of patterns of community-level sole-carbon-source utilization. *Applied and Environmental Microbiology*. 57 (8), pp. 2351–2359.

Ge, Z., Li, J., Xiao, L., Tong, Y. & He, Z. (2014) Recovery of electrical energy in microbial fuel cells. *Environmental Science & Technology Letters*. 1 (2), pp. 137–141.

Gil, G., Chang, I., Kim, B.H., Kim, M., Jang, J., Park, H.S. & Kim, H.J. (2003) Operational parameters affecting the performance of a mediator-less microbial fuel cell. *Biosensors & Bioelectronics*. 18pp. 327–334.

Giorgi, L., Antolini, E., Pozio, A. & Passalacqua, E. (1998) Influence of the PTFE content in the diffusion layer of low-Pt loading electrodes for polymer electrolyte fuel cells. *Electrochimica Acta*. 43 (24), pp. 3675–3680.

Gnana Kumar, G., Awan, Z., Suk Nahm, K. & Xavier, J.S. (2014) Nanotubular MnO2/graphene oxide composites for the application of open air-breathing cathode microbial fuel cells. *Biosensors & Bioelectronics*. 53pp. 528–534.

Gorby, Y.A., Yanina, S., McLean, J.S., Rosso, K.M., Moyles, D., Dohnalkova, A., Beveridge, T.J., Chang, I.S., Kim, B.H., Kim, K.S., Culley, D.E., Reed, S.B., Romine, M.F., Saffarini, D.A., et al. (2006) Electrically conductive bacterial nanowires produced by Shewanella oneidensis strain MR-1 and other microorganisms. *Proceedings of the National Academy of Sciences of the United States of America*. 103 (30), pp. 11358–11363.

Greenman, J., Gálvez, A., Giusti, L. & Ieropoulos, I. (2009) Electricity from landfill leachate using microbial fuel cells: Comparison with a biological aerated filter. *Enzyme and Microbial Technology*. 44 (2), pp. 112–119.

Ha, P.T., Tae, B. & Chang, I.S. (2008) Performance and bacterial consortium of microbial fuel cell fed with formate. *Energy and Fuels*. 22 (1), pp. 164–168.

Habermann, W. & Pommer, E.H. (1991) Biological fuel cells with sulphide storage capacity.

Applied Microbiology and Biotechnology. 35 (1), pp. 128–133.

HaoYu, E., Cheng, S., Scott, K. & Logan, B. (2007) Microbial fuel cell performance with non-Pt cathode catalysts. *Journal of Power Sources*. 171 (2), pp. 275–281.

Harnisch, F., Schröder, U. & Scholz, F. (2008) The suitability of monopolar and bipolar ion exchange membranes as separators for biological fuel cells. *Environmental Science & Technology*. 42 (5), pp. 1740–1746.

Harnisch, F., Warmbier, R., Schneider, R. & Schröder, U. (2009) Modeling the ion transfer and polarization of ion exchange membranes in bioelectrochemical systems. *Bioelectrochemistry*. 75 (2), pp. 136–141.

He, Z., Minteer, S.D. & Angenent, L.T. (2005) Electricity generation from artificial wastewater using an upflow microbial fuel cell. *Environmental Science & Technology*. 39 (14), pp. 5262–5267.

Heidrich, E.S., Curtis, T.P. & Dolfing, J. (2011) Determination of the internal chemical energy of wastewater. *Environmental Sciience & Technology*. 45 (2), pp. 827–832.

ter Heijne, A., Hamelers, H.V.M., Saakes, M. & Buisman, C.J.N. (2008) Performance of non-porous graphite and titanium-based anodes in microbial fuel cells. *Electrochimica Acta*. 53 (18), pp. 5697–5703.

Hirooka, K. & Ichihashi, O. (2013) Phosphorus recovery from artificial wastewater by microbial fuel cell and its effect on power generation. *Bioresource Technology*. 137pp. 368–375.

Huang, L., Chai, X., Cheng, S. & Chen, G. (2011) Evaluation of carbon-based materials in tubular biocathode microbial fuel cells in terms of hexavalent chromium reduction and electricity generation. *Chemical Engineering Journal*. 166 (2), pp. 652–661.

Ieropoulos, I. a, Ledezma, P., Stinchcombe, A., Papaharalabos, G., Melhuish, C. & Greenman, J. (2013) Waste to real energy: the first MFC powered mobile phone. *Physical Chemistry Chemical Physics*. 15 (37), pp. 15312–15316.

Ieropoulos, I. a., Greenman, J., Melhuish, C. & Hart, J. (2005) Comparative study of three types of microbial fuel cell. *Enzyme and Microbial Technology*. 37 (2), pp. 238–245.

Ieropoulos, I., Greenman, J. & Melhuish, C. (2003) Imitating metabolism : Energy autonomy in biologically inspired robots. In: *AISB '03, Second International Symposium on Imitation in Animals and Artifacts*. 2003 Aberystwyth, Wales: . pp. pp. 191–194.

Ieropoulos, I., Greenman, J. & Melhuish, C. (2010) Improved energy output levels from small-scale microbial fuel cells. *Bioelectrochemistry*. 78 (1), pp. 44–50.

Ieropoulos, I., Greenman, J. & Melhuish, C. (2012) Urine utilisation by microbial fuel cells; energy fuel for the future. *Physical Chemistry Chemical Physics*. 14 (1), pp. 94–98.

Ieropoulos, I., Greenman, J., Melhuish, C. & Horsfield, I. (2010) EcoBot-III: a robot with guts. In: *The 12th International Conference on the Synthesis and Simulation of Living Systems*. 2010 pp. pp. 733–740.

Ieropoulos, I., Melhuish, C. & Greenman, J. (2007) Artificial gills for robots: MFC behaviour in water. *Bioinspiration & Biomimetics*. 2 (3), pp. S83–S93.

Ieropoulos, I., Winfield, J. & Greenman, J. (2010) Effects of flow-rate, inoculum and time on the internal resistance of microbial fuel cells. *Bioresource Technology*. 101 (10), pp. 3520–3525.

Ieropoulos, I.A., Greenman, J. & Melhuish, C. (2013) Miniature microbial fuel cells and stacks for urine utilisation. *International Journal of Hydrogen Energy*. 38 (1), pp. 492–496.

Ieropoulos, I., Greenman, J., Melhuish, C. (2008) Microbial fuel cells based on carbon veil electrodes: Stack configuration and scalability. *International Journal of Energy Research*. 32pp. 1228–1240.

International Energy Agency (2014) *Key World Energy Statistics*.

International Energy Agency (2010) *World Energy Outlook 2010*.

International Renewable Energy Agency (2012) *Renewable energy technologies: Cost analysis series, Volume1: Power Sector, Issue 3/5 Hydropower*. 1 (3).

IPCC (2013) *Summary for Policymakers. In: Climate Change 2013: The Physical Science Basis. Contribution of Working Group I to the Fifth Assessment Report of the Intergovernmental Panel on Climate Change*. T.F. Socker, D. Qin, G.K. Plattner, M. Tignor, S.K. Allen, J. Boschung, A. Nauels, Y. Xia, V. Bex, & P.M. Midgley (eds.). Cambridge, United Kingdom and New York, NY, USA: Cambridge University Press.

Ishii, S., Watanabe, K., Yabuki, S., Logan, B.E. & Sekiguchi, Y. (2008) Comparison of electrode reduction activities of Geobacter sulfurreducens and an enriched consortium in an air-cathode microbial fuel cell. *Applied and Environmental Microbiology*. 74 (23), pp. 7348–7355.

Jambeck, J.R. & Damiano, L. (2010) *Microbial fuel cells in landfill applications*.

Jana, P.S., Behera, M. & Ghangrekar, M.M. (2010) Performance comparison of up-flow microbial fuel cells fabricated using proton exchange membrane and earthen cylinder. *International Journal of Hydrogen Energy*. 35 (11), pp. 5681–5686.

Jiang, D. & Li, B. (2009) Granular activated carbon single-chamber microbial fuel cells (GAC-SCMFCs): A design suitable for large-scale wastewater treatment processes. *Biochemical Engineering Journal*. 47 (1-3), pp. 31–37.

Jong, B.C., Kim, B.H., Chang, I.S., Liew, P.W.Y., Choo, Y.F. & Kang, G.S. (2006) Enrichment, performance, and microbial diversity of a thermophilic mediatorless microbial fuel cell. *Environmental Science & Technology*. 40 (20), pp. 6449–6454.

Jung, S. & Regan, J.M. (2007) Comparison of anode bacterial communities and performance in microbial fuel cells with different electron donors. *Applied Microbiology and Biotechnology*. 77 (2), pp. 393–402.

Kim, B.H., Chang, I.S. & Gadd, G.M. (2007) Challenges in microbial fuel cell development and operation. *Applied Microbiology and Biotechnology*. 76 (3), pp. 485–494.

Kim, B.H., Kim, H.J., Hyun, M.S. & Park, D.H. (1999) Direct electrode reaction of Fe(III)-reducing bacterium, Shewanella putrefaciens. *Journal of Microbiology and Biotechnology*.

Kim, B.H., Park, H.S., Kim, H.J., Kim, G.T., Chang, I.S., Lee, J. & Phung, N.T. (2004) Enrichment of microbial community generating electricity using a fuel-cell-type electrochemical cell. *Applied Microbiology and Biotechnology*. 63 (6), pp. 672–681.

Kim, G.T., Webster, G., Wimpenny, J.W.T., Kim, B.H., Kim, H.J. & Weightman, A.J. (2006) Bacterial community structure, compartmentalization and activity in a microbial fuel cell. *Journal of Applied Microbiology*. 101 (3), pp. 698–710.

Kim, J.R., Cheng, S., Oh, S.-E. & Logan, B.E. (2007) Power generation using different cation, anion, and ultrafiltration membranes in microbial fuel cells. *Environmental Science & Technology*. 41 (3), pp. 1004–1009.

Kim, J.R., Premier, G.C., Hawkes, F.R., Dinsdale, R.M. & Guwy, A.J. (2009) Development of a tubular microbial fuel cell (MFC) employing a membrane electrode assembly cathode. *Journal of Power Sources*. 187 (2), pp. 393–399.

Kim, J.R., Premier, G.C., Hawkes, F.R., Rodríguez, J., Dinsdale, R.M. & Guwy, A.J. (2010) Modular tubular microbial fuel cells for energy recovery during sucrose wastewater treatment at low organic loading rate. *Bioresource Technology*. 101 (4), pp. 1190–1198.

Kim, M., Youn, S.M., Shin, S.H., Jang, J.G., Han, S.H., Hyun, M.S., Gadd, G.M. & Kim, H.J. (2003) Practical field application of a novel BOD monitoring system. *Journal of Environmental Monitoring*. 5 (4), pp. 640–643.

Kim, N., Choi, Y., Jung, S. & Kim, S. (2000) Effect of initial carbon sources on the performance of microbial fuel cells containing Proteus vulgaris. *Biotechnology and Bioengineering*. 70 (1), pp. 109–114.

Kirchmann, H. & Pettersson, S. (1995) Human urine - chemical composition and fertilizer use efficiency. *Fertilizer Research*. 40pp. 149–154.

Kondo, T. & Ikeda, T. (1999) An electrochemical method for the measurements of substrate-oxidizing activity of acetic acid bacteria using a carbon-paste electrode modified with immobilized bacteria. *Applied Microbiology and Biotechnology*. 51 (5), pp. 664–668.

Konopka, A., Oliver, L. & Jr., R.F.T. (1998) The use of carbon substrate utilization patterns in environmental and ecological microbiology. *Microbial Ecology*. 35 (2), pp. 103–115.

Kuntke, P., Sleutels, T.H.J.A., Saakes, M. & Buisman, C.J.N. (2014) Hydrogen production and ammonium recovery from urine by a microbial electrolysis cell. *International Journal of Hydrogen Energy*. 39 (10), pp. 4771–4778.

Kuntke, P., Smiech, K.M., Bruning, H., Zeeman, G., Saakes, M., Sleutels, T.H.J.A., Hamelers, H.V.M. & Buisman, C.J.N. (2012) Ammonium recovery and energy production from urine by a microbial fuel cell. *Water Research*. 46 (8), pp. 2627–2636.

Larminie, J. & Dicks, A. (2003) *Fuel cell systems explained*. 2nd edition. SAE International.

Larrosa-Guerrero, A., Scott, K., Head, I.M., Mateo, F., Ginesta, A. & Godinez, C. (2010) Effect of temperature on the performance of microbial fuel cells. *Fuel*. 89 (12), pp. 3985–3994.

Larsen, T. & Gujer, W. (1996) Separate management of anthropogenic nutrient solutions (human urine). *Water Science and Technology*. 34 (3-4), pp. 87–94.

Ledezma, P., Greenman, J. & Ieropoulos, I. (2012) Maximising electricity production by controlling the biofilm specific growth rate in microbial fuel cells. *Bioresource Technology*. 118pp. 615–618.

Lee, S.A., Choi, Y., Jung, S. & Kim, S. (2002) Effect of initial carbon sources on the electrochemical detection of glucose by Gluconobacter oxydans. *Bioelectrochemistry*. 57 (2), pp. 173–178.

Lefebvre, O., Ooi, W.K., Tang, Z., Abdullah-Al-Mamun, M., Chua, D.H.C. & Ng, H.Y. (2009) Optimization of a Pt-free cathode suitable for practical applications of microbial fuel cells. *Bioresource Technology*. 100 (20), pp. 4907–4910.

Lefebvre, O., Shen, Y., Tan, Z., Uzabiaga, A., Chang, I.S. & Ng, H.Y. (2011) A comparison of membranes and enrichment strategies for microbial fuel cells. *Bioresource Technology*. 102 (10), pp. 6291–6294.

Lewis, N.S. & Nocera, D.G. (2006) Powering the planet: chemical challenges in solar energy utilization. *Proceedings of the National Academy of Sciences of the United States of America*. 103 (43), pp. 15729–15735.

Li, F., Sharma, Y., Lei, Y., Li, B. & Zhou, Q. (2010) Microbial fuel cells: the effects of configurations, electrolyte solutions, and electrode materials on power generation. *Applied Biochemistry and Biotechnology*. 160 (1), pp. 168–181.

Li, H., Tang, Y., Wang, Z., Shi, Z., Wu, S., Song, D., Zhang, J., Fatih, K., Zhang, J., Wang, H., Liu, Z., Abouatallah, R. & Mazza, A. (2008) A review of water flooding issues in the proton exchange membrane fuel cell. *Journal of Power Sources*. 178 (1), pp. 103–117.

Li, W.-W., Sheng, G.-P., Liu, X.-W. & Yu, H.-Q. (2011) Recent advances in the separators for microbial fuel cells. *Bioresource Technology*. 102 (1), pp. 244–252.

Lind, B.-B., Ban, Z. & Bydén, S. (2000) Nutrient recovery from human urine by struvite crystallization with ammonia adsorption on zeolite and wollastonite. *Bioresource Technology*. 73 (2), pp. 169–174.

Liu, H., Cheng, S. & Logan, B.E. (2005) Production of electricity from acetate or butyrate using a single-chamber microbial fuel cell. *Environmental Science & Technology*. 39 (2), pp. 658–662.

Liu, H., Hu, H., Chignell, J. & Fan, Y. (2010a) Microbial electrolysis: novel technology for hydrogen production from biomass. *Biofuels*. 1 (1), pp. 129–142.

Liu, H. & Logan, B.E. (2004) Electricity generation using an air-cathode single chamber microbial fuel cell in the presence and absence of a proton exchange membrane. *Environmental Science & Technology*. 38 (14), pp. 4040–4046.

Liu, Y., Harnisch, F., Fricke, K., Schröder, U., Climent, V. & Feliu, J.M. (2010b) The study of electrochemically active microbial biofilms on different carbon-based anode materials in microbial fuel cells. *Biosensors & Bioelectronics*. 25 (9), pp. 2167–2171.

Liu, Z., Liu, J., Zhang, S. & Su, Z. (2009) Study of operational performance and electrical response on mediator-less microbial fuel cells fed with carbon- and protein-rich substrates. *Biochemical Engineering Journal*. 45 (3), pp. 185–191.

Liu, Z., Zhao, Q., Wang, K., Lee, D., Qiu, W. & Wang, J. (2008) Urea hydrolysis and recovery of nitrogen and phosphorous as MAP from stale human urine. *Journal of Environmental Sciences (China)*. 20 (8), pp. 1018–1024.

Logan, B.E., Hamelers, B., Rozendal, R., Schröder, U., Keller, J., Freguia, S., Aelterman, P., Verstraete, W. & Rabaey, K. (2006) Microbial fuel cells: Methodology and technology. *Environmental Science and Technology*. 40 (17), pp. 5181–5192.

Logan, B.E. & Regan, J.M. (2006) Electricity-producing bacterial communities in microbial fuel cells. *Trends in Microbiology*. 14 (12), pp. 512–518.

Lovley, D.R. (2006) Microbial fuel cells: novel microbial physiologies and engineering approaches. *Current Opinion in Biotechnology*. 17 (3), pp. 327–332.

Lowy, D.A. & Tender, L.M. (2008) Harvesting energy from the marine sediment–water interface. *Journal of Power Sources*. 185 (1), pp. 70–75.

Lowy, D.A., Tender, L.M., Zeikus, J.G., Park, D.H. & Lovley, D.R. (2006) Harvesting energy from the marine sediment-water interface II. Kinetic activity of anode materials. *Biosensors & Bioelectronics*. 21 (11), pp. 2058–2063.

Lu, M. & Li, S.F.Y. (2012) Cathode reactions and applications in microbial fuel cells: A review. *Critical Reviews in Environmental Science and Technology*. 42 (23), pp. 2504–2525.

Malaisrie, S.C., Malekzadeh, S. & Biedlingmaier, J.F. (1998) In vivo analysis of bacterial biofilm formation on facial plastic bioimplants. *The Laryngoscope*. 108 (11 Pt 1), pp. 1733–1738.

Manomet Center for Conservation Sciences (2010) *Biomass sustainability and carbon policy study executive summary*. (June).

Mao, Y., Zhang, L., Li, D., Shi, H., Liu, Y. & Cai, L. (2010) Power generation from a biocathode microbial fuel cell biocatalyzed by ferro/manganese-oxidizing bacteria. *Electrochimica Acta*. 55 (27), pp. 7804–7808.

Matz, C. (2011) Competition, communication, cooperation: molecular crosstalk in multi-species biofilm. In: Hans-Curt Flemming, Jost Wingender, & Ulrich Szewzyk (eds.). *Biofilm Highlights*. Springer Berlin Heidelberg. pp. pp. 29–40. doi:10.1007/978-3-642-19940-0.

Mavrodi, D. V, Bonsall, R.F., Delaney, S.M., Soule, M.J., Phillips, G. & Thomashow, L.S. (2001) Functional analysis of genes for biosynthesis of pyocyanin and phenazine-1-carboxamide from Pseudomonas aeruginosa PAO1. *Journal of Bacteriology*. 183 (21), pp. 6454–6465.

McCarty, P.L., Bae, J. & Kim, J. (2011) Domestic wastewater treatment as a net energy producer--can this be achieved? *Environmental Sciience & Technology*. 45 (17), pp. 7100–7106.

Mew, M.C. (2016) Phosphate rock costs, prices and resources interaction. *The Science of the Total Environment*. 542 (Pt B), pp. 1008–1012.

Min, B., Kim, J., Oh, S., Regan, J.M. & Logan, B.E. (2005) Electricity generation from swine wastewater using microbial fuel cells. *Water Research*. 39 (20), pp. 4961–4968.

Min, B., Román, O.B. & Angelidaki, I. (2008) Importance of temperature and anodic medium composition on microbial fuel cell (MFC) performance. *Biotechnology Letters*. 30 (7), pp. 1213–1218.

Mino, T., van Loosdrecht, M.C.M. & Heijnen, J.J. (1998) Microbiology and biochemistry of the enhanced biological phosphate removal process. *Water Research*. 32 (11), pp. 3193–3207.

Mo, Y., Liang, P., Huang, X., Wang, H. & Cao, X. (2009) Enhancing the stability of power generation of single-chamber microbial fuel cells using an anion exchange membrane. *Journal of Chemical Technology & Biotechnology*. 84 (12), pp. 1767–1772.

Moon, H., Chang, I.S. & Kim, B.H. (2006) Continuous electricity production from artificial wastewater using a mediator-less microbial fuel cell. *Bioresource Technology*. 97 (4), pp. 621–627.

Morales, N., Boehler, M., Buettner, S., Liebi, C. & Siegrist, H. (2013) Recovery of N and P from urine by struvite precipitation followed by combined stripping with digester sludge liquid at full scale. *Water*. 5 (3), pp. 1262–1278.

Morris, J.M., Jin, S., Wang, J., Zhu, C. & Urynowicz, M.A. (2007) Lead dioxide as an alternative catalyst to platinum in microbial fuel cells. *Electrochemistry Communications*. 9 (7), pp. 1730–1734.

Münch, E. V & Barr, K. (2001) Controlled struvite crystallisation for removing phosphorus from anaerobic digester sidestreams. *Water Research*. 35 (1), pp. 151–159.

Natarajan, D. & Van Nguyen, T. (2003) Three-dimensional effects of liquid water flooding in the cathode of a PEM fuel cell. *Journal of Power Sources*. 115 (1), pp. 66–80.

Nelson, N.O. (2000) *Phosphorus removal from anaerobic swine lagoon effluent as struvite and its use as a slow-release fertilizer*. Raleigh, NC: North Carolina State University.

Nevin, K.P., Richter, H., Covalla, S.F., Johnson, J.P., Woodard, T.L., Orloff, a. L., Jia, H., Zhang, M. & Lovley, D.R. (2008) Power output and columbic efficiencies from biofilms of Geobacter sulfurreducens comparable to mixed community microbial fuel cells. *Environmental Microbiology*. 10 (10), pp. 2505–2514.

Niessen, J., Schröder, U., Rosenbaum, M. & Scholz, F. (2004) Fluorinated polyanilines as superior materials for electrocatalytic anodes in bacterial fuel cells. *Electrochemistry Communications*. 6 (6), pp. 571–575.

Oh, S., Min, B. & Logan, B.E. (2004) Cathode performance as a factor in electricity generation in microbial fuel cells. *Environmental Science & Technology*. 38 (18), pp. 4900–4904.

Oh, S.-E. & Logan, B.E. (2006) Proton exchange membrane and electrode surface areas as factors that affect power generation in microbial fuel cells. *Applied Microbiology and Biotechnology*. 70 (2), pp. 162–169.

Ohki, T., Nishikawa, N., Hasegawa, T., Okano, T. & Tanizawa, Y. (2009) Characterization of scale formed on the surfaces of toilet bowls. *Journal of Surfactants and Detergents*. 13 (1), pp. 19–26.

Oxfam (2015) *'Pee-power' to light camps in disaster zones*. Available from: https://www.oxfam.org/en/pressroom/pressreleases/2015-03-05/pee-power-light-camps-disaster-zones [Accessed 7 September 2015].

Paganin, V.A., Ticianelli, E.A. & Gonzalez, E.R. (1996) Development and electrochemical studies of gas diffusion electrodes for polymer electrolyte fuel cells. *Journal of Applied Electrochemistry*. 26 (3), pp. 297–304.

Pant, D., Van Bogaert, G., Diels, L. & Vanbroekhoven, K. (2010) A review of the substrates used in microbial fuel cells (MFCs) for sustainable energy production. *Bioresource Technology*. 101 (6), pp. 1533–1543.

Papaharalabos, G., Greenman, J., Melhuish, C., Santoro, C., Cristiani, P., Li, B. & Ieropoulos, I. (2013) Increased power output from micro porous layer (MPL) cathode microbial fuel cells (MFC). *International Journal of Hydrogen Energy*. 38 (26), pp. 11552–11558.

Papaharalabos, G., Greenman, J., Stinchcombe, A., Horsfield, I., Melhuish, C. & Ieropoulos, I. (2014a) Dynamic electrical reconfiguration for improved capacitor charging in microbial fuel cell stacks. *Journal of Power Sources*. 272pp. 34–38.

Papaharalabos, G., Greenman, J., Stinchcombe, A., Melhuish, C. & Ieropoulos, I. (2014b) Artificial control of microbial life : Towards a urine fuelled robot. In: *The 14th International Conference on the Synthesis and Simulation of Living Systems*. 2014

Parameswaran, P., Torres, C.I., Lee, H.-S., Krajmalnik-Brown, R. & Rittmann, B.E. (2009) Syntrophic interactions among anode respiring bacteria (ARB) and Non-ARB in a biofilm anode: electron balances. *Biotechnology and Bioengineering*. 103 (3), pp. 513–523.

Park, D.H. & Zeikus, J.G. (2002) Impact of electrode composition on electricity generation in a single-compartment fuel cell using Shewanella putrefaciens. *Applied Microbiology and Biotechnology*. 59 (1), pp. 58–61.

Park, D.H. & Zeikus, J.G. (2003) Improved fuel cell and electrode designs for producing electricity from microbial degradation. *Biotechnology and Bioengineering*. 81 (3), pp. 348–355.

Parliamentary Office of Science and Technology (2007) *postnote: Energy and sewage*. 7 (282).

Patil, S.A., Harnisch, F., Kapadnis, B. & Schröder, U. (2010) Electroactive mixed culture biofilms in microbial bioelectrochemical systems: The role of temperature for biofilm formation and performance. *Biosensors and Bioelectronics*. 26 (2), pp. 803–808.

Perera, P.W.A., Han, Z., Chen, Y. & Wu, W. (2007) Recovery of nitrogen and phosphorous

as struvite from swine waste. *Biomedical and Environmental Sciences*. 20pp. 343–350.

Pham, T.H., Boon, N., Aelterman, P., Clauwaert, P., De Schamphelaire, L., Vanhaecke, L., De Maeyer, K., Höfte, M., Verstraete, W. & Rabaey, K. (2008) Metabolites produced by Pseudomonas sp. enable a Gram-positive bacterium to achieve extracellular electron transfer. *Applied Microbiology and Biotechnology*. 77 (5), pp. 1119–1129.

Pham, T.H., Jang, J.K., Chang, I.S. & Kim, B.H. (2004) Improvement of cathode reaction of a mediatorless microbial fuel cell. *Journal of Microbiology and Biotechnology*. 14 (2), pp. 324–329.

Piccolino, M. (1998) Animal electricity and the birth of electrophysiology: the legacy of Luigi Galvani. *Brain Research Bulletin*. 46 (5), pp. 381–407.

Pinchuk, G.E., Hill, E. a., Geydebrekht, O. V., de Ingeniis, J., Zhang, X., Osterman, A., Scott, J.H., Reed, S.B., Romine, M.F., Konopka, A.E., Beliaev, A.S., Fredrickson, J.K. & Reed, J.L. (2010) Constraint-based model of Shewanella oneidensis MR-1 metabolism: A tool for data analysis and hypothesis generation. *PLoS Computational Biology*. 6 (6), pp. 1–8.

Pinto, R.P., Srinivasan, B., Guiot, S.R. & Tartakovsky, B. (2011) The effect of real-time external resistance optimization on microbial fuel cell performance. *Water research*. 45 (4), pp. 1571–1578.

Pinto, R.P., Srinivasan, B., Manuel, M.-F. & Tartakovsky, B. (2010) A two-population bio-electrochemical model of a microbial fuel cell. *Bioresource Technology*. 101 (14), pp. 5256–5265.

Pocaznoi, D., Calmet, A., Etcheverry, L., Erable, B. & Bergel, A. (2012) Stainless steel is a promising electrode material for anodes of microbial fuel cells. *Energy & Environmental Science*. 5 (11), pp. 9645.

Polley, M.H. & Boonstra, B.B.S.T. (1957) Carbon Blacks for Highly Conductive Rubber. *Rubber Chemistry and Technology*. 30 (1), pp. 170–179.

Potter, M.C. (1911) Electrical effects accompanying the decomposition of organic compounds. *Proceedings of the Royal Society B: Biological Sciences*. 84 (571), pp. 260–276.

Premier, G.C., Kim, J.R., Michie, I., Dinsdale, R.M. & Guwy, A.J. (2011) Automatic control of load increases power and efficiency in a microbial fuel cell. *Journal of Power Sources*. 196 (4), pp. 2013–2019.

Price-Whelan, A., Dietrich, L.E.P. & Newman, D.K. (2006) Rethinking 'secondary' metabolism: physiological roles for phenazine antibiotics. *Nature Chemical Biology*. 2 (2), pp. 71–78.

Putnam, D.F. (1971) *Composition and concentrative properties of human urine*.

Quitzau, M.-B. (2007) Water-flushing toilets: Systemic development and path-dependent characteristics and their bearing on technological alternatives. *Technology in Society*. 29 (3), pp. 351–360.

Rabaey, K., Boon, N., Siciliano, S.D., Verhaege, M. & Verstraete, W. (2004) Biofuel cells select for microbial consortia that self-mediate electron transfer. *Applied and Environmental Microbiology*. 70 (9), pp. 5373–5382.

Rabaey, K., Clauwaert, P., Aelterman, P. & Verstraete, W. (2005) Tubular microbial fuel cells for efficient electricity generation. *Environmental Science & Technology*. 39 (20), pp. 8077–8082.

Rabaey, K. & Keller, J. (2008) Microbial fuel cell cathodes: from bottleneck to prime

opportunity? *Water Science and Technology*. 57 (5), pp. 655–659.

Rabaey, K., Rodríguez, J., Blackall, L.L., Keller, J., Gross, P., Batstone, D., Verstraete, W. & Nealson, K.H. (2007) Microbial ecology meets electrochemistry: electricity-driven and driving communities. *The ISME Journal*. 1 (1), pp. 9–18.

Rao, J.R., Richter, G.J., Von Sturm, F. & Weidlich, E. (1976) The performance of glucose electrodes and the characteristics of different biofuel cell constructions. *Bioelectrochemistry and Bioenergetics*. 3 (1), pp. 139–150.

Reimers, C.E., Girguis, P., Stecher, H.A., Tender, L.M., Ryckelynck, N. & Whaling, P. (2006) Microbial fuel cell energy from an ocan cold seep. *Geobiology*. 4pp. 123–136.

Richter, H., McCarthy, K., Nevin, K.P., Johnson, J.P., Rotello, V.M. & Lovley, D.R. (2008) Electricity generation by Geobacter sulfurreducens attached to gold electrodes. *Langmuir : the ACS journal of surfaces and colloids*. 24 (8), pp. 4376–4379.

Röder, M., Whittaker, C. & Thornley, P. (2015) How certain are greenhouse gas reductions from bioenergy? Life cycle assessment and uncertainty analysis of wood pellet-to-electricity supply chains from forest residues. *Biomass and Bioenergy*. 79pp. 50–63.

Roller, S.D., Bennetto, H.P., Delaney, G.M., Mason, J.R., Stirling, J.L. & Thurston, C.F. (1984) Electron-transfer coupling in microbial fuel cells: 1. comparison of redox-mediator reduction rates and respiratory rates of bacteria. *Journal of Chemical Technology and Biotechnology*. 34 (1), pp. 3–12.

Rozendal, R. a, Hamelers, H.V.M. & Buisman, C.J.N. (2006) Effects of membrane cation transport on pH and microbial fuel cell performance. *Environmental Science & Technology*. 40 (17), pp. 5206–5211.

Rozendal, R.A., Sleutels, T.H.J.A., Hamelers, H.V.M. & Buisman, C.J.N. (2008) Effect of the type of ion exchange membrane on performance, ion transport, and pH in biocatalyzed electrolysis of wastewater. *Water Science and Technology*. 57 (11), pp. 1757–1762.

Ryu, H., Lim, C., Kang, M. & Lee, S. (2012) Evaluation of struvite obtained from semiconductor wastewater as a fertilizer in cultivating Chinese cabbage. *Journal of Hazardous Materials*. 221-222pp. 248–255.

Santoro, C., Agrios, A., Pasaogullari, U. & Li, B. (2011) Effects of gas diffusion layer (GDL) and micro porous layer (MPL) on cathode performance in microbial fuel cells (MFCs). *International Journal of Hydrogen Energy*. 36 (20), pp. 13096–13104.

Santoro, C., Lei, Y., Li, B. & Cristiani, P. (2012) Power generation from wastewater using single chamber microbial fuel cells (MFCs) with platinum-free cathodes and pre-colonized anodes. *Biochemical Engineering Journal*. 62pp. 8–16.

Schröder, U. (2007) Anodic electron transfer mechanisms in microbial fuel cells and their energy efficiency. *Physical Chemistry Chemical Physics*. 9 (21), pp. 2619–2629.

Scott, K., Rimbu, G.A., Katuri, K.P., Prasad, K.K. & Head, I.M. (2007) Application of modified carbon anodes in microbial fuel cells. *Process Safety and Environmental Protection*. 85 (5), pp. 481–488.

Shi, L., Squier, T.C., Zachara, J.M. & Fredrickson, J.K. (2007) Respiration of metal (hydr)oxides by Shewanella and Geobacter: a key role for multihaem c-type cytochromes. *Molecular Microbiology*. 65 (1), pp. 12–20.

Shukla, A.K., Suresh, P., Berchmans, S. & Rajendran, A. (2004) Biological fuel cells and their applications. *Current Science*. 87 (4), pp. 455–468.

Sleiti, A.K. (2015) Overview of tidal power technology. *Energy Sources, Part B: Economics,*

Planning, and Policy. 10 (1), pp. 8–13.

Sun, J., Hu, Y., Bi, Z. & Cao, Y. (2009) Improved performance of air-cathode single-chamber microbial fuel cell for wastewater treatment using microfiltration membranes and multiple sludge inoculation. *Journal of Power Sources*. 187 (2), pp. 471–479.

Sun, J.-J., Zhao, H.-Z., Yang, Q.-Z., Song, J. & Xue, A. (2010) A novel layer-by-layer self-assembled carbon nanotube-based anode: Preparation, characterization, and application in microbial fuel cell. *Electrochimica Acta*. 55 (9), pp. 3041–3047.

Tender, L.M., Reimers, C.E., Stecher, H.A., Holmes, D.E., Bond, D.R., Lowy, D.A., Pilobello, K., Fertig, S.J. & Lovley, D.R. (2002) Harnessing microbially generated power on the seafloor. *Nature Biotechnology*. 20 (8), pp. 821–825.

The New York Times (2007) *Microbial 'fuel cell' squeezes energy from brewery wastewater*. Available from: http://www.nytimes.com/2007/05/02/business/worldbusiness/02iht-beer.1.5529489.html [Accessed 14 September 2015].

Torres, C.I., Kato Marcus, A. & Rittmann, B.E. (2008) Proton transport inside the biofilm limits electrical current generation by anode-respiring bacteria. *Biotechnology and Bioengineering*. 100 (5), pp. 872–881.

Treter, J. & Macedo, A.J. (2011) Catheters : a suitable surface for biofilm formation. In: A. Mendez-Vilas (ed.). *Science against Microbial Pathogens: Communicating Current Research and Technological Advances*. Formatex Research Center. pp. pp. 835–842.

Udert, K.M., Larsen, T.A. & Gujer, W. (2003) Biologically induced precipitation in urine-collecting systems. *Water Science and Technology: Water Supply*. 3 (3), pp. 71–78.

Velasquez-Orta, S.B., Curtis, T.P. & Logan, B.E. (2009) Energy from algae using microbial fuel cells. *Biotechnology and Bioengineering*. 103 (6), pp. 1068–1076.

Venkata Mohan, S., Veer Raghavulu, S. & Sarma, P.N. (2008) Biochemical evaluation of bioelectricity production process from anaerobic wastewater treatment in a single chambered microbial fuel cell (MFC) employing glass wool membrane. *Biosensors & Bioelectronics*. 23 (9), pp. 1326–1332.

Verstraete, W., Morgan-Sagastume, F., Aiyuk, S., Waweru, M., Rabaey, K. & Lissens, G. (2005) Anaerobic digestion as a core technology in sustainable management of organic matter. *Water Science and Technology*. 52 (1-2), pp. 59–66.

Viti, C. & Giovannetti, L. (2005) Characterization of cultivable heterotrophic bacterial communities in Cr-polluted and unpolluted soils using Biolog and ARDRA approaches. *Applied Soil Ecology*. 28 (2), pp. 101–112.

Walan, P., Davidsson, S., Johansson, S. & Höök, M. (2014) Phosphate rock production and depletion: Regional disaggregated modeling and global implications. *Resources, Conservation and Recycling*. 93pp. 178–187.

Walter, X.A., Greenman, J. & Ieropoulos, I.A. (2014) Intermittent load implementation in microbial fuel cells improves power performance. *Bioresource Technology*. 172pp. 365–372.

Wang, H., Wu, Z., Plaseied, A., Jenkins, P., Simpson, L., Engtrakul, C. & Ren, Z. (2011) Carbon nanotube modified air-cathodes for electricity production in microbial fuel cells. *Journal of Power Sources*. 196 (18), pp. 7465–7469.

Wang, X., Feng, C., Ding, N., Zhang, Q., Li, N., Li, X., Zhang, Y. & Zhou, Q. (2014) Accelerated OH(-) transport in activated carbon air cathode by modification of quaternary ammonium for microbial fuel cells. *Environmental Sciience & Technology*. 48 (7), pp. 4191–4198.

Wang, X., Feng, Y.J. & Lee, H. (2008) Electricity production from beer brewery wastewater using single chamber microbial fuel cell. *Water Science and Technology : A Journal of the International Association on Water Pollution Research*. 57 (7), pp. 1117–1121.

Wang, X.L., Zhang, H.M., Zhang, J.L., Xu, H.F., Tian, Z.Q., Chen, J., Zhong, H.X., Liang, Y.M. & Yi, B.L. (2006) Micro-porous layer with composite carbon black for PEM fuel cells. *Electrochimica Acta*. 51 (23), pp. 4909–4915.

Watanabe, K., Manefield, M., Lee, M. & Kouzuma, A. (2009) Electron shuttles in biotechnology. *Current Opinion in Biotechnology*. 20 (6), pp. 633–641.

Weber, A.Z. & Newman, J. (2005) Effects of microporous layers in polymer electrolyte fuel cells. *Journal of The Electrochemical Society*. 152 (4), pp. A677.

Wei, J., Liang, P. & Huang, X. (2011) Recent progress in electrodes for microbial fuel cells. *Bioresource Technology*. 102 (20), pp. 9335–9344.

Wilkinson, S. (2000) 'Gastrobots' - benefits and challenges of microbial fuel cells in food powered robot applications. *Autonomous Robots*. 9 (2), pp. 99–111.

Winfield, J., Greenman, J., Huson, D. & Ieropoulos, I. (2013) Comparing terracotta and earthenware for multiple functionalities in microbial fuel cells. *Bioprocess and Biosystems Engineering*. 36 (12), pp. 1913–1921.

Winfield, J., Ieropoulos, I., Greenman, J. & Dennis, J. (2011) The overshoot phenomenon as a function of internal resistance in microbial fuel cells. *Bioelectrochemistry*. 81 (1), pp. 22–27.

World Nuclear Association (2014) *Transport and the hydrogen economy*. Available from: http://www.world-nuclear.org/info/Non-Power-Nuclear-Applications/Transport/Transport-and-the-Hydrogen-Economy/ [Accessed 4 February 2015].

Xiao, L., Damien, J., Luo, J., Jang, H.D., Huang, J. & He, Z. (2012) Crumpled graphene particles for microbial fuel cell electrodes. *Journal of Power Sources*. 208pp. 187–192.

Yang, S., Jia, B. & Liu, H. (2009) Effects of the Pt loading side and cathode-biofilm on the performance of a membrane-less and single-chamber microbial fuel cell. *Bioresource Technology*. 100 (3), pp. 1197–1202.

You, J., Greenman, J., Melhuish, C. & Ieropoulos, I. (2015) Electricity generation and struvite recovery from human urine using microbial fuel cells. *Journal of Chemical Technology & Biotechnology*. pp. n/a – n/a.

You, J., Santoro, C., Greenman, J., Melhuish, C., Cristiani, P., Li, B. & Ieropoulos, I. (2014) Micro-porous layer (MPL)-based anode for microbial fuel cells. *International Journal of Hydrogen Energy*. 39 (36), pp. 21811–21818.

Yu, E.H., Cheng, S., Logan, B.E. & Scott, K. (2008) Electrochemical reduction of oxygen with iron phthalocyanine in neutral media. *Journal of Applied Electrochemistry*. 39 (5), pp. 705–711.

Yu, L., Chen, W., Qin, M. & Ren, G. (2009) Experimental research on water management in proton exchange membrane fuel cells. *Journal of Power Sources*. 189 (2), pp. 882–887.

Yuan, H., Chen, Y., Zhang, H., Jiang, S., Zhou, Q. & Gu, G. (2006) Improved bioproduction of short-chain fatty acids (SCFAs) from excess sludge under alkaline conditions. *Environmental Science & Technology*. 40 (6), pp. 2025–2029.

Yuan, Y., Chen, Q., Zhou, S., Zhuang, L. & Hu, P. (2012) Improved electricity production from sewage sludge under alkaline conditions in an insert-type air-cathode microbial fuel cell. *Journal of Chemical Technology & Biotechnology*. 87 (1), pp. 80–86.

Zak, J., Willig, M., Moorhead, D. & Wildman, H. (1994) Functional diversity of microbial communities: a quantitative approach. *Soil Biology and Biochemistry*. 26 (9), pp. 1101–1108.

Zang, G.-L., Sheng, G.-P., Li, W.-W., Tong, Z.-H., Zeng, R.J., Shi, C. & Yu, H.-Q. (2012) Nutrient removal and energy production in a urine treatment process using magnesium ammonium phosphate precipitation and a microbial fuel cell technique. *Physical Chemistry Chemical Physics*. 14 (6), pp. 1978–1984.

Zhang, E., Xu, W., Diao, G. & Shuang, C. (2006) Electricity generation from acetate and glucose by sedimentary bacterium attached to electrode in microbial-anode fuel cells. *Journal of Power Sources*. 161 (2), pp. 820–825.

Zhang, F., Chen, G., Hickner, M. a. & Logan, B.E. (2012) Novel anti-flooding poly(dimethylsiloxane) (PDMS) catalyst binder for microbial fuel cell cathodes. *Journal of Power Sources*. 218pp. 100–105.

Zhang, L., Liu, C., Zhuang, L., Li, W., Zhou, S. & Zhang, J. (2009) Manganese dioxide as an alternative cathodic catalyst to platinum in microbial fuel cells. *Biosensors & Bioelectronics*. 24 (9), pp. 2825–2829.

Zhang, L., Zhu, X., Li, J., Liao, Q. & Ye, D. (2011a) Biofilm formation and electricity generation of a microbial fuel cell started up under different external resistances. *Journal of Power Sources*. 196 (15), pp. 6029–6035.

Zhang, T., Zeng, Y., Chen, S., Ai, X. & Yang, H. (2007) Improved performances of E. coli-catalyzed microbial fuel cells with composite graphite/PTFE anodes. *Electrochemistry Communications*. 9 (3), pp. 349–353.

Zhang, X., Cheng, S., Huang, X. & Logan, B.E. (2010) The use of nylon and glass fiber filter separators with different pore sizes in air-cathode single-chamber microbial fuel cells. *Energy & Environmental Science*. 3 (5), pp. 659.

Zhang, Y., Min, B., Huang, L. & Angelidaki, I. (2011b) Electricity generation and microbial community response to substrate changes in microbial fuel cell. *Bioresource Technology*. 102 (2), pp. 1166–1173.

Zhao, F., Harnisch, F., Schröder, U., Scholz, F., Bogdanoff, P. & Herrmann, I. (2005) Application of pyrolysed iron(II) phthalocyanine and CoTMPP based oxygen reduction catalysts as cathode materials in microbial fuel cells. *Electrochemistry Communications*. 7 (12), pp. 1405–1410.

Zhao, F., Harnisch, F., Schröder, U., Scholz, F., Bogdanoff, P. & Herrmann, I. (2006) Challenges and constraints of using oxygen cathodes in microbial fuel cells. *Environmental Science & Technology*. 40 (17), pp. 5193–5199.

Zhou, M., Wang, H., Hassett, D.J. & Gu, T. (2013) Recent advances in microbial fuel cells (MFCs) and microbial electrolysis cells (MECs) for wastewater treatment, bioenergy and bioproducts. *Journal of Chemical Technology & Biotechnology*. 88 (4), pp. 508–518.

Zhuang, L., Feng, C., Zhou, S., Li, Y. & Wang, Y. (2010a) Comparison of membrane- and cloth-cathode assembly for scalable microbial fuel cells: Construction, performance and cost. *Process Biochemistry*. 45 (6), pp. 929–934.

Zhuang, L., Zhou, S., Li, Y. & Yuan, Y. (2010b) Enhanced performance of air-cathode two-chamber microbial fuel cells with high-pH anode and low-pH cathode. *Bioresource Technology*. 101 (10), pp. 3514–3519.

Zuo, Y., Cheng, S., Call, D. & Logan, B.E. (2007) Tubular membrane cathodes for scalable power generation in microbial fuel cells. *Environmental Science & Technology*. 41 (9),

pp. 3347–3353.

Zuo, Y., Cheng, S. & Logan, B.E. (2008) Ion exchange membrane cathodes for scalable microbial fuel cells. *Environmental Science & Technology*. 42 (18), pp. 6967–6972.

Appendices

Appendix A – Summary of MFC Configuration and Power Output

Reactor	Anode	Cathode	Membrane	Feedstock	P_{MAX}[1]
4.2. Multiple Membrane Comparison					
R-MFC	CV20, S.A.[2]: 270 cm^2	CV20, S.A.: 270 cm^2 Open-to-air cathode	VWR-C, VWR-A, MI-C, MI-A, FT-C, FT-A, AGC-C, AGC-A, MEGA-A S.A.: 30 cm^2	AS[3] + 0.1 M acetate Batch fed	115.6 µW
4.3. MPL Based Anode					
C-MFC	CV20, CV30, CV20-MPL, CC, CC-MPL, S.A.: 67 cm^2	AC[4], S.A.: 4.9 cm^2 Open-to-air cathode	MI-C, S.A.: 4.9 cm^2	Human urine Continuous fed	304.3 µW
5.2. Thermophilic Biofilm					
S-MFC	CV20, S.A.: 28 cm^2	CV20, S.A.: 28 cm^2 Re-circulating water cathode	VWR-C, S.A.: 1.8 cm^2	Modified 2SPYN (x10) Continuous fed	35.3 µW

* (1) calculated from polarisation measurements (2) surface area (3) activated sludge (4) activated carbon

Reactor	Anode	Cathode	Membrane	Feedstock	P_{MAX}
5.3. Effect of External Resistance eon Anodic Biofilm					
R-MFC	CV20, S.A.: 270 cm^2	CV20, S.A.: 270 cm^2 Open-to-air cathode	VWR-C, S.A.: 30 cm^2	Human urine Batch fed	203.4 µW
5.4. Stability and Variability of Anodic Biofilm					
C-MFC	CV30, S.A.: 10 cm^2	AC, S.A.: 4.9 cm^2 Open-to-air cathode	MI-C, S.A.: 4.9 cm^2	Modified M1 + acetate/casein as a sole carbon source Continuous fed	242.6 µW
6.2. Human Urine as a Power Source					
R-MFC	CV20, S.A.: 270 cm^2	CV20, S.A.: 270 cm^2 Open-to-air cathode	VWR-C, S.A.: 30 cm^2	Human urine Batch fed	203.4 µW

Reactor	Anode	Cathode	Membrane	Feedstock	P_{MAX}
6.3. Uric Salts Utilisation					
R-MFC	CV20, S.A.: 270 cm^2	CV20, S.A.: 270 cm^2 Open-to-air cathode	VWR-C, S.A.: 30 cm^2	Urine or uric salts Batch fed	-
S-MFC	CV20, S.A.: 28 cm^2	CV20, S.A.: 28 cm^2 Re-circulating water cathode	VWR-C, S.A.: 1.8 cm^2	Sludge + uric salts Batch fed	31.1 µW
6.4. Struvite Recovery from Human Urine					
C-MFC	CV30, S.A.: 50 cm^2	AC, S.A.: 4.9 cm^2 Open-to-air cathode	MI-C, S.A.: 4.9 cm^2	Human urine Continuous fed	557.2 µW (for a group of 4 MFCs)
Appendix D – Additional Pin Electrode					
R-MFC	CV20, S.A.: 270 cm^2	CV20, S.A.: 270 cm^2 1) Open-to-air cathode 2) Batch type water/ ferricyanide cathode	VWR-C, S.A.: 30 cm^2	Human urine or TYE Batch fed	58.8 µW (for water cathode)

Appendix B – Preparation of Modified M1 Minimal Medium

Growing medium

The preparation steps for the medium employed in section 5.4 are presented below.

SL10 trace elements solution (for 1 L)

Reagent	g/L
$FeCl_2 \cdot 4H_2O$	1.5
7.7 M HCl	10 mL
$CoCl_2 \cdot 6H_2O$	0.006
$MnCl_2 \cdot 4H_2O$	0.036
$ZnCl_2$	0.024
H_3BO_3	0.002
$Na_2MnO_4 \cdot 2H_2O$	0.19
$NiCl_2 \cdot 6H_2O$	0.1
$CuCl_2 \cdot 2H_2O$	0.07

Preparation steps for SL10 trace elements solution

1. $FeCl_2$ is added to a beaker which contains HCl and mixed until it is dissolved completely.
2. About 800 mL of DIW is added to the beaker and all other ingredients are followed. The solution is mixed well.
3. pH adjusted to 6.0 then DIW is added to complete volume of 1 L.

The solution should be stored in a dark bottle to be protected from light.

Wolfe's vitamin solution (for 1L)

Reagent	mg/L
Pyridoxine hydrochloride	10
Thiamine-HCl	5
Riboflavin	5
Nicotinic acid	5
Calcium D-(+)-pantothenate	5
p-Aminobenzoic acid	5
Thioctic acid	5
Biotin	2
Folic acid	2
Vitamin B12	0.1

Preparation steps for Wolfe's vitamin solution

1. All ingredients are dissolved completely in 900 mL of DIW
2. Q.S to 1000 mL.
3. Solution is filter sterilised

Main reagents

Reagent	g/mol	mM employed
PIPES buffer	302.37	3
NaOH	40	7.5
NH_4Cl	53.56	28
KCl	74.55	1.34
$NaH_2PO_4 \cdot H_2O$	137.99	4.35
NaCl	58.44	30
$MgCl_2 \cdot 6H_2O$	203.3	3
$CaCl_2$	110.98	0.0068
Sodium acetate*	82.03	18
Casein*	-	
Glutamine*	146.14	
Glucose*	180.16	

*sole carbon sources: equivalent COD value of 1150 ppm
(1.48 g/L sodium acetate, 0.83 g/L casein, 1.17 g/L glutamine, 1.08 g/L glucose)

Modified M1 medium preparation

1. All main reagents are dissolved, except for casein, in 700 mL DIW (per L wanted)
2. pH adjusted to 7.0 with 100 mM NaOH solution
3. Q.S. to 980 mL per L wanted
4. Solution is autoclaved

5. 10 mL of SL10 trace elements solution and Wolfe's vitamin solution each (x100 concentrated, per L medium wanted) are then added. Final volume of the solution is now 1000 mL

6. (for casein) casein is added to 5 mL of 1M NaOH (the amount of NaOH for this mixture is taken out from the preparation procedure step 1 above so the final concentration of NaOH is equal to 7.5 mM) then heated until it is dissolved completely. This solution is autoclaved separately then transferred to the main media bottle aseptically

Appendix C – Calculus-based proof of R_{INT}

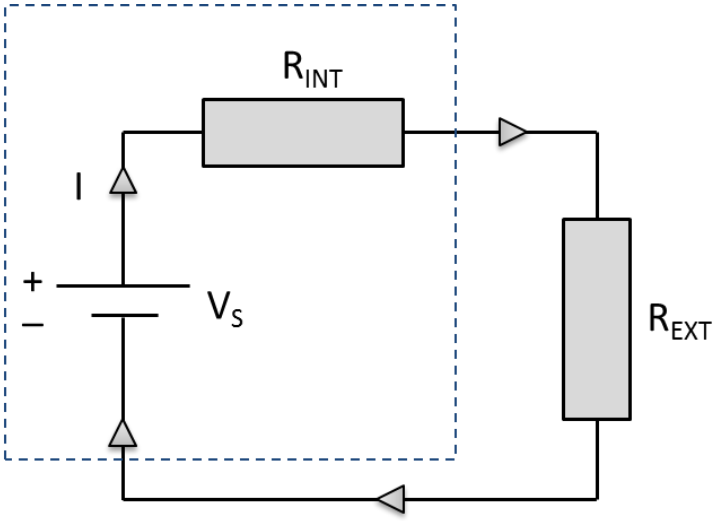

In the diagram, power is being transferred from the source, with voltage V_S (voltage of the source) and internal resistance of the source R_{INT} (representative of losses), to a load with resistance R_{EXT} (external resistance), resulting in a current I.

Kirchhoff's voltage law states the directed sum of the electrical potential differences (voltage) around any closed network is zero.

$$V_S - V_{R_{INT}} - V_{R_{EXT}} = 0$$

where $V_{R_{INT}}$ is voltage drop across the internal resistance and $V_{R_{EXT}}$ is voltage drop across the external resistance.

By Ohm's law,

$$V_S = (I \times R_{INT}) + (I \times R_{EXT})$$

$$V_S = I(R_{INT} + R_{EXT})$$

$$R_{INT} = \left(\frac{V_S}{I}\right) - R_{EXT}$$

In a Thevenin's equivalent circuit, V_S is equal to open circuit voltage of the source $V_{O/C}$.

$$R_{INT} = \left(\frac{V_{O/C}}{I_L}\right) - R_{EXT}$$

For the power P_L dissipated in the load is the square of the current multiplied by the resistance:

$$P_L = I^2 R_{EXT} = \left(\frac{V_S}{R_{INT} + R_{EXT}}\right)^2 R_{EXT} = \frac{{V_S}^2}{\frac{{R_{INT}}^2}{R_{EXT}} + 2R_{INT} + R_{EXT}}$$

Under maximum power transfer to load condition:

$$\frac{d}{dR_{EXT}} P_L = \frac{d}{dR_{EXT}} \left(\frac{{V_S}^2}{\frac{{R_{INT}}^2}{R_{EXT}} + 2R_{INT} + R_{EXT}}\right) = 0$$

$$\frac{d}{dR_{EXT}} \left(\frac{{R_{INT}}^2}{R_{EXT}} + 2R_{INT} + R_{EXT}\right) = -\frac{{R_{INT}}^2}{{R_{EXT}}^2} + 1 = 0$$

$$\frac{{R_{INT}}^2}{{R_{EXT}}^2} = 1$$

$$R_{EXT} = \pm R_{INT}$$

$$R_{EXT} = R_{INT}$$

Thus when R_{EXT} equals to R_{INT}, maximum power from a source is obtained. This is referred to as 'Jacobi's impedance matching law' named after Moritz von Jacobi, who published the maximum power transfer theorem.

Appendix D - Calculation of Shannon-Wiener Index from Biolog AN Plates

The Shannon-Wiener index (H) uses the function $\mathbf{H} = -\sum_{i=1}^{n} \boldsymbol{p_i}(\mathbf{ln}\, \boldsymbol{p_i})$ where $p_i = \frac{OD_i}{\sum OD_i}$, OD_i is the optical density value of an well containing a particular substrate (OD_i), $\sum OD_i$ is the sum of optical density values of all the wells of the AN plates, n is the number of substrates on a plate (n = 95).

A worked example of calculating the H for a sample presented in Fig. 5.15 is as follows;

The raw data, measured ODs at 590 nm, are shown below.

	1	2	3	4	5	6	7	8	9	10	11	12
A	0.167	0.589	1.513	1.349	0.191	0.149	0.237	0.469	0.912	0.222	0.228	1.351
B	0.278	0.185	0.965	0.284	1.002	1.103	0.203	1.349	0.254	1.208	0.261	1.638
C	0.298	0.795	0.186	0.957	0.197	1.185	1.347	1.361	1.274	0.786	1.033	0.432
D	0.366	0.277	0.207	1.062	0.234	0.861	0.835	0.455	1.077	0.242	1.350	1.259
E	0.191	0.306	0.191	0.694	0.135	0.145	0.605	0.130	0.182	0.187	0.989	0.993
F	0.296	0.160	1.218	0.168	0.868	0.751	0.752	0.281	0.858	0.355	0.352	0.235
G	0.188	0.207	0.831	0.636	0.190	1.093	0.955	0.222	0.228	0.417	0.227	0.273
H	0.146	0.137	0.458	0.150	0.138	0.455	0.126	0.479	0.337	0.972	0.379	0.221

1) Normalise the raw values by subtracting the OD value of the control well (A1) from them. If a raw value is smaller than the control's, replace the result with 0. e.g. (for A2 well) 0.589 – 0.167 = 0.422

	1	2	3	4	5	6	7	8	9	10	11	12
A	0.000	0.422	1.346	1.182	0.024	0.000	0.070	0.302	0.745	0.055	0.061	1.184
B	0.111	0.018	0.798	0.117	0.835	0.936	0.036	1.182	0.087	1.041	0.094	1.471
C	0.131	0.628	0.019	0.790	0.030	1.018	1.180	1.194	1.107	0.619	0.866	0.265
D	0.199	0.110	0.040	0.895	0.067	0.694	0.668	0.288	0.910	0.075	1.183	1.092
E	0.024	0.139	0.024	0.527	0.000	0.000	0.438	0.000	0.015	0.020	0.822	0.826
F	0.129	0.000	1.051	0.001	0.701	0.584	0.585	0.114	0.691	0.188	0.185	0.068
G	0.021	0.040	0.664	0.469	0.023	0.926	0.788	0.055	0.061	0.250	0.060	0.106
H	0.000	0.000	0.291	0.000	0.000	0.288	0.000	0.312	0.170	0.805	0.212	0.054

2) Calculate the relative abundance ($= \boldsymbol{P_i}$) of an utilised substrate; this is the normalised OD value of an utilised substrate, divided by the sum of normalised OD values of all the substrates. e.g. (for A2 well) 0.422/38.912 = 0.011

3) Perform a natural log on each relative abundance result ($= \mathbf{ln}\, \boldsymbol{P_i}$) e.g. (for A2 well) ln 0.011 = −4.524

4) Next multiply each **ln Pi** by **Pi** e.g. (for A2 well) 0.011 x −4.524 = −0.049

	1	2	3	4	5	6	7	8	9	10	11	12
A	0.000	-0.049	-0.116	-0.106	-0.005	0.000	-0.011	-0.038	-0.076	-0.009	-0.010	-0.106
B	-0.017	-0.004	-0.080	-0.017	-0.082	-0.090	-0.006	-0.106	-0.014	-0.097	-0.015	-0.124
C	-0.019	-0.067	-0.004	-0.079	-0.006	-0.095	-0.106	-0.107	-0.101	-0.066	-0.085	-0.034
D	-0.027	-0.017	-0.007	-0.087	-0.011	-0.072	-0.070	-0.036	-0.088	-0.012	-0.106	-0.100
E	-0.005	-0.020	-0.005	-0.058	0.000	0.000	-0.051	0.000	-0.003	-0.004	-0.081	-0.082
F	-0.019	0.000	-0.098	0.000	-0.072	-0.063	-0.063	-0.017	-0.072	-0.026	-0.025	-0.011
G	-0.004	-0.007	-0.069	-0.053	-0.004	-0.089	-0.079	-0.009	-0.010	-0.032	-0.010	-0.016
H	0.000	0.000	-0.037	0.000	0.000	-0.036	0.000	-0.039	-0.024	-0.080	-0.028	-0.009

5) Now add up all the results to give total ($= \sum_{i=1}^{n} \boldsymbol{p_i}(\mathbf{ln}\, \boldsymbol{p_i})$) e.g. 0.000 + –0.049 + –0.116 … + –0.009 = –3.990

6) Multiply by -1 to give a positive number ($= -\sum_{i=1}^{n} \boldsymbol{p_i}(\mathbf{ln}\, \boldsymbol{p_i})$) e.g. H = –1 x –3.990 = 3.990

Appendix E - Additional Pin Electrodes

For a practical application of MFC technology, one of the biggest hurdles to overcome is voltage/current increase since the power output of a single MFC is relatively low. In order to do this, conventional configurations such as serial or parallel connection (or combination of the two) is usually applied. As an alternative to these common ways, a new connection method with the introduction of another electrode (pin electrode) was suggested and the preliminary work is presented.

For the first part of work investigating power boosting effect of additional pins, single-chamber R-MFCs were used. An additional electrode, '3rd pin' electrode, was inserted into the anode chamber. The pin electrodes were made of carbon fibre veil which is the same material as the anode. Its size was 27 cm^2 which is 1/10th of the anode electrode size. Apart from the top and bottom, 3rd pins were wrapped up with a plastic paraffin film in order to avoid short circuit by contacting the anodes, 'working electrodes', in the same chamber of MFCs.

A 3rd pin of an MFC (referred as a 'target cell') was connected to the cathode of another MFC (referred as a 'driver cell') which was not connected with R_{EXT} (open circuit condition). While this connection, 'poise period', the anode of the driver cell was connected to the anode of the target cell. Figure E.1 describes how the connections and disconnections were performed.

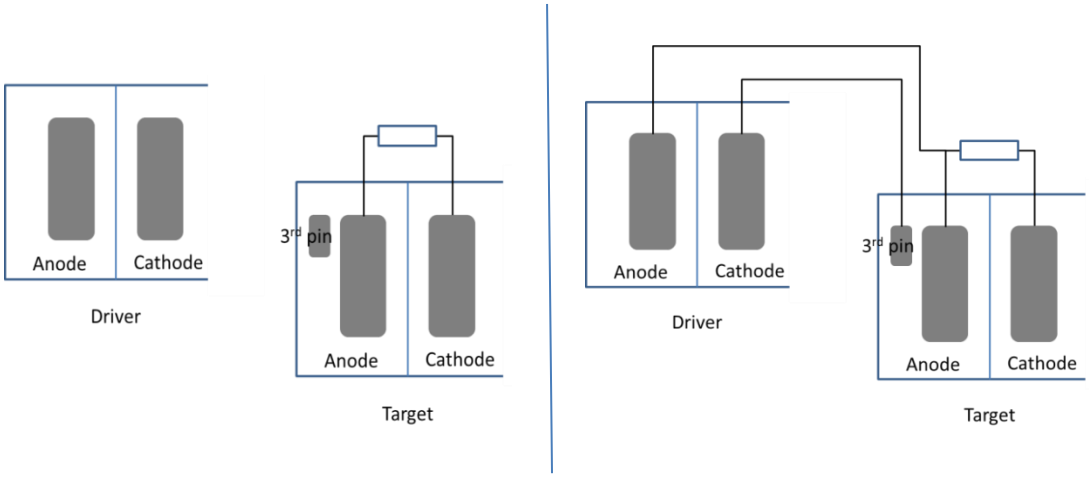

Figure E.1. Configuration of target cell (working cell) and driver cell; break time (left) and poise period (right)

In the second part of work, two-chamber R-MFCs with ferricyanide or water cathodes were employed in order to introduce 4th pins in the cathode chambers. MFCs were fed with neat human urine.

Power boosting effect

Figure E.2 illustrates power producing behaviour of target cells when they were poised by driver cells (open circuit condition) through 3rd pins. In this case, target cells and working cells were connected for 10 seconds and disconnected for 90 seconds. When two cells were connected (poised), target cell voltage peaked up and driver cell voltage fell instantly. The amount of increased voltage by poising was 32 % and 26.2 % for both target cells. This boosting effect becomes even bigger when power is considered as in 74.6 % and 59.1 % respectively. Although the first time of connection showed the biggest increase, the boosting effect did not vanish after repeating a few more times.

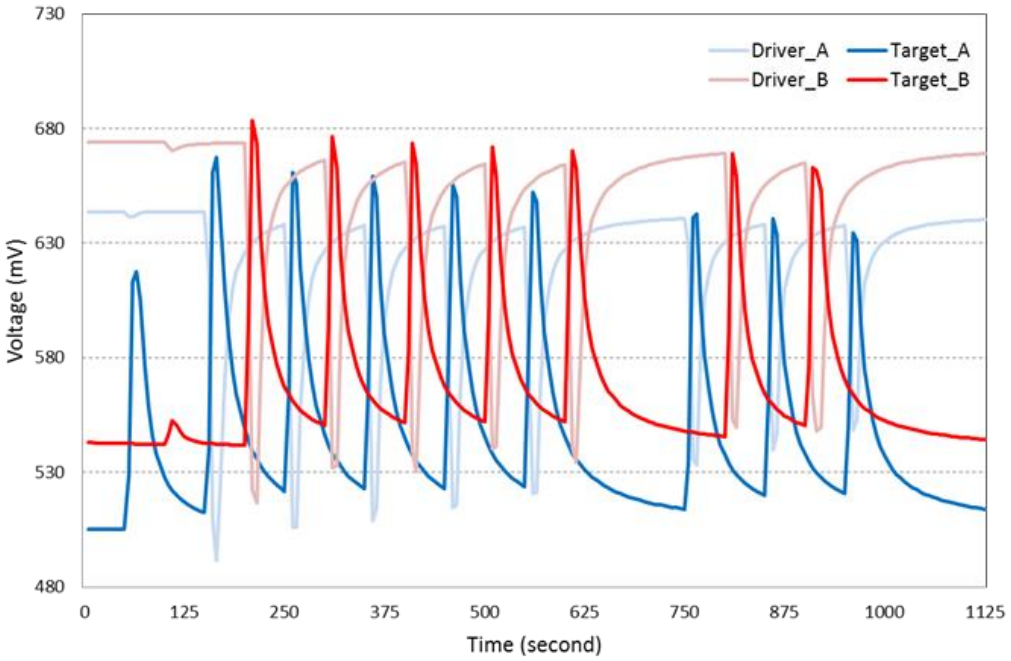

Figure E.2. Voltage increase by poising target cells

Comparison with conventional connecting methods

In order to compare this new connection method with conventional connections, driver cells were connected with target cells in series or parallel. As shown in Fig. E.3, connecting a driver cell to the 3rd pin had a unique effect unlike the serial or parallel connection. It is very well known that serial and parallel connections bring increase of voltage and current respectively. However neither ways can increase both voltage and current, whereas the new configuration raises both. Therefore poising is a completely novel connecting method and can be used when different strategy is required.

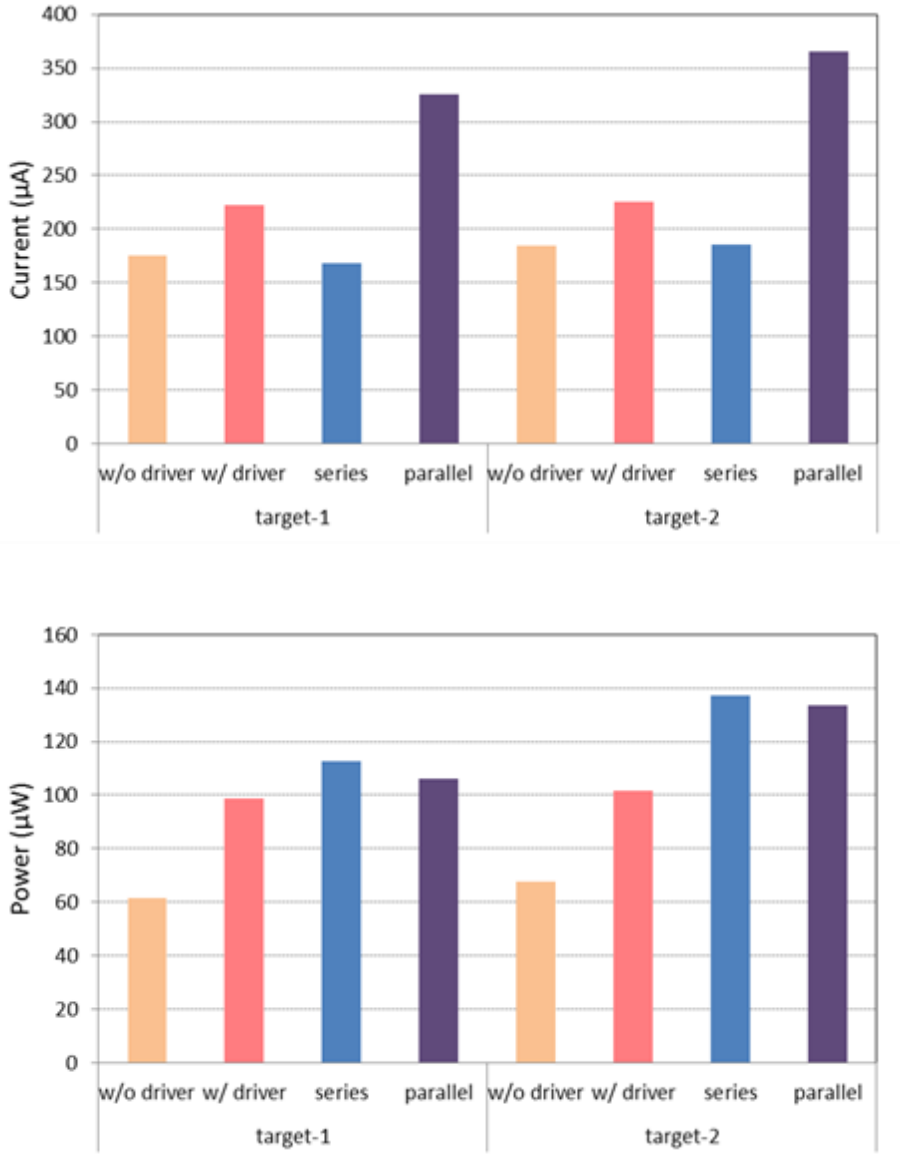

Figure E.3. Poising effect compared to conventional connections in current and power

Potential for open circuit voltage real-time monitoring

As discussed in section 5.3 .3, for maximum power output, it is important to run an MFC system under the load that matches to the R_{INT} of the system. The R_{INT} might vary with changes in operational conditions such as temperature, pH, ionic strength of anolyte, substrate composition and COD concentration. For maintaining the best condition for MFC power generation, therefore, constant control of R_{EXT} is required (Pinto *et al.*, 2011; Premier *et al.*, 2011). In this respect, it would be extremely beneficial if the R_{INT} is measured in real-time without disturbing the system performance.

Another potential application of the additional pins is real-time monitoring of OCV of an MFC system. In order to investigate this, another pin electrode, 4^{th} pin, was introduced and inserted in the closed cathode chamber. Because pin electrodes were isolated from main anode and cathode electrodes, it seemed like that the pins were not affected by loading the main electrodes. Figure E.4 shows that the potential difference between two pins did not change when polarisation experiments of main electrodes were carried out. This value was not exactly the same as the open circuit value of the MFCs but almost half of it. If there is a relationship between the OCV of main electrodes and potential difference of the two pins, pin cells could be used as a monitoring tool which can sense OCV of an MFC in real time. This is potentially an exploitable finding.

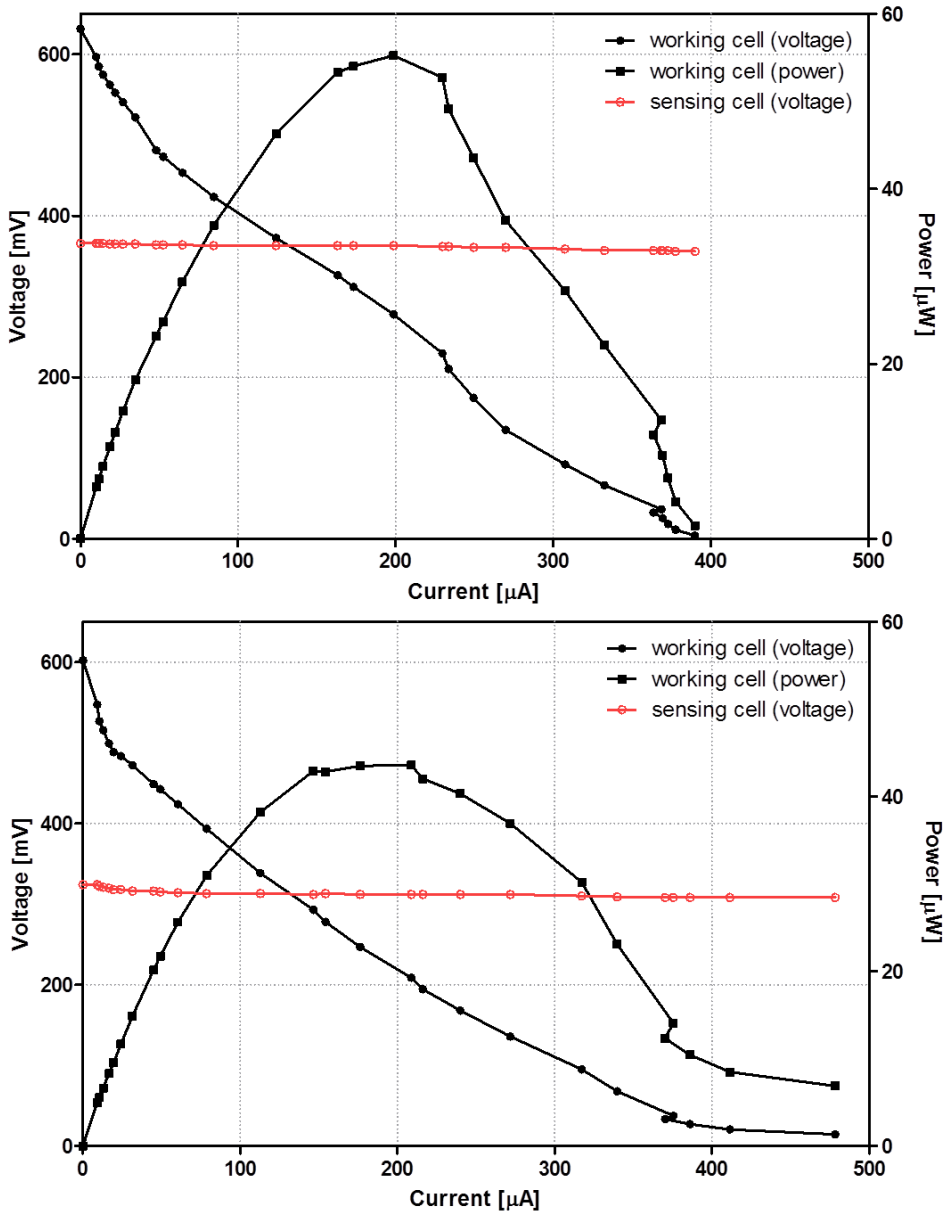

Figure E.4. Pin electrodes performing open circuit potential sensing during polarisation experiment